

# PHYSICS OF BLOWN SAND AND COASTAL DUNES

The Title of this thesis relates to the pioneering and inspiring work of R.A. Bagnold; "The Physics of Blown Sand and Desert Dunes". It is not the intention to compare this thesis that took 4 years to complete to the fantastic lifetime legacy of R.A. Bagnold. The work of R.A. Bagnold continues to inspire and with using this title it is intended to make a (humble) reference to his excellent work.

Sierd de Vries



# PHYSICS OF BLOWN SAND AND COASTAL DUNES

Proefschrift

ter verkrijging van de graad van doctor  
aan de Technische Universiteit Delft  
op gezag van de Rector Magnificus prof.ir. K.C.A.M. Luyben  
voorzitter van het College voor Promoties  
in het openbaar te verdedigen op 20 september 2013 om 10.00 uur

door

Sierd DE VRIES  
civiel ingenieur  
geboren te Gouda

Dit proefschrift is goedgekeurd door de promotor:

Prof.dr.ir. M.J.F. Stive

Co-promotor:

Dr. R. Ranasinghe

Samenstelling promotiecommissie:

Rector Magnificus	voorzitter
Prof.dr.ir. M.J.F. Stive	Technische Universiteit Delft, promotor
Dr. R. Ranasinghe	Technische Universiteit Delft, co-promotor
Prof.dr. P. Hoekstra	Universiteit Utrecht
Prof.dr.ir. J.A. Roelvink	Unesco-IHE institute for water education
Dr. S.M. Arens	Arens bureau voor Duinonderzoek
Dr.ir. J.S.M. van Thiel de Vries	Technische Universiteit Delft
Prof.dr. H. Hanson	Lund University
Prof.dr.ir. W.S.J. Uijttewaal	Technische Universiteit Delft, reservelid

## Samenvatting

Het doel van deze studie is het identificeren en kwantificeren van processen die verantwoordelijk zijn voor de ontwikkeling van kustduinen op de ingenieurstijdschaal. Deze studie is onderdeel van het Building with Nature (Bouwen met de Natuur) project. Binnen het Building with Nature project wordt geprobeerd om natuurlijke processen te gebruiken en mogelijkheden voor natuur te scheppen terwijl kust gerelateerde infrastructuur wordt gerealiseerd.

Om inzichten te ontwikkelen in op welke manier processen die leiden tot de vorming van duinen verantwoordelijk zijn voor het gedrag van duinen op jaarlijkse-decennia tijdschaal is de Nederlandse Jarkus dataset geanalyseerd. De JARKUS dataset bevat gemeten morfologische profielen langs de gehele Nederlandse kust die verzameld zijn van 1965 tot heden. Het gedeelte van deze dataset met betrekking tot de Hollandse Kust is gebruikt. Uit deze dataset zijn veranderingen van duinvolumes bepaald en deze volumeveranderingen zijn gebruikt als parameters die representatief zijn voor duingedrag. De metingen van deze duinvolumeveranderingen laten vaak een positieve lineaire ontwikkeling in de tijd zien op de tijdschaal van decennia. Hieruit volgt dat op een aanzienlijk deel van de locaties een constante duinaangroei kan worden aangenomen. Dit schept potentieel mogelijkheden om duingedrag beter te kunnen voorspellen. De mate van deze constante duinaangroei in de tijd varieert in de ruimte in kustlangse richting. Ruimtelijke en temporele variabiliteiten in veranderingen van duinvolumes zijn afgeleid en deze zijn gecorreleerd met windcondities en strandhelling. Er is op geen enkele van de beschouwde locaties een correlatie gevonden tussen windcondities en volumeveranderingen in het duin op de tijdschaal van jaren tot decennia. Het lijkt daarom onwaarschijnlijk dat het gebruik van modellen die duingedrag voorspellen op de tijdschaal van decennia met wind als belangrijkste parameter tot bevredigende resultaten zal leiden. Veranderingen in duinvolume correleren significant met strandhelling. Strandhelling zou een aanbod limiterende parameter kunnen zijn. Dit alles suggereert dat het duingedrag op de beschouwde locaties bepaald wordt door zandaanbod in plaats van forcering door de wind. Een model voor duinontwikkeling waar sediment aanbod een significante rol speelt lijkt daarom geschikt.

Terwijl de ontwikkeling van duinvolumes en strandhellingen gecorreleerd blijken te zijn kan het zo zijn dat beiden worden bepaald door de sediment uitwisseling in kustdwarse richting tussen de brandingszone en het droge strand. Om deze reden is sediment uitwisseling vanuit de brandingzone naar het droge strand erg interessant. Aanvullend ten opzichte van de voorgaande jaarlijkse dataset zijn er morfologische strandprofielen geanalyseerd die met maandelijkse intervallen zijn verzameld. Deze datasets maken het mogelijk om morfologische activiteit op maandelijkse tijdschaal te analyseren. Er zijn data gebruikt die zijn verzameld op drie verschillende locaties; 1. Vlugtenburg (NL) 2. Noordwijk (NL) 3. Narrabeen (AU). Op deze locaties zijn de gemeten morfologische veranderingen op maandelijkse tijdschaal door marine processen significant groter dan door eolische processen. In hoeverre marine processen morfologische ontwikkelingen beïnvloeden verandert in tijd en

ruimte. Geen significante erosie of aanzanding van het droge strand is gemeten en dus zijn transport gradiënten door eolisch transport op het droge strand beperkt. Vanwege deze beperkte morfologische activiteit op het droge strand is het onwaarschijnlijk dat dit droge strand een grote zandbron is voor eolische transportprocessen. Een grote bron van sediment kent een vermoedelijke oorsprong in het intergetijdengebied. Op basis hiervan is een model voor een ruimtelijke verdeling van zandaanbod voorgesteld.

Een nieuw model om sediment transporten te schatten in aanbod gelimiteerde situaties waarbij gebruikt wordt gemaakt van het eerdergenoemde ruimtelijke model is gepresenteerd. In dit 1D lineaire advectionmodel worden sedimenttransporten berekend aan de hand van conventionele transportformuleringen terwijl er expliciet rekening wordt gehouden met aanbod beperkingen. Het model verklaart verschillende waarnemingen zoals de aanwezigheid van een fetch effect, discontinuïteiten in sediment transport en de dominante rol van aanbod limitaties. Een beperkt sediment aanbod kan een fetch effect tot gevolg hebben waarbij het sediment transport toeneemt in de richting van de wind. De lengte van dit fetch effect (kritieke fetch lengte) is afhankelijk van de mate van zandaanbod. Wanneer het zandaanbod beperkt is correleert de variabiliteit van het sediment transport maar in kleine mate met traditionele sedimenttransportformuleringen. Als een alternatief is er een lineaire relatie tussen wind en sedimenttransporthoeveelheden geadopteerd. De parameters van deze lineaire relatie geven informatie over de mate van sediment aanbod. Veld data die zijn verzameld in aanbod gelimiteerde situaties (stranden) ondersteunen dat een lineair verband tussen windsnelheid en sedimenttransport bestaat en dat deze mogelijk wordt bepaald door de mate van zandaanbod. Om het model toe te passen in toekomstige modellen om eolisch sedimenttransport te voorspellen moeten drempelsnelheden voor transport worden meegenomen en het sedimentaanbod moet een gegeven zijn. Kennis op het gebied van de mate van sedimentaanbod is van belang maar momenteel beperkt.

Om de relatie tussen windsnelheid, sedimentaanbod en eolisch transport verder te testen is er extra veld data verzameld. Windsnelheden en sedimenttransporten zijn gemeten gedurende 5 dagen op het strand bij Vlugtenburg in Nederland. De variabiliteit in de gemeten transporten is sterk bepaald door het getijdeniveau. Dit impliceert een expliciete link tussen eolisch sedimenttransport en het intergetijdengebied. Gedurende de metingen was het sedimentaanbod in het intergetijdengebied van grotere orde dan op het droge strand. Volgens fetch theorieën neemt de hoeveelheid sedimenttransport toe in de richting van de wind tot de transportcapaciteit is bereikt na een kritieke fetchafstand. Ondanks dat er fetch achtige effecten zijn gemeten kunnen conventionele fetchtheorieën niet worden bevestigd omdat het onduidelijk is of er een wind gedreven transportcapaciteit is bereikt. Als er geen wind gedreven transportcapaciteit wordt bereikt dan volgt de relatie tussen wind en sedimenttransport de traditionele formuleringen voor sedimenttransport niet. Het eerder voorgestelde 1D lineaire model, waarin een kleine aanpassing is gedaan, past succesvol op de gemeten data. De daarmee afgeleide model parameters zijn de drempelwaarde van de windsnelheid voor transport en de gemiddelde sedimentconcentratie. De afgeleide drempelwaarden voor transport laten weinig

variatie in tijd en ruimte zien waar de gemiddelde sedimentconcentraties sterk variëren in tijd en ruimte. Dit suggereert mogelijk dat gedurende dit experiment de variabiliteit in transport niet worden veroorzaakt door een variërende drempelsnelheid voor transport.

De belangrijkste conclusies van deze studie zijn dat in het geval van een strand-situatie het systeem van eolisch transport aanbod gelimiteerd is. Dit wordt ondersteund door het gebrek aan correlatie tussen veranderingen van duin volume en wind condities op de jaarlijkse tijdschaal, het verschil in morfologische activiteit in het kustdwarse profiel op de maandelijkse tijdschaal, de door een 1D model afgeleide lineaire relatie tussen sediment transport en windsnelheid en het beperkte verband tussen gemeten windsnelheden en sedimenttransporten op de procestijdschaal. Een belangrijke parameter die de mate van sedimenttransport bepaald in een aanbodgelimiteerd systeem is de mate van aanbod en deze kan variëren in tijd en ruimte. Dit wordt ondersteund door de relatie tussen strandhelling en de mate van duinaangroei op de jaarlijkse tijdschaal, de gemodelleerde sedimenttransporthoeveelheden waarbij de mate van aanbod wordt gevarieerd en de grote correlatie tussen gemeten transporten en getijdeniveau. Huidige kennis over de mate van zandaanbod is nog steeds beperkt en is mogelijk een interessant onderwerp voor toekomstig onderzoek.





## Abstract

The aim of this study is to identify and quantify the processes governing the development of coastal dunes at the engineering timescale. This study is part of the Building with Nature project. Within the Building with Nature project it is intended to utilize natural processes and provide opportunities for nature while realizing coastal infrastructure.

To gain initial insight in how dune building processes govern dune behavior on the yearly to decadal timescales, the Dutch JARKUS dataset is analyzed. The JARKUS dataset contains measured morphological profiles along the entire Dutch coast since 1965 to date of which a 'Holland coast' subset is used. From this dataset, dune volume changes are extracted and used as a parameter representing dune behavior. The measurements of dune volume changes over decadal timescales often show a positive linear trend with respect to time. Therefore a constant dune growth rate in time can be assumed at specific locations. This might offer possibilities for predicting dune behavior. The magnitude of the measured linear dune growth in time varies in space in alongshore direction. Spatial and temporal variations in dune volume changes are derived and have been correlated with wind and beach slope. No correlation between dune behavior and wind forcing is found on the yearly to decadal timescale at any of the considered locations. It seems therefore unlikely that the use of models predicting dune behavior on the decadal timescale with wind as the main (forcing) parameter will lead to satisfying results. The dune volume changes are found to depend significantly on beach slope. Beach slope could represent a supply limiting parameter. This suggests that, at the considered sites, dune behavior is governed by sediment supply rather than wind forcing. Therefore a model for dune development where supply plays a significant role seems appropriate.

While the development of dune volume changes and beach slopes appear to be correlated, cross shore sediment supply from the surf zone to the beach/dune system could influence both beach slope and dune volume changes. Therefore sediment supply from the surf zone towards the aeolian beach is of particular interest. In addition to the analysis of annual data, morphological beach profiles collected at monthly intervals are analyzed. These datasets allow morphological activity to be analyzed on a monthly timescale. Data collected at three sites are considered; 1. Vlughtenburg (NL) 2. Noordwijk (NL) 3. Narrabeen (AU). At these study sites, the measured morphological changes on monthly timescales due to marine processes are significantly larger than morphological changes due to aeolian processes. The extent of the marine processes' influences varies in time and space and largely determine morphological development. No significant erosion or sedimentation due to aeolian transport is measured at the upper beach. Therefore, only small transport gradients related to aeolian transports occur at the upper beach. Due to this limited morphological activity at the upper beach, the upper beach is unlikely to function as a significant source area for aeolian transport processes. A large sediment supply to the aeolian system is expected to originate from the intertidal zone. Based on the above, a spatial distribution of sediment

supply is proposed which can be used for modeling purposes.

Using this spatial arrangement of supply, A new model to estimate aeolian sediment transport rates in supply limited situations is presented. In the 1D linear advection model sediment transport rates are calculated as a function of wind using traditional sediment transport formulations where a limited sediment supply magnitude is explicitly taken into account. The model successfully explains several physical observations such as the occurrence of a fetch effect, intermittency in sediment transport and the dominant role of supply magnitude. Limited supply can cause fetch effects where sediment transport rates increase in the direction of the wind. The length of these fetch effects (critical fetch) is dependent on supply magnitude. When supply is limited, variability in sediment transport rates show limited correlation with traditional sediment transport formulations. Alternatively, a linear relationship between wind and sediment transport could be adopted. The parameters of the fitted linear relationship provides information on source magnitude. Field data collected at supply limited locations (beaches) provide evidence that linear relationships between wind and transport rates can also be found in the field and are possibly governed by supply magnitude. For the model to be applicable in future models predicting aeolian sediment transport, threshold velocities should be accounted for and supply magnitudes should be a given. Gaining knowledge on the supply magnitude is of major concern since current quantitative knowledge on sediment supply is limited.

To further test relations between wind velocity, sediment supply and aeolian transport, field data is collected. Data of wind velocity and sediment transport rates are collected during a 5 day field campaign at Vlugtenburg beach located in The Netherlands. The variability in measured transports is found to be governed by the tide elevation to a large extent. This indicates an explicit link between aeolian sediment transport rates and the intertidal area. During the measurements, the sediment supply in the intertidal area is considered of larger order of magnitude than at the upper beach. According to fetch theories, sediment transport increases in the direction of the wind until wind-driven transport capacity is reached at critical fetch distance. While fetch alike effects are measured, conventional fetch theories are not confirmed because it is unclear if a wind driven transport capacity is reached. If wind driven transport capacity is not reached, the relationship between wind speed and sediment transport rates does not follow traditional formulations. The proposed 1D linear model, slightly adapted to be applicable to this field data, is used to successfully fit the measured data. The fitting parameters of the linear model are the threshold velocity for transport and the average sediment concentration. For this particular dataset the derived threshold velocities show limited spatial and temporal variability but the derived averaged sediment concentrations show significant spatial and temporal variability. This could suggests that during the experiment the variability in measured sediment transport is not governed by the variability in threshold velocity for transport.

The main conclusions of this study are that in beach situations, the system of aeolian sediment transport can be supply limited. This is shown by the lack of correlation between dune volume changes and wind conditions on the annual

timescale, the difference in morphological activity in the cross shore profile on the monthly timescale, the derived linear relation between sediment transport and wind speed using the 1D model and the limited correlation between measured aeolian sediment transport rates and wind speed on the process timescale. An important governing parameter of aeolian sediment transport rates in a supply limited system is the supply magnitude which can vary in space and time. This is reflected by the dependence between beach slope and dune volume changes on the annual timescale, the modeled sediment transport rates using varying source magnitude and the large correlation between the measured sediment transport rates and tide elevation. Current knowledge on the quantification of sediment supply remains limited and is an interesting topic for further research.



# Contents

<b>1</b>	<b>Introduction</b>	<b>1</b>
1.1	Motivation . . . . .	1
1.2	Approach . . . . .	2
1.3	Reader . . . . .	2
<b>2</b>	<b>Measured decadal dune behavior.</b>	<b>3</b>
2.1	Introduction . . . . .	4
2.1.1	Background on aeolian transport . . . . .	5
2.2	Data . . . . .	9
2.2.1	JARKUS dataset . . . . .	9
2.2.2	Wind data and drift potentials . . . . .	13
2.2.3	Effects of marine processes . . . . .	15
2.2.4	Nourishments . . . . .	18
2.3	Methodology . . . . .	18
2.4	Analysis . . . . .	20
2.4.1	Linear trends in Dune Volumes . . . . .	20
2.4.2	Autocorrelations in time . . . . .	20
2.4.3	Autocorrelation in Space . . . . .	23
2.4.4	Cross correlations . . . . .	23
2.5	Discussion . . . . .	32
2.5.1	Modeling dune behavior . . . . .	32
2.5.2	Balancing erosion vs. accretion . . . . .	33
2.5.3	Timescale of erosion and accretion . . . . .	33
2.5.4	Sediment availability, beach slope and Dune volume change . . . . .	33
2.6	Conclusions . . . . .	34
<b>3</b>	<b>Seasonal development of the cross shore profile</b>	<b>37</b>
3.1	Introduction . . . . .	38
3.1.1	Cross shore interaction between foreshore, beach and dune . . . . .	39
3.1.2	Chapters Aim . . . . .	40
3.2	Field sites . . . . .	40
3.2.1	Vlugtenburg Beach . . . . .	40
3.2.2	Noordwijk . . . . .	43
3.2.3	Narrabeen . . . . .	45
3.3	Analysis & Results . . . . .	47
3.3.1	Defining a discrete separation point between the marine and aeolian zone . . . . .	48
3.3.2	Separation point and profile development . . . . .	51
3.4	Discussion . . . . .	52
3.4.1	Marine-, aeolian processes and beach morphology . . . . .	52
3.4.2	The intertidal zone as source area for aeolian transport . . . . .	52
3.4.3	A model for spatial zonation . . . . .	55
3.5	Conclusions . . . . .	55

<b>4</b>	<b>A numerical implementation of processes.</b>	<b>57</b>
4.1	Introduction . . . . .	58
4.2	Model concept . . . . .	60
4.3	Results . . . . .	64
4.3.1	Test Case I; Continuous wind . . . . .	64
4.3.2	Test Case II; Increasing and decreasing winds . . . . .	65
4.3.3	Test Case III; Random wind (short term variability) . . . . .	66
4.4	Comparison with field data . . . . .	70
4.5	Discussion . . . . .	73
4.5.1	Supply limited vs Abundant supply . . . . .	73
4.5.2	Variability in Supply . . . . .	73
4.5.3	Threshold velocity for transport . . . . .	75
4.5.4	Fetch effects . . . . .	75
4.5.5	Implications for future modeling . . . . .	75
4.6	Conclusions . . . . .	76
<b>5</b>	<b>Measured aeolian sediment transport processes.</b>	<b>77</b>
5.1	Introduction . . . . .	78
5.2	Measurement location and experimental design . . . . .	80
5.3	Results . . . . .	82
5.3.1	Temporal variability of aggregated parameters . . . . .	83
5.3.2	Relation between Wind speed and sediment transport rates . . . . .	83
5.3.3	Spatial gradients in transport. . . . .	90
5.4	Discussion . . . . .	93
5.4.1	Measured cross shore gradients and the role of supply . . . . .	93
5.4.2	The Fetch effect . . . . .	95
5.4.3	Transport capacity vs Supply limitations . . . . .	95
5.5	Conclusions . . . . .	96
<b>6</b>	<b>Conclusions and Perspective</b>	<b>99</b>
6.1	Conclusions . . . . .	99
6.1.1	Measured morphologic behavior along the Holland coast . . . . .	99
6.1.2	Seasonal development of the cross shore profile . . . . .	100
6.1.3	A numerical implementation of processes . . . . .	101
6.1.4	Measured aeolian sediment transport processes . . . . .	101
6.2	Perspective . . . . .	102
6.2.1	Research on aeolian sediment transport in coastal environments . . . . .	103
6.2.2	Building with nature . . . . .	103
	<b>References</b>	<b>105</b>
	<b>CV and Publications</b>	<b>111</b>
	<b>Acknowledgments</b>	<b>115</b>

# Chapter 1

## Introduction

### *Building with Nature and aeolian transport*

#### 1.1 Motivation

The research presented in this thesis is driven by the Building with Nature philosophy (Waterman, 2010). The aim of Building with Nature is to utilize natural processes and provide opportunities for nature while realizing coastal infrastructure. Recently, Building with Nature type strategies to manage the development of coastal situations are gaining popularity. This popularity could be attributed to the increase of economic pressure on coastal regions and the need for a multidisciplinary approach towards the implementation of coastal development. Within this multidisciplinary approach it is aimed to combine social economic interests with the natural development of a coastal system during and after construction of coastal infrastructure. Moreover, with natural processes doing part of the work, building with nature type solutions could provide a cost efficient alternative in the realisation of coastal infrastructure.

Along the Holland coast, much coastal infrastructure and coastal maintenance is present. Coastal dunes are maintained while they provide safety against flooding for the lower lying hinterland. This maintenance at the Holland coast generally involves sand nourishments at the dunes, beach and foreshore. Occasionally, these sand nourishments are applied in combination with the planting of vegetation, stabilizing natural dynamics of the dune system. In 1990, the Dutch Government adopted the national policy of "Dynamic Preservation" which aimed at a sustainable preservation of safety against flooding, as well as values and functions in the dune area (Ministry of transport and Public Works, 1990). As a result, sand nourishments were increased and concentrated at the beach and foreshore rather than nourishing the foredunes directly. Nourishing the beach and shoreface has the advantage that it is relatively easy in terms of logistics but also the natural dynamics of the dune area are not directly influenced. After the implementation of the 1990's Dynamic Preservation act, studies have shown that dunes grow due to increased sand input and increased aeolian dynamics (Arens et al., 2012). However the interaction between shoreface, beach and dunes remains poorly understood.

The framework of this thesis is defined within the overarching objective of Building with Nature case HK; to develop a perspective for the sustainable development of the coast from the Hook of Holland up to Den Helder, over a timescale of 50 to 100 years (see [www.ecoshape.nl](http://www.ecoshape.nl) for details). The aim of this thesis is more specifically: *to identify and quantify the processes governing the development of coastal foredunes at the engineering timescale (5-50 yrs).*

## 1.2 Approach

The dynamics of coastal foredunes at the engineering timescale are characterized by interchanging periods of erosion and growth. While coastal foredunes erode mainly due to marine forces, the foredunes grow mainly due to aeolian processes. Due to the importance of dune erosion as a failing mechanism of the protective function provided by dunes, much research focuses on predicting dune erosion. As a result, quantitative tools to predict dune erosion are available (see for instance den Heijer et al. (2012) and references therein). The capability to quantitatively predict dune growth due to aeolian processes is less well established and the availability of predictive tools is limited. While several models for predicting aeolian sediment transport in desert type situations are available, the complex physics of beach situations are less well understood. Especially the quantitative influence of supply limitations towards the aeolian system is relatively unknown.

Due to the lack of quantitative knowledge on dune growth due to aeolian processes, the dynamics of dunes as a function of both growth and erosion are difficult to predict. Moreover, where datasets on the temporal and spatial development of dunes due to combined growth and erosion are available (e.g. JARKUS), measured behavior is difficult to reproduce.

This thesis' overall aim is to "identify and quantify the processes governing the development of coastal dunes at the engineering timescale" by analyzing collected morphological data, analyzing collected process data and formulating a conceptual model. While all chapters contribute to this aim, chapter specific aims are further specified in each chapter's starting section.

## 1.3 Reader

This thesis is build around three article manuscripts of which one is currently accepted for publication. These article manuscript are presented in Chapters 2, 4 and 5 and can be read separately. In Chapter 2, decadal dune behavior is analyzed using a unique 40 year dataset containing yearly measured coastal profiles along the entire Dutch coast. In Chapter 3 three morphological datasets which cover a shorter timescale than the data presented in Chapter 2 are analyzed to cover event based behavior of the beach. Going more into the details of aeolian sediment transport, Chapter 4 describes a numerical model which is designed to model the supply limited conditions which are typically found on beaches. In Chapter 5 field data is presented where it is aimed to quantify model parameters fitting traditional and new sediment transport formulations. Chapters 4 and 5 complement each other where data is used to validate the model concept and the numerical model is used as a tool to analyze the measurement data.

Chapters 2, 3, 4 and 5 each start with a separate section which contains the highlights of the chapter. These highlights include specific aims and the lessons learned relevant for the Building with Nature design guidelines. In Chapter 6, all conclusions of the previous Chapters are summed up and a perspective is given.



## Chapter 2

# Dune Behavior and Aeolian Transport on Decadal Timescales

### *A Statistical Analysis using Jarkus Data*

---

This chapter is published in Coastal Engineering (de Vries, S., Southgate, H., Kanning, W., Ranasinghe, R., 2012. Dune behavior and aeolian transport on decadal timescales. Coastal Engineering 67 (0), 41–53). No changes have been made with respect to the CE publication other than this text.

The chapter aims to gain insight in how dune building processes govern dune behavior on the yearly to decadal timescale. Therefore, the Dutch JARKUS dataset is used to analyze yearly to decadal dune behavior where dune volume changes are taken as a measurable parameter of dune behavior. Spatial and temporal variability in dune behavior along the Holland coast is correlated with wind conditions and beach slope.

Lessons learned:

- Measurements of dune volume changes over decadal timescales often show a positive linear trend. Therefore a constant dune growth could be assumed for specific profiles. This might simplify possibilities of predicting dune behavior.
  - The magnitude of the measured linear dune behavior in time varies in space in alongshore direction. Spatial and temporal variation in dune volume changes can easily be derived and correlated with parameters of interest. This chapter focusses on wind conditions and beach slope but many other parameters of interest are possible to derive from the JARKUS dataset.
  - No correlation between dune behavior and wind forcing is found on the yearly to decadal timescale at any of the considered locations. Therefore the use of models where wind is the main forcing, predicting dune behavior on the decadal timescale, should be reconsidered.
  - The dune volume changes are found to depend significantly on beach slope. Beach slope could represent a supply limiting parameter which suggests that, at the considered site, dune behavior is governed by sediment supply rather than wind forcing.
  - Annually averaged erosion volumes as a result of extreme marine events are found to be of similar order as the aeolian growth along the considered Hollands coast.
- 
-

## 2.1 Introduction

At many places dunes function as a natural barrier protecting coasts from flooding during storms. Opposed to sea dikes, dunes have the advantage of being built by naturally occurring processes and are in favor of recreational use. The disadvantage is that dune systems are dynamic and the safety level provided by dunes is variable in time. Therefore significant management and frequent safety assessments are needed.

Traditional management is often based on reactive strategies where dunes are stabilized and/or reinforced when certain safety criteria are not met. However, recent coastal management strategies explore the possibilities of how to use natural processes in a proactive way to build, maintain and reinforce dunes and the accompanying protective function (see for example Aarninkhof et al. (2010)). This approach is driven by the challenging possibility of integrating coastal protection and natural development in an interdisciplinary coastal management strategy (Building with Nature; Waterman (2010)).

The development of coastal dunes on decadal timescales is a result of erosive and accretive processes. In some cases (such as the Dutch case), nourishments and management interventions also influence the development of coastal dunes. The net result determines the dunes to be either in an erosive or accretive state. Previous publications on decadal dune behavior describe dune behavior in terms of coastal retreat in meters per year (Pye and Blott, 2008; Ruessink and Jeuken, 2002) or morphologic variability via EOF analysis (Bochev-van der Burgh et al., 2011). In this paper we choose dune volume changes per year as a parameter to describe dune behavior because it gives direct and quantitative information on accretion and erosion rates.

Erosive processes are commonly linked to storm events where marine processes erode the dunes. Over the years, a lot of research has been invested in predicting dune erosion under storm (or even super storm) conditions to assess coastal safety (e.g. van de Graaff (1977); Kriebel and Dean (1985); Vellinga (1986); Larson et al. (2004); Callaghan et al. (2008); den Heijer et al. (2012)). However, dunes are only affected by marine processes if water levels are high enough to reach the dunes and wave conditions strong enough to erode the dunes. Erosive (storm) periods are separated by much longer periods where water does not reach the dunes and only aeolian processes govern dune development. When sufficient (onshore) wind occurs and sediment is available for transport, sediment is transported from the beach towards the dunes leading to an increase of dune volume.

Sufficient winds needed for sediment transport are typically in the order of  $> 5-10$  m/s (Arens, 1996) which frequently occur during moderate conditions. Extreme conditions with larger wind speeds usually coincide with precipitation which stops aeolian transport because the sand surface becomes wet and non erodible. Therefore, the cumulative effect of aeolian sediment transport is largely governed by relatively mild conditions instead of rare extreme conditions (Arens, 1996; Wolman and Miller, 1960; Jungerius et al., 1991). It is unclear however to what extent aeolian recovery is able to compensate for the event based marine erosion.

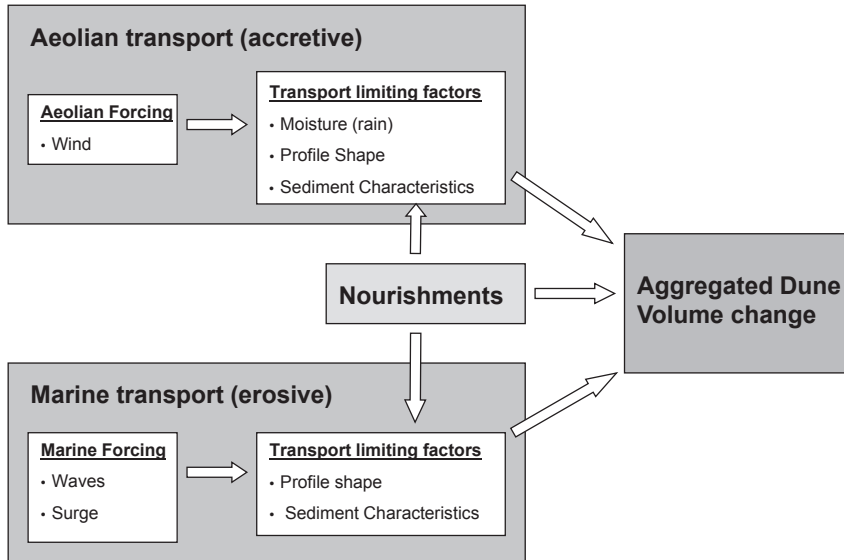


Figure 2.1: Conceptual representation of dune volume change aggregated over time. Accretive periods are alternated with erosive periods. Nourishments directly affects the dune volume changes as well as transport limiting factors.

Figure 2.1 shows a summary of processes influencing dune volume changes. Recent progress has been made predicting aggregated coastal behavior within the framework of climate change where both erosive and accretive processes are considered (Ranasinghe et al., 2011). However, quantitative knowledge on dune building processes is still limited.

This paper aims to gain insight in the aggregated effects of wind speed and beach slope on annual aeolian sediment transport quantities and their effect on dune behavior on the yearly to decadal timescale. This timescale is of interest as it represents the most relevant engineering timescale for coastline development and management for which data are available.

In the next Section, additional background on aeolian transport is discussed. Then the Dutch JARKUS dataset is used for statistical analysis for which the aim is to find spatial and temporal variations in dune behavior and how these correlate with wind conditions and beach slope. The main focus is aeolian transport but marine influences are discussed where appropriate.

### 2.1.1 Background on aeolian transport

Literature on aeolian sediment transport in desert environments is abundant starting with the pioneering work of Bagnold (1954). He identified the main factors

influencing aeolian transport rates ( $q$ ) as the grain diameter ( $d$ ) relative to a reference grain diameter ( $D$ ), the air density ( $\rho$ ), the gravitational acceleration ( $g$ ), the drag velocity ( $u_*$ ) and an empirical coefficient ( $C_b$ ).

$$q = C_b \frac{\rho}{g} \sqrt{\frac{d}{D}} (u_*)^3 \quad (2.1)$$

This work was followed by Kawamura (1951) who slightly reformulated the equation and added a threshold drag velocity ( $u_{*t}$ ).

$$q = C_k \frac{\rho}{g} (u_* - u_{*t})(u_* + u_{*t})^2 \quad (2.2)$$

The threshold drag velocity is dependent on the grain diameter ( $D$ ), the gravitational acceleration ( $g$ ), the density of the sand grains ( $\rho_s$ ), the density of the air ( $\rho$ ) and an empirical coefficient ( $A_b$ ) (Bagnold, 1954).

$$u_{*t} = A_b \sqrt{Dg(\rho_s - \rho)/\rho} \quad (2.3)$$

Over the years these principles have been followed by many researchers where measuring, deriving and defining appropriate  $C_b$  and  $A_b$  values for various conditions was of interest.

These Bagnold type formulations generally assume conditions where all parameters in Equation 2.1 are considered constant in time except the wind speed. This makes the temporal variability in transport solely dependent on variability in wind speed.

On beaches, sediment transport is typically limited by additional time varying effects (Davidson-Arnott and Law, 1990). Threshold drag velocity ( $u_{*t}$ ) can vary in time as a function of (amongst others) moisture content (Davidson-Arnott et al., 2008) and beach slope (Iversen and Rasmussen, 1994). On beaches, both moisture content and beach slope are very variable in time as a result of tides and varying meteorological and morphological conditions. As a result sediment transport rates ( $q$ ) may vary in time independently from wind conditions.

Additionally, the amount of aeolian sediment transport ( $q$ ) is often assumed to depend on fetch length ( $F$ ) (see for instance Bauer et al. (2009) or Delgado-Fernandez (2010) for an overview). The fetch effect states that longer fetch lengths lead to higher transport under given wind conditions until a certain limit is reached. This limit is the critical fetch ( $F_c$ ) where wind reaches transport saturation ( $q_m$ ), see Figure 2.2. While winds are directly or obliquely onshore on a beach, the maximum available fetch distance ( $F_m$ ) is limited by beach width ( $W$ ). When the maximum available fetch is smaller than the critical fetch, aeolian sediment transport towards the dunes is limited due to beach width. Therefore variable beach width might induce variable sediment transport rates towards the dunes if the beach width is less than the critical fetch.

Values of critical fetch measured in the field vary from 10-40 m (Davidson-Arnott and Law, 1990) up to over 200m (Davidson-Arnott et al., 2008). There have also been reports of field campaigns where no significant fetch effects are

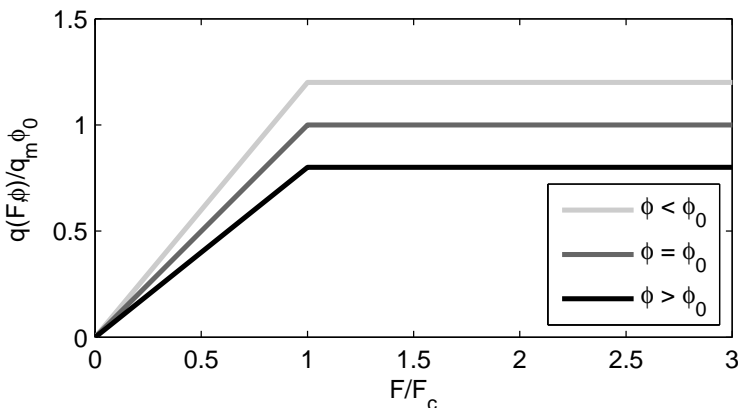


Figure 2.2: Conceptual representation of the fetch effect, where transport increases with increasing fetch towards a certain limit. Different lines show different bed slopes ( $\phi$ ) with respect to a reference bed slope ( $\phi_0$ ). Bed slopes influence the transport capacity where steeper slopes limit transport to a larger extent than milder slopes (Hardisty and Whitehouse, 1988). For the  $\phi_0 = 0$  case, reference is made to Bauer and Davidson-Arnott (2002) who suggests similar curves including a smoother transition between the increasing and stable transport.

measured (Jackson and Cooper, 1999; Lynch et al., 2008). The magnitude of the critical fetch length on the process scale has proven to be highly variable and dependent on wind speed (Davidson-Arnott and Law, 1990), surface moisture content (Davidson-Arnott et al., 2005) and the presence of lag deposits (van der Wal, 1998). Lynch et al. (2008) remark that under specific conditions, any of the mentioned variables controlling sediment transport can affect the critical fetch, influencing the distance required for the transport rate to reach a maximum value. While these variables influence the sediment available for transport it could be argued that their influence represent a supply effect rather than a fetch effect (Lynch et al., 2008). This complicates matters since it is not always possible to isolate the measured fetch effects from transport limiting variables. Additionally the actual fetch is highly dependent on wind direction since oblique winds result in a larger distance between waterline and dune in the direction of the wind (Bauer and Davidson-Arnott, 2002).

Another transport limiting process is the effect of surface slope. Several authors have investigated the effects of surface slope on sediment transport for both aeolian (Iversen and Rasmussen, 1994; Hardisty and Whitehouse, 1988) and marine applications (Allen, 1982; Bagnold, 1973). Much of this work is based on theory derived from observations in wind tunnels or observations in flumes. For the present work, the empirical work of Hardisty and Whitehouse (1988) is adopted. While the results of their field observations deviate somewhat from the laboratory studies (possibly due to scale effects), the concept is easily applicable and it

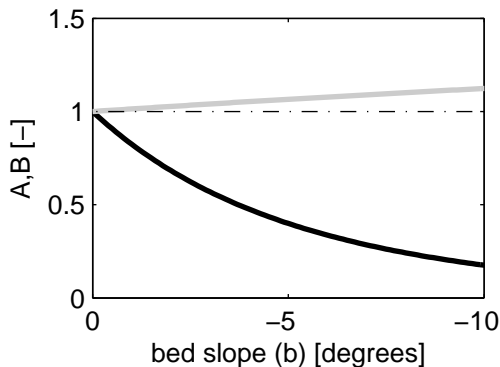


Figure 2.3: Constants A in black and B in gray as a function of bed slope given by Hardisty and Whitehouse (1988). Negative slopes indicate upslope values.

connects to our field oriented analysis.

On the process scale, the bed slope influences two parameters: (1) the transport capacity, (2) the threshold velocity needed for sediment motion. Limiting either or both of these parameters on the process scale could result in significant smaller cumulative (aggregated) transports.

Hardisty and Whitehouse (1988) measured the influence of bed slope on the threshold wind velocity and rate of transport for desert dunes. The slopes they analyzed were between -30 and +30 degrees. Hardisty and Whitehouse (1988) use the Bagnold type equation:

$$q = k(u^2 - u_{t0}^2)u \quad (2.4)$$

where  $u$  represents wind speed,  $u_{t0}$  threshold wind speed with bed slope ( $b = 0$ ) and  $k$  is a constant. They convert Equation 2.4 to introduce slope effects to

$$q = Ak(u^2 - B^2u_{t0}^2)u \quad (2.5)$$

where

$$A = \left[ \frac{\tan i}{\tan i - \tan b} \right]^7 \quad (2.6)$$

and

$$B = \sqrt{\frac{\tan i - \tan b}{\tan i} \cos b} \quad (2.7)$$

Constants  $A$  and  $B$  are empirical functions of internal friction of the sediment ( $i$ ) and the bed slope ( $b$ ) alone. As a result Bagnold type sediment transport equations can be corrected for slope using separate factors for threshold velocity ( $B$ ) and total transport ( $A$ ).

In Figure 2.3 it is shown how constants A and B vary for different slopes according to Hardisty and Whitehouse (1988). Where bed slopes increase from 0 to only

2 degrees, threshold velocities increase by a factor  $B = 1.03$  and total transport decreases by a factor  $A = 0.68$ . The overall effect is a decrease in transport rates of the order of 30-40 %. While the theory presented is largely empirical based on measurements in desert environments, it lacks physical argumentation. However, few (field) alternatives with respect to coastal environments are available and at this stage it is used in an indicative manner only.

For wind velocities exceeding the threshold and perpendicular to the beach, the conceptual influence of the beach slope on the transport capacity combined with fetch effects is illustrated in Figure 2.2. Looking at this Figure it is stressed that there are two separate causes of variability. One is due to fetch effects when the critical fetch is larger than the actual fetch (Bauer and Davidson-Arnott, 2002). The other is due to varying transport capacity which is related to bed slope effects. We have initially assumed that bed slope does not influence the fetch effect other than by a proportional reduction of the sediment transport capacity, shown in Figure 2.2. While it remains unclear from the literature if bed slope influences the fetch effect, the method presented in Figure 2.2 is based on combining the beach slope and fetch effects assuming they act independently of each other. This assumption allows analyzing variability in transport due to slope effects independently from beach width related fetch effects.

Whereas the beach slope only represents the bed slope in the direction perpendicular to the coast, wind directions vary in nature. However, since wind speed is considered a vector, beach slope could be expected to have some influence on aeolian sediment transport quantities if any landward component of wind direction is present.

With time dependent transport limiting parameters, sedimentary systems on beaches are more complex compared to deserts and as a result more difficult to model. This is reflected by the consistent over-prediction of sediment transport rates at the coast by most wind driven sediment transport models (Sherman et al., 1998).

In the next sections we use collected data and statistical techniques to gather evidence of parameters controlling annual dune volume changes. The parameters discussed are beach slope, wind speed and water levels.

## 2.2 Data

### 2.2.1 JARKUS dataset

The morphological dataset used is part of the Dutch JAarlijkse KUSmeting (JARKUS). This dataset consists of yearly profile measurements along the entire Dutch coast since 1965 with an alongshore spacing of approximately 250 m. The data covers beach, dune and foreshore. For this study we specifically focus on the sub aerial data of the Holland coast where elevation measurements are taken at 5 m intervals along the transect in the cross shore direction (Southgate, 2011)

The Holland coast is a subsection of the Dutch coast and extends for 117 km

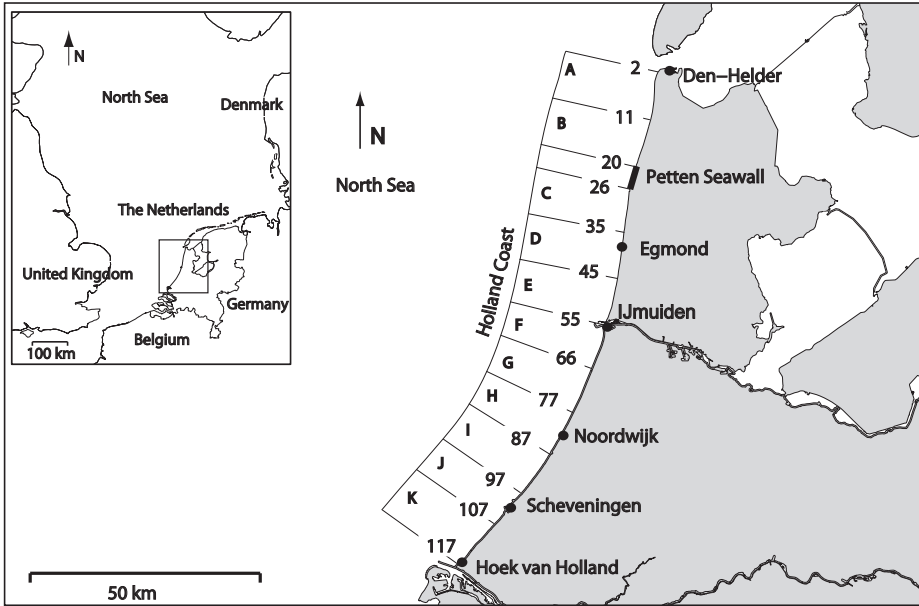


Figure 2.4: Overview of the Holland coast. Numbers indicate alongshore kilometers with respect to the most northern point of the Holland coast. Sub-areas for analysis are shown together with the Petten sea wall and the harbors of IJmuiden and Scheveningen.

uninterrupted by tidal inlets. The north side is bordered by a tidal inlet and the south side by the large harbor moles at Hoek van Holland. There are some man-made features, namely the seawall near Petten and the harbor inlets at IJmuiden and Scheveningen. Figure 2.4 shows the measurement area.

During the period of data gathering the measurements techniques measuring sub aerial topography have changed. See Bochev-van der Burgh et al. (2011) and references therein for a description of the data gathering techniques including accuracies. For the current work it is important to mention that the early leveling (before 1977) has a fundamental limitation for calculating yearly budgets with respect to the later stereo photogrammetry (from 1977) and laser altimetry (from 1996 to date). The later measurement techniques are capable of measuring the entire Holland coast in a relative short time. Leveling is more labor intensive taking almost the entire year to measure the Dutch coast. This variability in measurement time creates an unwanted bias when extracting year to year sediment budgets. For this reason we limit the analysis to years after 1980. The accuracy of the measurements after 1980 is about 0.1 m in vertical direction (Bochev-van der Burgh et al., 2011). For additional descriptions of the dataset see also Southgate (2011) and Wijnberg and Terwindt (1995).



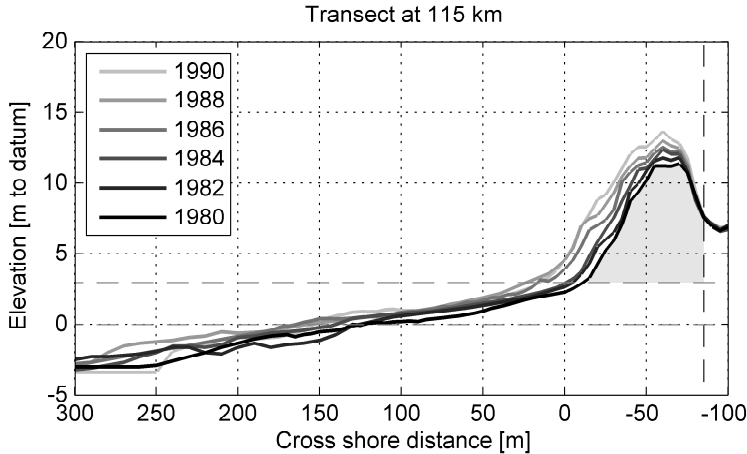


Figure 2.5: Example of evolution of a growing dune volume in time. Dune volume is indicated by the gray area where the lower boundary is the +3m NAP line and the landward boundary the point where the vertical variability is lower than a certain threshold.

### Dune Volume (Changes)

For the dune volume ( $DV$ ) no general definition exists. Here we define the dune volume as the volume of sand above the dunefoot level until a certain landward limit. The dunefoot level along the Dutch coast is widely assumed to be +3 m NAP. NAP is the Dutch reference level (Normaal Amsterdams Peil) and is located around mean sea level. In early measurements along the Dutch coast the dunefoot was defined as the point where there was a visible break in slope between beach and dune, see for instance Van Straaten (1961). This position roughly corresponds to + 3 m NAP (Ruessink and Jeuken, 2002).

The landward limit is determined using a multiple year profile time series. For all profiles this limit is defined from where the vertical variability is negligible in the landward direction. The dune volume is defined as the volume enclosed by the sand surface, the +3 m NAP line and the landward point where variability is negligible. See Figure 2.5 for reference.

Absolute dune volumes are largely influenced by the landward reference point. However, considering the dune volume changes (where  $DVC = DV_t - DV_{t-1}$ ) the chosen landward reference is not of relevance. As a result annual dune volume changes of different profiles can be compared.

Figure 2.6 shows an overview of all Dune Volume change data available. de Vries et al. (2011a) compared a part of these extracted dune volume changes (period 1980-1990) from the JARKUS dataset to possible fetch effects but found only limited correlations. Moreover, their results did not support the critical fetch theory.

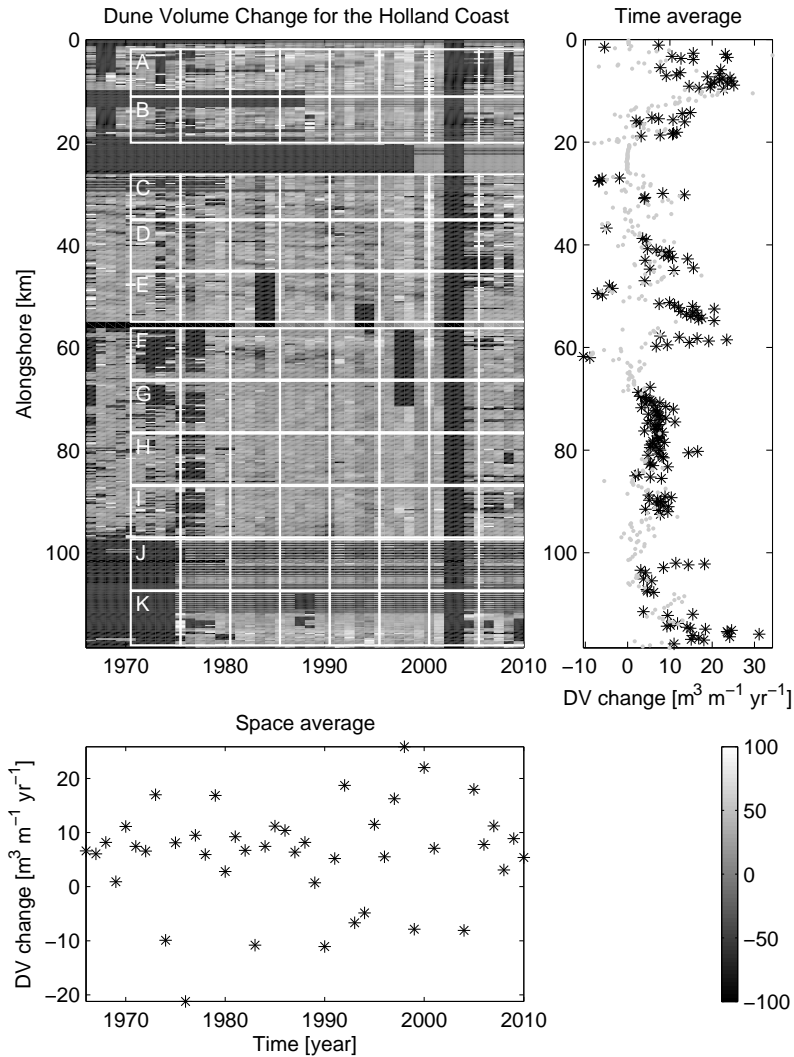


Figure 2.6: Top left panel gives a data overview of available data on dune volume changes along the Holland coast. Black sections (for instance around the Petten sea wall 20-26 km) indicate missing data. White squares indicate 11 sub-areas where data is grouped in 5 year intervals with a spatial extent of 10 km. Time averages are given in the right subplot where the black stars indicate the correlation coefficient, fitting a linear trend, is larger than 0.9 (see Section 2.4.1). Gray dots indicate smaller correlation coefficients. The space average is given in the bottom panel. Note that the bottom panel is similar to the bottom right panel of Figure 2.12.

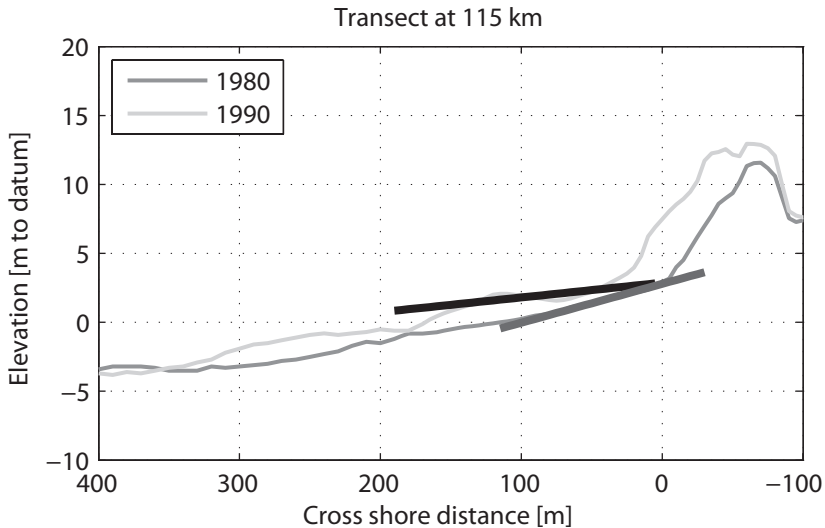


Figure 2.7: Calculated beach slopes for two years of an arbitrary transect. The beach slope is calculated as the best fit line through the beach area (from MWL until + 3 m NAP). The dark gray lines indicate the fitted lines for beach slopes at 1980 and 1990.

### Beach width and Beach gradient

The beach width is defined as the horizontal distance between the dune foot and the waterline. Various definitions of the waterline location have been used in the literature. In line with Ruessink and Jeuken (2002) we take the average between MHW and MLW. The beach gradient is the slope of the best fit line through the vertical elevation over the horizontal extent of the beach width. Figure 2.7 shows an example of the fitted beach slopes. The mean beach widths over all profiles is in the order of 80-90 m where the accompanying beach gradient is typically in the order of 1:15-1:20 m (bed slopes in the order of 2-4 degrees). Figure 2.8 gives an overview of the available beach gradient data. It is interesting to note that the variability in beach slope (and width) is very limited with the exception of the areas around harbors where relatively mild slopes are found.

### 2.2.2 Wind data and drift potentials

The Royal Dutch Meteorological Institute (KNMI) collects time series of meteorological data. Data collected at the wind station of IJmuiden is used. IJmuiden is located near the center of the Holland coast and the wind station is situated on the lighthouse of the old southern Harbor mole (practically next to the beach). The height of the wind sensor is +13 m NAP.

Figure 2.9 (top panel) shows the wind rose measured at the weather station

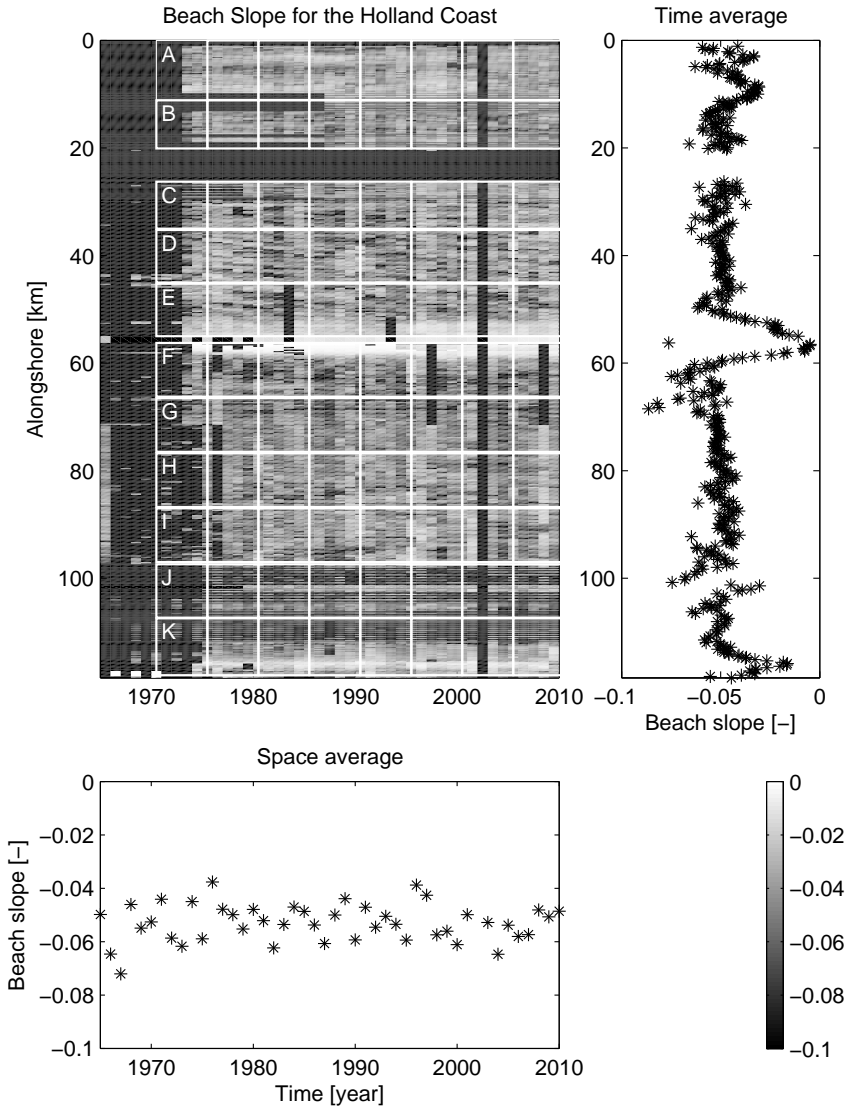


Figure 2.8: Top left panel gives a data overview of available data on beach slope along the Holland coast. Beach slopes are defined using the definition presented in Figure 2.7. Black sections (for instance around the Petten sea wall 20-26 km) indicate missing data. White squares indicate 11 sub-areas where data is grouped in 5 year intervals with a spatial extent of 10 km. Space and time averages are given in the bottom and right subplots respectively.

of IJmuiden. A large west to south-west component of the wind is measured over the period 1970-2010. West to south-west winds are oblique onshore with respect to the Holland coast.

Several authors have attempted to parameterize meteorological conditions with respect to coastal behavior and dune behavior in particular. Whenever dune erosion is of interest, several authors (Guillen et al., 1999; Ruessink and Jeuken, 2002) find correlations (to some significant degree) between defined annual "storminess parameters" and dunefoot behavior. These analyses are based on hydrodynamic processes alone.

Considering wind conditions, reference is made to Fryberger (1979). He calculated drift potentials (DP [ $\text{m}^3\text{m}^{-1}\text{year}^{-1}$ ]) by grouping wind data in a limited number (e.g. 16) of wind direction sectors. Generally, a Bagnold type 3<sup>rd</sup> power function is used to calculate sediment transport from the wind speed. Many (3<sup>rd</sup> power) alternatives are available (overviews are given in Sørensen (2004), Sherman et al. (1998), Iversen and Rasmussen (1999)). All Bagnold type formulations follow the 3<sup>rd</sup> power principle with respect to wind velocity resulting in similar values of wind induced variability of calculated transports. Since it connects to the earlier discussion on bed slope, we choose to use the equation proposed by Hardisty and Whitehouse (1988). For the purpose of analyzing variability of transports due to wind forcing only, we have simplified Equation 2.4 to

$$q_r \propto (u^2 - u_{t0}^2)u \quad (2.8)$$

where the absolute value of  $q_r$  is of minor interest and the focus is on the relative variability of  $q_r$  as a function of wind. Aggregating towards a yearly interval we use one wind speed and direction value representative for 1 day. This value is the vector mean wind speed (provided by KNMI) of that particular day. The Resultant Drift Potential (RDP) of a particular year is calculated to be the vector sum of all daily  $q_r$  values, and the Resultant Drift Direction (RDD) is the direction of that vector (assuming transport is in the same direction as the wind). As a result, the RDP describes the relative net sand transport over a certain period in the direction of the RDD. Figure 2.9 shows the yearly RDP and RDD for the period 1980-2010 derived from measurements at IJmuiden weather station (see also Figure 2.4). Figure 2.9 shows a varying RDP relative to the mean. Variations are roughly between 0.5 times to 2 times the mean. This implies that for some years the RPD is up to 4 times larger than other years. The mean RDD over all years is 256 degrees with a standard deviation of 8 degrees indicating that the RDD is fairly constant over the years.

### 2.2.3 Effects of marine processes

Dune volume changes are, besides aeolian processes, also influenced by marine erosion (Figure 2.1). In this section we present annual maximum water levels as one of the main drivers for marine erosion. Moreover, three documented events are discussed to illustrate the order of dune volume changes due to marine processes.

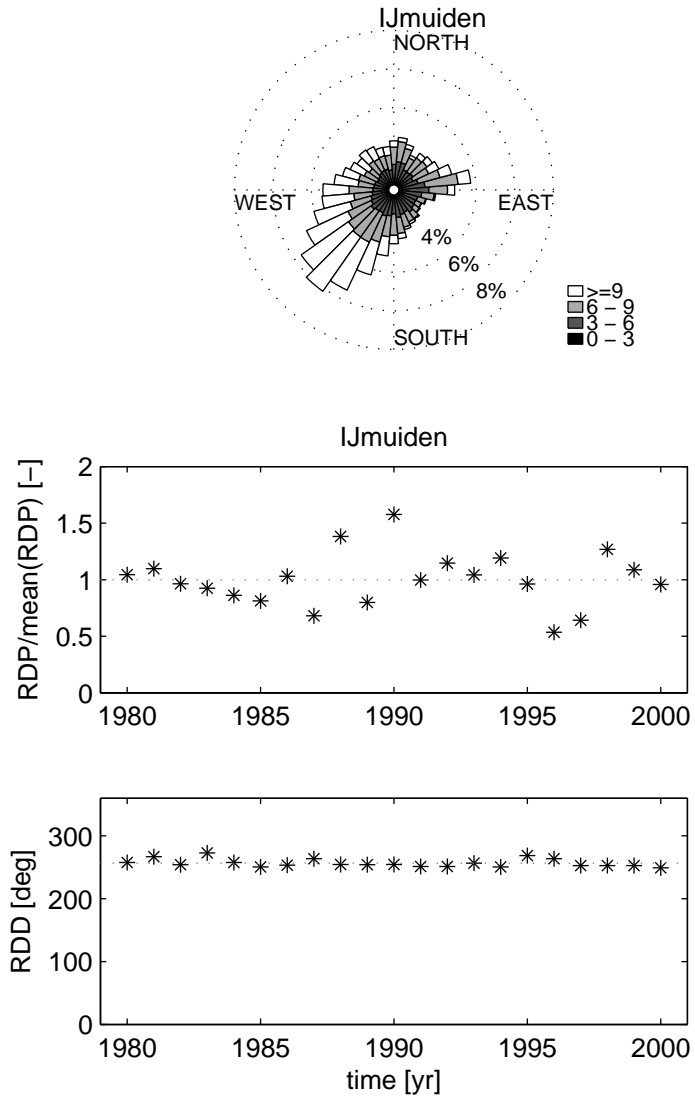


Figure 2.9: Meteorological data from IJmuiden station (provided by KNMI). Top panel shows wind rose. Middle and bottom panels show RDP and RDD respectively.

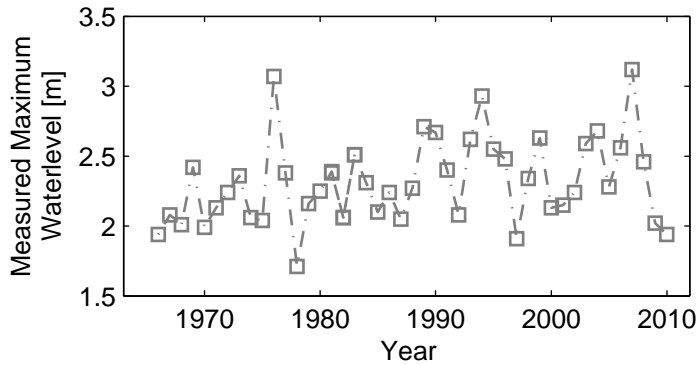


Figure 2.10: Time series of annual maxima tide level measured at IJmuiden

### Measured waterlevels.

At several locations along the Dutch coast, tide stations measure water levels. Ruessink and Jeuken (2002) argue that the annual maximum is representative for the storm induced effects on dune foot dynamics for that year. Moreover, Ruessink and Jeuken (2002) show that the variability in time of the measured annual maxima is similar between stations alongshore. For these reasons we use the annual maxima derived from the dataset gathered at IJmuiden as a proxy for forcing conditions causing dune erosion. It is shown in Figure 2.10 that annual maxima vary between +2 and +3 m NAP showing some variability in time.

### Impact of storms

For extreme storms under design conditions along the Dutch coast, van de Graaff (1986) mentions theoretically expected storm erosion of about  $400 \text{ m}^3/\text{m}$  with a return probability of  $10^{-5}$  per year. However, the likelihood of such a big storm happening in an arbitrary decade is limited. To focus on less rare storms with lower impacts the effects of three recent well documented storms are summarized below.

Since data from only three erosion events are available over the last 60 years, field data from storm erosion is limited for the Holland coast. However, we value this data to be very insightful to be used to quantify typical erosion rates due to storm events in an illustrative manner.

1. The most severe storm measured along the Dutch coast was in 1953 and caused an estimated average amount of  $80\text{-}100 \text{ m}^3/\text{m}$  erosion during a single event (WL/Delft Hydraulics, 1978). The return probabilities for storm surge and waves are both estimated at 1 in 50 years (Wolf and Flather, 2005). While not further specified by Wolf and Flather (2005), the return probability of this storm surge and waves combined is consequently estimated to be smaller than 1 in 50 years.

2. On 03-01-1976 a 1 in 20 year return probability storm occurred (WL/Delft Hydraulics, 1978). For the Holland coast a mean erosion of  $36 \text{ m}^3/\text{m}$  of dune erosion above storm surge level was recorded. The maximum and minimum recorded dune erosion was  $80 \text{ m}^3/\text{m}$  and  $15 \text{ m}^3/\text{m}$  respectively. Storm surge levels were measured by tide stations inside harbors and interpolated in between. The storm surge level was about 3.00-3.50 for the 1976 storm.
3. On 01-02-1983 another big storm occurred (WL/Delft Hydraulics, 1984). Measured storm surge levels were around 2.50-3.20 (typically 2.68 in Noord Holland) which are lower than the 1976 storm. The mean storm erosion along the Holland coast was measured to be  $23 \text{ m}^3/\text{m}$ . The highest and lowest measured values were  $55.13 \text{ m}^3/\text{m}$  and  $1.45 \text{ m}^3/\text{m}$  respectively on the North Holland coast. Evidence of this storm can be found in Figure 2.12 where dune volume changes in 1984 are smaller than the average trend. The trend itself however is not significantly influenced.

A large part of the sand eroded from the dunes during marine events gets typically deposited on the beach between the dunefoot and the low-water level (Edelman, 1972; Vellinga, 1986). This leads to post storm profiles with relatively modest beach slopes where the sand eroded from the dunes is not entirely extracted from the aeolian system. Therefore conditions are favorable for fast recovery of the dunes due to aeolian processes. Pye and Blott (2008) observe that dune recovery can be very fast in the order of several days at the Sefton Coast (UK). Aeolian recovery has not been widely quantified in detail which makes it difficult to estimate the annual contribution of storm events and their recovery along arbitrary coasts.

Based on the above we summarize that dune erosion due to the described extreme events is in the order of  $0\text{-}100 \text{ m}^3/\text{m}$  per event. The events have estimated return periods for dune erosion of 10-50 years. At this stage it can be concluded that these erosion budgets per event are of similar order than the measured growth.

#### 2.2.4 Nourishments

Due to the implementation of the dynamic preservation policy, adopted in 1990, nourishments are used to keep the sediment budgets along the Dutch coast positive. As a result, nourishment volumes along the Dutch coast have increased since 1990 and even more since 2000, see Figure 2.11. Nourishments have been applied both on the beach and also on the shoreface. In both cases natural processes account for redistribution over the profile and alongshore.

### 2.3 Methodology

Section 2.2 presents the dataset and presents variables and possible relations with different forcing conditions. Sections 2.3 and 2.4 attempt to derive statistical properties of the main parameters presented in Section 2.2. The initial focus is



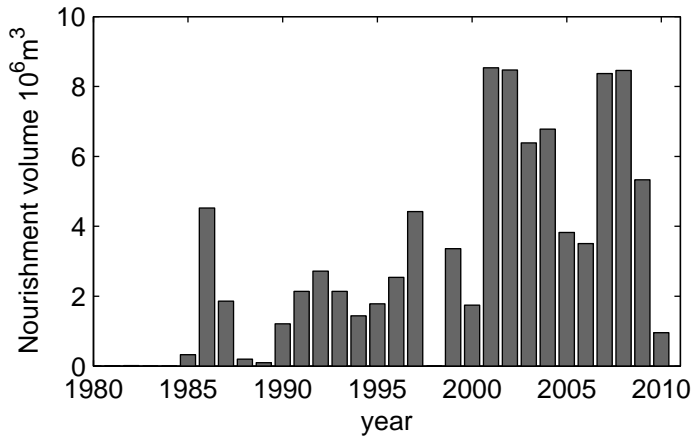


Figure 2.11: Total nourished volume along the Holland coast. Source: Dutch water board (Rijkswaterstaat).

on linear trend analysis of dune volumes, autocorrelation and the cross correlation between dune volume changes and beach slope in space and time where:

1. Linear trend analysis is used to identify and quantify linear trends and their associated correlation properties. Linear trends are fitted using basic least squares algorithms.
2. The autocorrelation of a variable's times series plotted against time lag indicates the magnitude of temporal variability relative to possible trends. If a significant correlation in time is found, this could indicate that a trend is present and the main acting processes are longer than the time interval between measurements (1 year in this case). If there is no significant correlation, this could indicate that the process is independent in time (random in time). This independence in time is possibly due to governing time-scales which are less than the used interval, or due to a relatively large measurement uncertainty.
3. The autocorrelation of a variable's spatial series plotted against space lag could indicate the spatial scales on which the process acts. No correlation either shows there is no spatial coherence between the profiles (the behavior of one profile is independent of the behavior of its neighbors), an underlying random process or measurement/transformation uncertainty.
4. The cross-correlations between parameters indicate if the tested parameters show any significant dependence (in time and in space). When significant cross correlations are identified an empirical predictive model can be derived.

Details of the correlation procedure including the tests for significance are discussed in Appendix A. Results of the correlations are shown in the form of correlograms

showing correlations of properties as a function of lag (in space or time). The scale of fluctuation is the longest time/space lag at which there is still a correlation between a property's value, see for instance Chatfield (1996) for details.

## 2.4 Analysis

### 2.4.1 Linear trends in Dune Volumes

Figure 2.12 shows the dune volumes and dune volume changes at two arbitrary transect locations together with the total mean considering all transect locations. At the transects locations shown in the left panels of Figure 2.12 the dune volume is found to develop rather linearly in time. To test how well dune volume could be represented by a linear model we have fitted linear trends at all transect locations.

After fitting the linear trend for all transect locations, the difference between the linear fit and the actual measured dune volume is calculated for every year and transect location. Figure 2.13 shows the standard deviation of the differences between the linear fit and the measured data for all profiles combined. Relatively small standard deviations for the period between 1978 and 2000 imply that the linearity in time is specifically representative for that period. Periods before 1978 and after 2001 show relatively large standard deviations from the linear trend. Assuming an underlying linear process, the relatively large standard deviation before 1977 can largely be explained by the scatter caused by the used measurement technique. After 2001 the scatter might be caused by the large nourishments specified in Section 2.2.4. To focus on a possible underlying linear process we will consider the period between 1980-2000 in the remainder of this paper.

To check to what extent this linearity in time is valid for the alongshore extent of the dataset, we calculate the correlation coefficient for all transect locations. From the 1980-2000 period, only transect locations that have more than 15 measurements (out of 21 available in time) are considered. It is found that from the 433 profiles considered, 45% have correlation coefficients ( $r$ ) larger than 0.9. This percentage decreases towards smaller correlation coefficients, see Figure 2.14. This indicates that a large part of the dune volume data is well represented using a linear model in time. Figure 2.6 (right panel) shows that the transect locations where correlations coefficients are larger than 0.9 are distributed over the entire domain.

### 2.4.2 Autocorrelations in time

Per individual profile, beach slopes are generally stable in time. Figure 2.15 shows all autocorrelations and the mean autocorrelation as a function of time lag for all profiles respectively. Temporal correlograms of beach slope data show a sudden drop in correlation between lags of zero and one year. This indicates a dataset without a periodic signal and significant trend. In other words the year to year variance exceeds the trend and/or periodic signal. Having the same properties, this data would be well represented as a random Gaussian process in time.

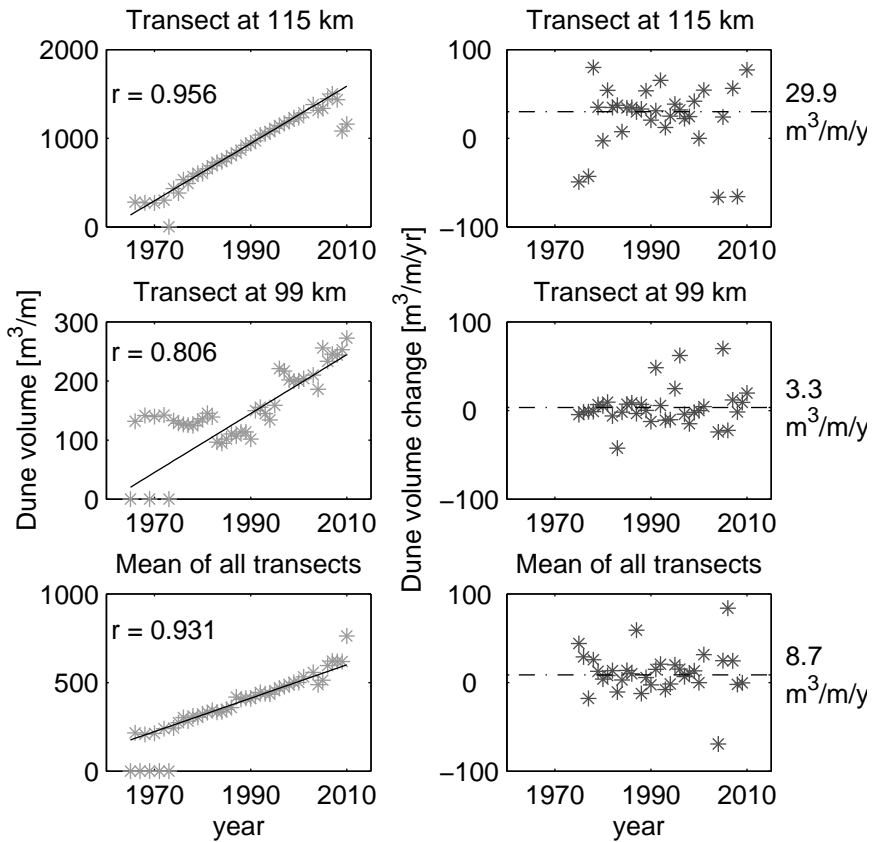


Figure 2.12: Left panels show examples of dune volume ( $DV$ ) in time together with a linear fit. Right panels shows dune volume change ( $DVC$ ) in time which generally show a stationary mean. Note that the fitted trend in the left panels is equal to the mean dune volume change in the right panels.

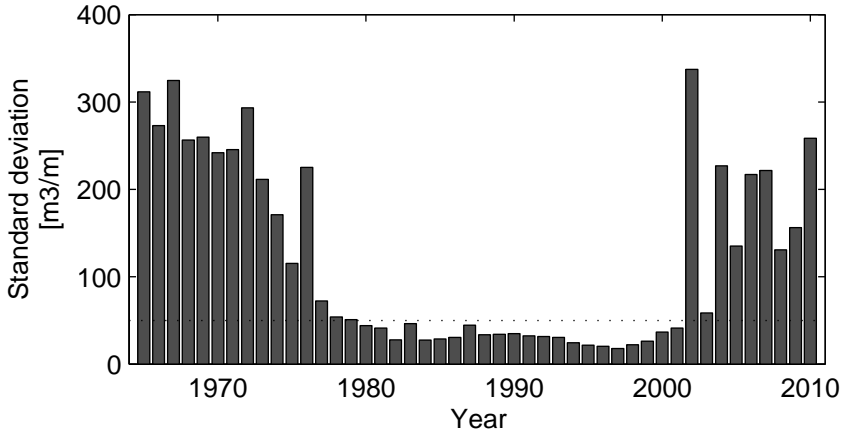


Figure 2.13: Standard deviation of the differences between the linear trend and the actual measured dune volume. Each year is plotted separately.

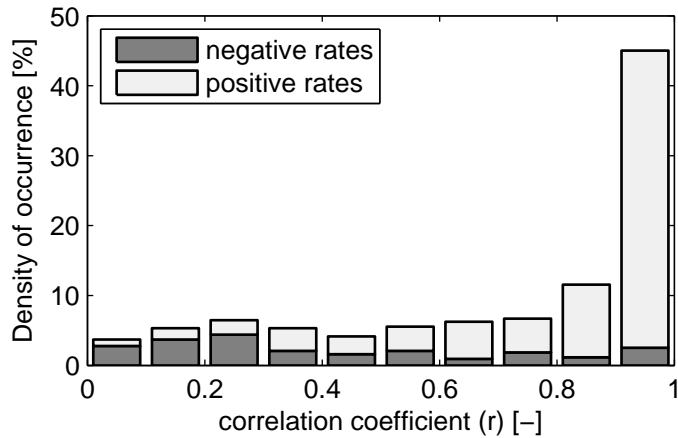


Figure 2.14: Density of occurrence of linear behavior in the period 1980-2000. 433 out of 593 transect locations are used for the calculation. Transect locations are discarded if there are fewer than 15 (out of 21) years of measurements available. 45% of the considered transect locations show correlation coefficients larger than 0.9. Both positive and negative linear behavior is found where positive behavior is dominant for large correlation coefficients.

Intuitively beach slope might be expected to follow some time dependent pattern where at least the beach slope in an arbitrary year is expected to correlate with the previous and next year. However, this is not found and is a result of a stable mean beach slope in time which is subject to small annual variability. See the bottom panel of Figure 2.8 for reference.

For dune volume changes (*DVC*) the signal is similar. Based on the mean autocorrelation shown in Figure 2.16, no periodic signal and/or trend is found as well. Based on these autocorrelations shown in Figures 2.15 and 2.16 it is concluded that both dune volume changes and beach slopes show random behavior in time with stable mean.

### 2.4.3 Autocorrelation in Space

Autocorrelations in space provide information on how dune behavior is correlated in the alongshore direction. Figure 2.17 shows that there is some alongshore correlation in dune behavior for a single arbitrary year (1980). The autocorrelation (blue line in Figure 2.17) shows a sudden drop for a spatial lag of one transect (250 m). For a lag of 500 m or more, autocorrelations decrease below the level of significance indicating data dominated by random noise at these spatial lags. This apparent random data is possibly caused by measured short term variability due to small scale processes and/or measurement errors.

When autocorrelating the same dataset but now averaging the behavior over 5-20 years some significant alongshore correlation appears. This is most likely a result of averaging short term variability or measurement uncertainty over time. Autocorrelations with a lag of 1 transect (250 m) increase as the averaging periods increase. When averaging over 5-10 years, autocorrelations for a lag of 1 transect (250 m) increase to 0.6-0.8. Averaging over more than 10 years increases correlation to a lesser extent. Overall it is concluded that, when averaging over more than 10 years a significant alongshore autocorrelation is measured which is possibly the result of underlying processes relevant to decadal timescales. The spatial scale of fluctuation of this correlation is about 2.2 km.

### 2.4.4 Cross correlations

When cross-correlating dune growth rates and beach slopes difficulties occur because the dune growth rate and RDP are cumulative values over a year whereas the beach slope is a momentary sample from that year, and is prone to vary over much smaller timescales due to short term variability of wave forcing. Using this dataset it is not possible to derive a true annual representative value. However, every year two 'snapshot' measurements of beach slope (one at the beginning and one at the end of the year) are available. Estimating an annual representative value we average the derived beach slope of two consecutive years.

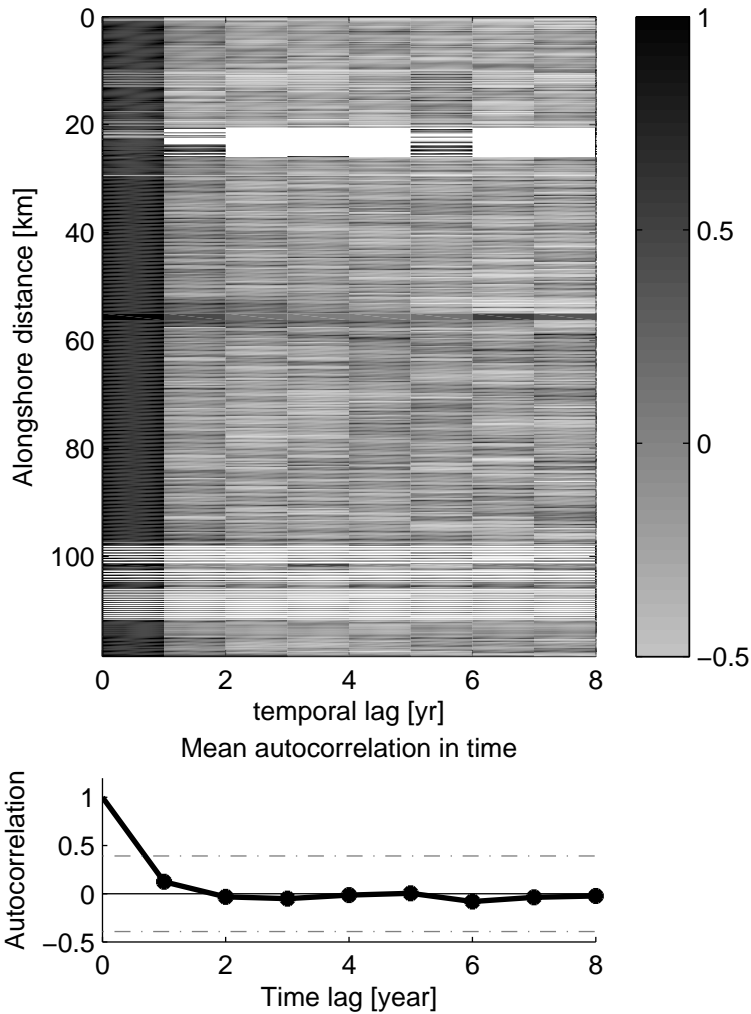


Figure 2.15: Autocorrelation versus time lag for beach slope. Top panel shows all individual profiles where the colorbar indicates the autocorrelation coefficients. Bottom panel shows the mean autocorrelation for all profiles where the dash-dotted lines show 95 % confidence intervals based on the average number of observations of all transect locations.

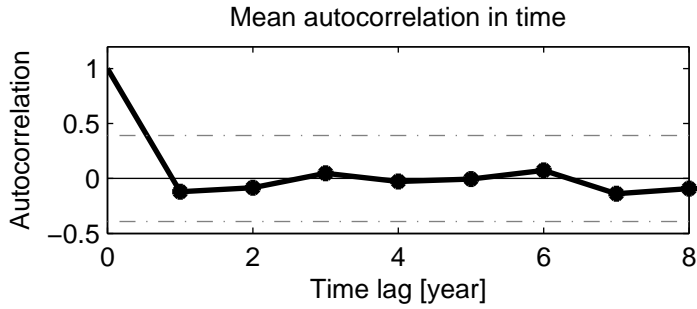


Figure 2.16: Mean autocorrelation versus time lag of dune volume changes considering all profiles (similar procedures as for the beach slopes shown in Figure 2.15 are used). The dash-dotted lines show 95 % confidence intervals based on the average number of observations of all transect locations

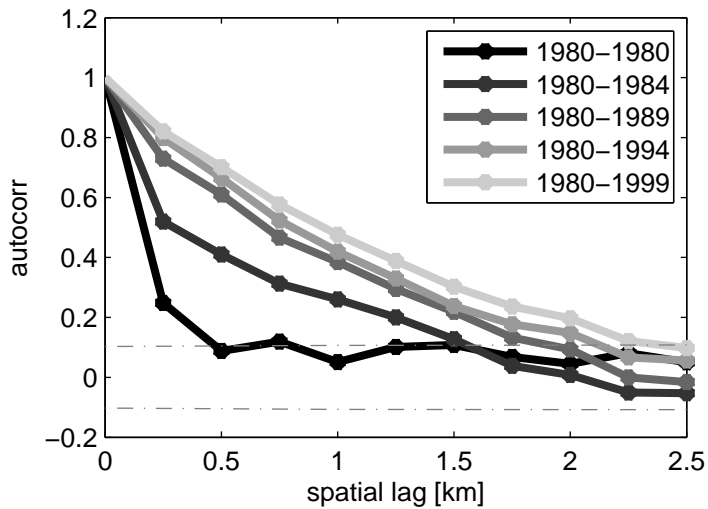


Figure 2.17: Spatial autocorrelation of dune volume changes. Dune volume changes are averaged over different periods up to 20 years. An averaging period of 1 year shows limited alongshore correlation while averaging over more consecutive years show more correlation alongshore

### **Cross correlation RDP and Dune volume changes in time**

Intuitively, dune volume changes should be correlated in time with RDP calculated earlier. The more wind there is the more aeolian transport and therefore the more dune growth is expected. However, no significant positive (or negative) correlation is found between RDP and dune volume change at a temporal lag of 0 years. Considering all profiles, fewer than 5% show a significant correlation (using 95 % confidence limits) between dune volume changes and RDP. This indicates that variability in RDP is not correlated to the variability in dune volume changes at this time and space scale. Note that the value of  $u_t$  is chosen arbitrarily at 5 m/s. Choosing other values of  $u_t$  (from 0 to 10 m/s) shows no significant changes in the results.

### **Cross correlation between annual maximum of waterlevel and dune volume change**

To test if any evidence of marine events is present in the dune volume change, we correlate the measured annual maximum water level (AMWL) to the dune volume changes. Figure 2.18 (Right panels) shows that for no temporal lag 17.5% of the transect locations show significant negative correlations between annual maxima of the water level and dune volume changes. The results of this correlation are similar to the results of earlier work by Ruessink and Jeuken (2002) and Guillen et al. (1999) and confirm that erosive events are partly responsible for the interannual behavior of dunes.

Fast recovery after a stormy year could induce a positive correlation between AMWL and Dune Volume changes with a lag of 1 or 2 years. Although a very small peak in the percentage of positively correlating transect locations is found (Figure 2.18 right bottom panel at a lag of 2 years) we cannot conclude there is any evidence of recovery after a stormy year.

High water levels might have an effect on beach slope which, if true, would be shown in a correlation analysis. Therefore we have also correlated beach slopes with the annual maxima of the water level. No discernible positive or negative correlations were found for different definitions of beach slope. The definitions of beach slope tested are the single values of two neighboring years as well as the average over these neighboring years.

### **Cross correlation Beach slope and Dune volume change in time**

Disregarding variability of dune volume changes caused by wind conditions, profile parameters (beach slope) could possibly influence dune volume changes. The beach slope could continuously influence (limit) aeolian transport processes according to the model suggested in Figure 2.2. In this section beach slope and dune volume change in time are cross correlated. Figure 2.18 shows that for no temporal lag, 11% of all transect locations show significant positive cross correlations between dune volume changes and beach slopes.



It was stated in Section 2.4.4 that the used annual estimate of beach slope might be rendered less accurate as a true annual estimate because of forcing by processes on shorter timescales. Variability on shorter timescales will introduce random noise on the annual timescale and will therefore influence the cross correlation negatively. However a correlation between the derived beach slope and dune volume changes is still identified.

Following these results we continue correlating beach slope and dune volume change in a more aggregated approach in the next section.

### Cross correlation Beach slope and Dune volume change (5yr avg.)

Based on the spatial autocorrelations which increase when averaging over time (shown in Section 2.4.3), we have chosen to do an additional cross correlation where both values (beach slope and dune volume change) are averaged over a period of 5 years. The 5 year averaging procedure might be expected to exclude short term variability which overshadows longer term processes. Figure 2.19 shows an arbitrary 5 year average of the total beach slope and dune volume change data available (shown in Figures 2.6 and 2.8). It is shown that mostly positive but also negative dune volume changes are measured together with a varying slope in space. For practical reasons the data is subdivided in spatial areas of about 60 transect locations (10-15 km). The total of 11 spatial subsets (of which 5 are shown in Figure 2.19) provide a less cumbersome autocorrelation than correlating the entire dataset as a whole while additionally, spatial differences (between subsets) could be identified. Spatial differences could be expected due to the influence of the harbor moles at IJmuiden, Scheveningen and Hook of Holland or the inlet at the northern boundary of the domain. The resulting space-time blocks which will be used for further analysis are shown in Figures 2.6 and 2.8.

Cross correlating the spatial series of dune volume change and beach slope is influenced by the increased scale of fluctuation indicating a serial dependence in dune volume changes which occur after averaging (see Figure 2.19). The (averaged) beach slope shows a similar serial dependence (not shown). The presence of serial dependence might give rise to apparently large cross correlation coefficients and the method of significance testing based on independent sampling is not valid. When testing both datasets for significant cross correlation, using significance testing described in Appendix A, the datasets should be filtered to convert them to white noise first (Chatfield, 1996). We have chosen to use a regression filter where we assume that at each transect location the value of the parameter is considered a function of its value at the neighboring transect locations.

$$X'_d = X_d - \zeta \frac{(X_{d-1} + X_{d+1})}{2} \quad (2.9)$$

where  $X'$  represents a new dataset containing the residuals after filtering. Subscript  $d$  stands for distance alongshore in accordance with Figure 2.19. All datasets are filtered and autocorrelation analysis on the residuals is used to estimate an appropriate value of  $\zeta$ . After a procedure of trial and error, it is found that  $\zeta = 0.7$

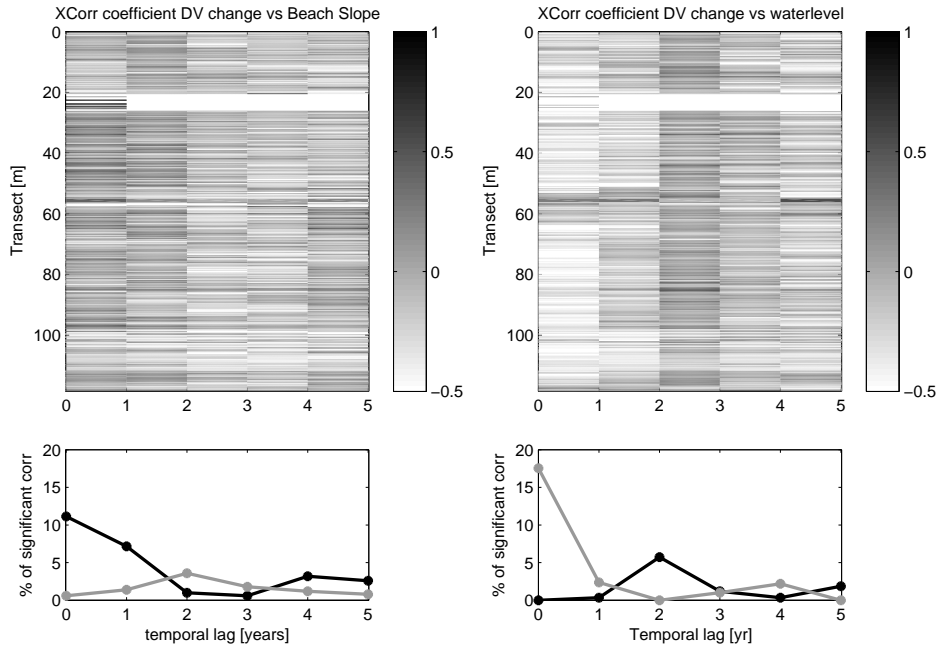


Figure 2.18:

LEFT:

Top panel shows cross correlation between dune volume change and beach slope with temporal lag showing all transects. Bottom panel shows the percentages of significant correlations found where the gray and black lines represent negative and positive correlations respectively. A positive correlation between beach slope and DV changes is found indicated by the slightly darker band at 0 lag in the top panel and the black peak at zero lag in the bottom panel. No negative correlations seem to be present. (this figure shows subset between 1980-2000)

RIGHT:

Top panel shows cross correlation between dune volume change and annual maximum water level with temporal lag showing all transects. Bottom panel shows the percentages of significant correlations found where the gray and black lines represent negative and positive correlations respectively. A negative correlation between beach slope and annual maxima is found indicated by the slightly lighter band at 0 lag in the top panel and the gray peak at zero lag in the bottom panel. No positive correlations seem to be present. (this figure shows subset between 1980-2000)

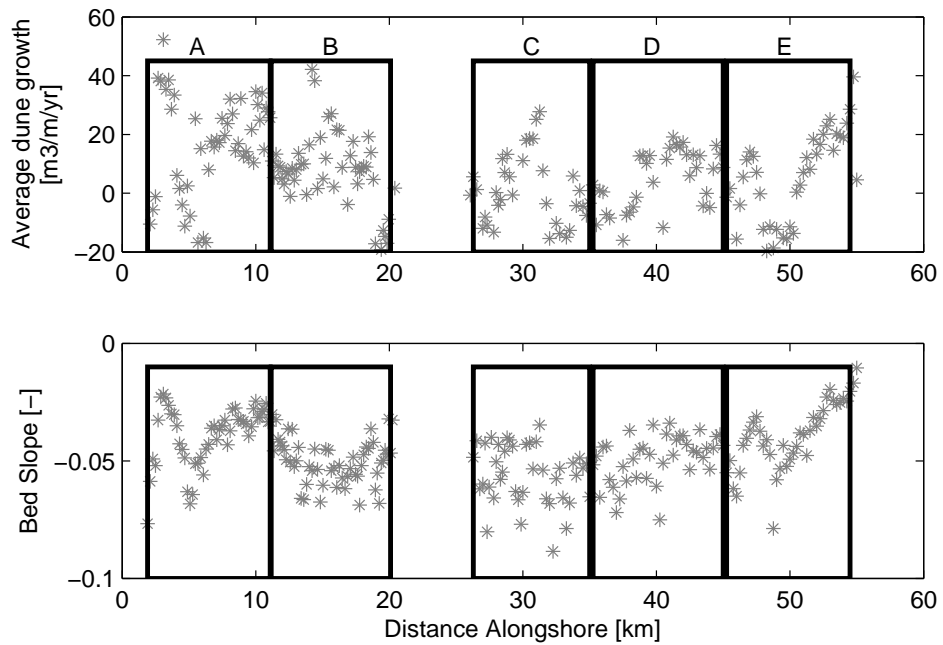


Figure 2.19: Average dune volume changes and beach slope for 1986-1990 along the North Holland coast. Black boxes indicate sub-areas which correspond to the white squares in Figures 2.6 and 2.8. See also Figure 2.4.

Area	Time subset			
	81-85	86-90	91-95	96-00
7A	-0.06	0.42	0.05	0.36
7B	0.58	-0.10	0.29	0.24
7C	0.25	0.45	0.20	-0.03
7D	0.32	0.57	0.55	0.36
7E	0.03	0.56	0.56	0.56
8A	0.32	0.39	0.17	-0.19
8B	0.22	-0.05	0.53	0.21
8C	0.45	0.29	0.04	0.09
8D	-0.08	0.39	0.08	0.21
9A	0.46	0.29	0.71	0.15
9B	0.56	0.48	0.50	0.29

Table 2.1: Values of cross correlation coefficients (spatial lag of 0) between beach slope (5 yr. avg. and filtered) and dune volume changes (5 yr. avg. and filtered) within each sub-area. Each year/area cell refers to the white squares in Figures 2.6 and 2.8. Gray cells indicate significant cross correlations while white cells show no significant cross correlations.

reduces the signals' scale of fluctuation to one alongshore interval and therefore the serial dependence is removed in all datasets.

The left panels of Figure 2.20 shows the cross correlation between the filtered beach slope and dune volume changes associated with the data of Figure 2.19. A significant cross correlation (at spatial lag 0) is found for 4 out of 5 space-time blocks shown.

Because the dominant winds are oblique to the coastline, a spatial lag between beach slope and dune volume change could be expected. However, no consistent evidence of such a spatial lag is found indicating that the cross correlation between beach slope and dune volume changes is strongest in the cross shore direction.

Applying the averaging, filtering and cross correlation to all available data the results are shown in Table 2.1. All gray cells indicate significant cross correlations (at lag 0) between 5 year averaged values of dune volume change and beach slope. It is shown that within the 1980-2000 time window, 18 out of 44 (40%) of the space-time subsets show significant correlations between dune volume change and beach slope after filtering using the regression model.

The right panels of Figure 2.20 show the fitted linear relation between beach slope and dune volume change for 5 space time blocks. The variance explained by the fitted trends represent the combination of both the serial dependence and residual behavior. Similar positive relations are found for the different blocks. Lumping all averaged beach slopes and dune volume changes for all space time blocks the total relation between the two is given in Figure 2.21. It is shown that, despite some scatter, a significant positive relation is found. This fitted trend can be quantified and possibly be used as a predictive relation for forecasting decadal

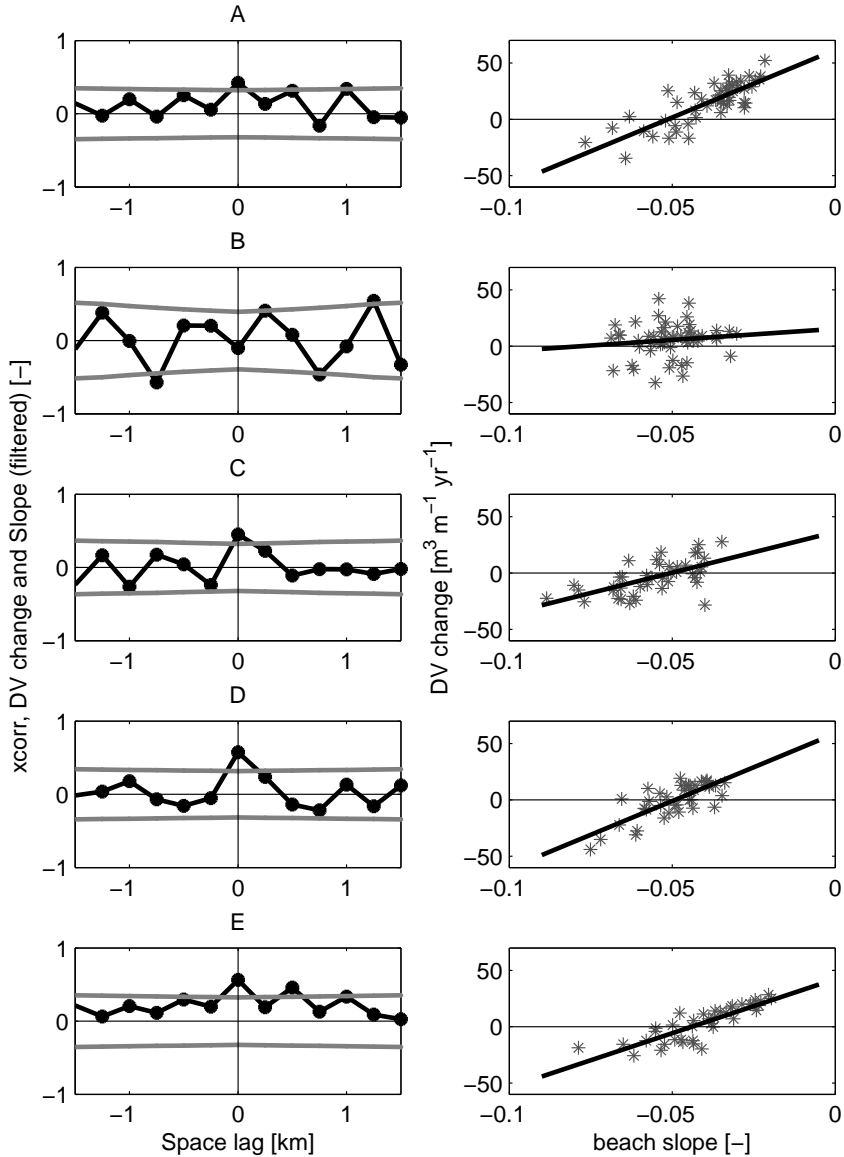


Figure 2.20: Left panels show cross-correlation between the averaged and filtered beach slope and dune volume change versus space lag for the zones indicated in Figure 2.19. Gray lines indicate limits of the 95% significance interval, see Appendix A. Right panels show empirically fitted linear relations between 5 year averages of beach slope and dune volume change for each zone (unfiltered).

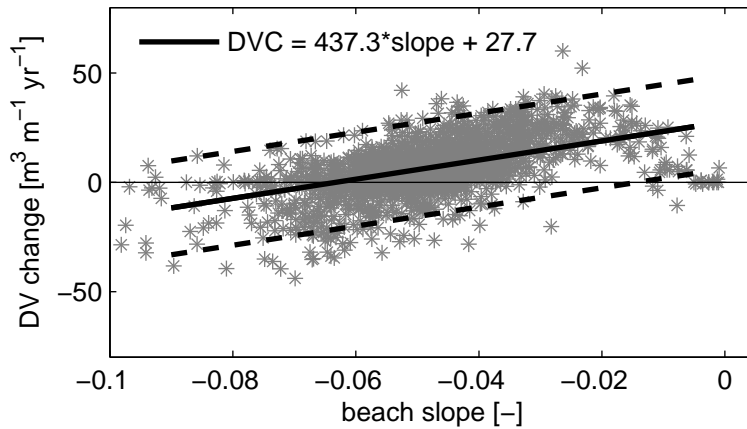


Figure 2.21: Averaged beach slope versus averaged dune volume changes. Black solid line indicates significant linear trend ( $r=0.52$ ). Dashed lines show 95% confidence intervals of the linear fit.

behavior of spatial variability.

## 2.5 Discussion

### 2.5.1 Modeling dune behavior

Existing sediment transport relations are used to determine annual resultant drift potentials. The variability in the determined RDP values, representing the variability in wind conditions and a constant threshold wind velocity, do not agree well with the measured variability in dune volume change. The latter is likely to be overshadowed by transport limiting effects. Looking back at Equation 2.8 for calculating RDP's, the threshold velocity of transport  $u_t$  and transport capacity might vary alongshore as a result of varying beach slopes. Therefore RDP values could be corrected for beach slope effects using the theoretical relations of Equations 2.5, 2.6 and 2.7. When calculating RDP values taking into account the correction for beach slope, the percentage of significantly correlating profiles does not change with respect to the results presented in Section 2.4.4. This could possibly be caused by the fact that temporal variability of beach slopes is limited and therefore overshadowed by temporal variability of wind conditions when calculating the corrected RDPs. Moreover, other limiting effects such as precipitation could also play a large role. The lack of a correlation between dune behavior and wind conditions, even when corrected for slope effects, underlines the importance of transport limiting processes. Future modeling efforts of larger than annual dune behavior are likely to benefit from quantitative knowledge of transport limiting processes rather than fine tuning and aggregating wind based sediment transport

relations.

### 2.5.2 Balancing erosion vs. accretion

The analysis above shows that in general the upper limit of measured dune growth is around  $30 \text{ m}^3/\text{m}/\text{yr}$  (see also Figure 2.6). It could be assumed that the potential dune growth due to wind alone along the entire measurement area (assuming no large differences in wind conditions) is at least this measured upper limit. Dunes behind beaches with steep slopes show much smaller accretion rates or even erosion. This could be caused by the occurrence of storm events which limits the measured dune volume changes (Damsma, 2009). However, based on historic storm records it is unlikely that the assumed potential of  $30 \text{ m}^3/\text{m}/\text{yr}$  (upper limit) of aeolian accretion is eroded every year by storm events. Not all annual maximum water levels reach the dunefoot and therefore erosion due to extreme marine events will not occur every year and expected erosion rates are smaller than the assumed potential accretion. We feel it is more likely that the assumed potential accretion of  $30 \text{ m}^3/\text{m}/\text{yr}$  is limited due to transport limiting conditions which vary between profiles. This means that if transport is limited the dune volume change is still constant ( $DV$  evolves linearly in time) but reduced due to limiting processes.

### 2.5.3 Timescale of erosion and accretion

The right panels of Figure 2.20 and Figure 2.21 suggest a linear relation between 5 year averaged beach slope and dune volume changes. This linear trend seems to be representative for both positive and negative 5 year averaged dune volume changes. While on the short timescale negative dune volume changes are driven by marine erosion and positive changes by aeolian accretion, differences in behavior between positive and negative dune volume changes could be expected with respect to the averaged beach slope. However these 5 year averaged results show no explicit difference. This result questions the relevance of the different short term processes while looking at erosion on the longer timescales while no evidence of increased variability is found for eroding situations.

### 2.5.4 Sediment availability, beach slope and Dune volume change

Based on Figure 2.21 it could be concluded that the spatial variability in 5 year averaged dune volume changes is explained to some degree (27%) by the variability in beach slope (also 5 year averaged). A possible physical process behind this correlation is the limitation of sediment transport due to the beach slope. However, at this stage we can not exclude the possibility that the sediment supply from the marine zone governs both the beach slope and the dune volume change directly. Large sediment supply from the marine zone is likely to cause coastline extension and therefore a milder beach slope. This milder beach slope would accommodate more aeolian transport. However, aeolian transport quantities are possibly

directly influenced by marine supply as well. Marine supply from the intertidal zone (deposition of loosely packed sand in the intertidal zone) could function as a direct source for aeolian transport, reducing supply limiting effects. While concepts describing dune behavior as a function of the beach state are available (e.g. Short and Hesp (1982)), the current lack of quantitative knowledge on sediment exchange processes between marine and sub aerial zones makes it impossible to address the question to what extent the sediment supply from the marine zone could influence dune volume changes. Future research might shed more light on this.

## 2.6 Conclusions

Dune behavior along the Holland coast is analyzed using the Dutch JARKUS dataset. Based on this analysis it is concluded that:

1. Dune volume changes along the Holland coast are often found to be linear in time. A constant dune growth rate can be defined at many transect locations and is used to quantify dune growth rates. The linear dune growth rates at the Holland coast are found to be in the order 0-40 m<sup>3</sup>/m/yr. These fitted relations could simplify future predictions of dune volume changes.

The spatial scale of fluctuation of the auto correlation of dune volume changes in alongshore direction is in the order of 2 km when averaging over 5-10 years. On shorter timescales, smaller alongshore correlation distances are found.

2. No significant correlation is found between the variability of yearly wind conditions (RDP) and yearly dune volume changes. This suggests that traditional aeolian transport models developed for desert dunes overestimate the importance of variability in wind conditions for aeolian transport rates across the beach towards the foredunes.
3. Significant temporal correlation is found between variability of yearly beach gradients and dune volume change for part of the analyzed spatial domain (11% of the transect locations). This correlation is likely to be governed by transport limiting processes with respect to aeolian transport.
4. Significant spatial correlations are found between 5 year averaged beach slopes and dune volume changes. Moreover, it is found that alongshore variability of the 5 year averaged beach slope explains 27% of the alongshore variability of the 5 year averaged dune volume changes.
5. In future modeling of yearly to decadal dune volume changes, variability of transport limiting parameters is of interest rather than time varying forcing conditions such as varying wind speeds and drift potentials.
6. The capacity of aeolian processes to build dunes is of similar order to the capacity of (extreme) marine events to erode dunes. Alongshore variability



in dune volume changes at decadal scales is therefore likely to be governed by aeolian processes as well as marine erosion.

## Acknowledgements

Sierd de Vries was funded by the innovation program Building with Nature. The Building with Nature program is funded from several sources, including the Subsidierregeling Innovatieketen Water (SIW, Staatscourant nrs 953 and 17009) sponsored by the Dutch Ministry of Transport, Public Works and Water Management and partner contributions of the participants to the Foundation EcoShape. The program receives co-funding from the European Fund for Regional Development EFRO and the Municipality of Dordrecht.

## Appendix A Correlation and significance testing

Illustrating the procedure of correlation, the correlation coefficient (Pearson product-moment  $r$ ) is given as:

$$r = \frac{\sum_{i=1}^N (x_i - \bar{x})(y_i - \bar{y})}{\sqrt{\sum_{i=1}^N (x_i - \bar{x})^2 \sum_{i=1}^N (y_i - \bar{y})^2}} \quad (2.10)$$

When cross correlating,  $x$  and  $y$  are separate datasets representing different variables. When auto correlating,  $x$  is a lagged version of  $y$  where the overlapping parts of the datasets are used in equation (2.10).  $N$  is the number of (paired) samples. The square of the sample correlation coefficient, which is also known as the coefficient of determination, estimates the fraction of the variance in  $x$  that is explained by  $y$  in a linear regression analysis.

Values of  $r$  of  $\pm 2/\sqrt{N}$  represent the 95% significance levels of a random process where samples are assumed to be independent. Values of  $r$  outside this range will generally indicate significant correlations, although about 1 in 20 (5%) of such values could be expected to occur as a result of purely random processes.

The datasets analyzed in this paper contain data gaps. The correlation is done ignoring these missing values using the method described by Wijnberg et al. (2011). They propose to ignore the observation pair  $(x_i, y_i)$  if either of the observations  $x_i$  or  $y_i$  has no value. This method has the advantage that it is not needed to interpolate data while interpolation would bias results of lagged correlations. The number of samples used for the correlation ( $N$ ) is limited due to the data gaps. This has been accounted for while testing significance.



## Chapter 3

# Seasonal development of the cross shore dune and beach profile

### *An analysis using monthly morphological data collected at three field sites*

---

This chapter elaborates on the previous Chapter (2). In the previous chapter, annual to decadal dune behavior is quantified using annual (JARKUS) data along the Dutch coast. The general trend is that dune volumes increase due to onshore aeolian sediment transport and difference in dune growth rates are partly explained by a difference in beach slope. Cross shore sediment supply to the dunes and beach can however influence both beach slope and dune volume changes which makes sediment exchange between the beach and surfzone and sediment supply from the surf zone towards the beach in particular, a relevant parameter of interest. It is currently not addressed how sediment supply varies in space and time and therefore it is unclear from where the sediment which is found in the dunes originates and how profile morphology changes due to aeolian processes.

In this Chapter, it is tried to gain detailed insight in sediment supply and profile shape by analyzing morphological data which is collected monthly at three distinctly different field sites. At the end of this chapter a spatial model is presented to be used for describing the spatial distribution of the sediment supply for aeolian sediment transport towards the dunes.

Lessons learned:

- Measured morphological changes, at the study sites, due to marine processes are significantly larger than morphological changes due to aeolian processes. The extent of the marine processes influences vary in time and space and largely determine morphological development.
  - No significant erosion or sedimentation due to aeolian transport is measured at the upper beach. Therefore, only small transport gradients related to aeolian transports occur at the upper beach. Due to this limited morphological activity at the upper beach, the upper beach is unlikely to function as a large source area for aeolian transport processes. A large sediment supply to the aeolian system is expected to originate from the intertidal zone.
  - While morphological changes due to marine processes is of higher order than due to aeolian processes. The shape of the cross shore coastal profile seems to be determined by marine conditions rather than aeolian conditions.
- 
-

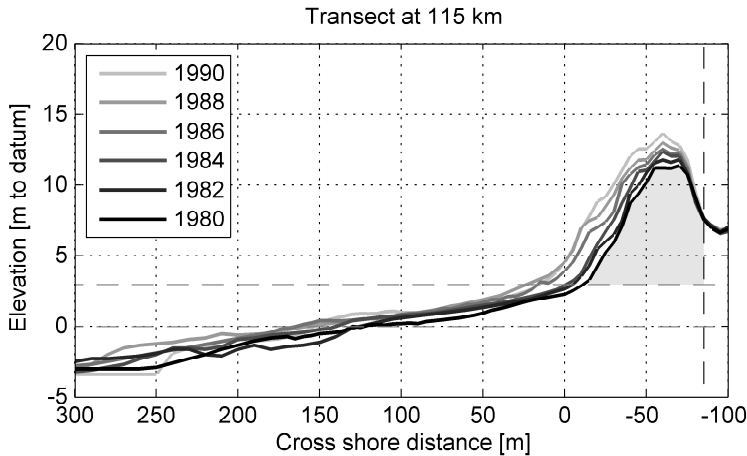


Figure 3.1: Example of cross shore profile evolution at an arbitrary location at the Holland coast.

### 3.1 Introduction

This chapter elaborates on the previous chapter (Chapter 2). In the previous chapter, annual to decadal dune behavior is quantified using annual (JARKUS) data collected along the Dutch coast. Dune behavior is quantified using dune volume changes. While the general trend is that dune volumes increase due to onshore sediment transport, it is not addressed where from this sediment originates and how the profile morphology develops. In the common case that beaches are rather alongshore uniform in width, gradient and orientation, conditions do not vary in alongshore direction and significant alongshore gradients in transport are not expected. If alongshore gradients in transport are neglected, sediment can either originate from the beach or from the intertidal zone during aeolian transport events. Assuming a sediment balance in cross shore direction and that the dunes are growing, it could be expected that the beach and intertidal morphology are eroding. The sediment exchange between the growing dunes and eroding beach is likely to be governed by aeolian processes.

Figure 3.1 shows an example of arbitrary growing profile along the Dutch coast. It is shown that both the dune area and the beach are accreting. Where the dunes grow in volume, the beach level rises keeping a more or less constant beach slope. Both the beach and the dune volumes are increasing indicating that an external sediment source is present. Assuming limited alongshore transport gradients, a sediment source at the seaward extent of the profile must be present. With an external sediment source present it is not possible to quantify exchange between beach and dune based on a cross shore sediment balance.

Despite the obvious change in dune and beach volume, parts of the profile morphology remain constant in the example given in Figure 3.1. The beach slope

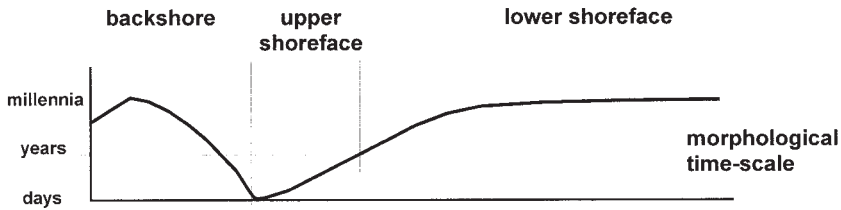


Figure 3.2: Cross shore representation of morphological timescale. Copied from Cowell et al. (2003).

(between 0-3m NAP) seems fairly constant in time (around  $1/50$ ) while the beach itself translates in seaward direction. A similar seawards translation occurs at the seaward foredune slope (above the dunefoot at 3m NAP) where the slope remains constant (around  $1/5$ ). Therefore, at this particular profile location both the beach and the foredune are increasing in volume but their respective shapes remain constant.

Changes in profile volume and shape are governed by processes which act on different morphological timescales. The marine foreshore is typically governed by hydrodynamic processes and the aeolian beach is typically governed by aeolian processes. Chapter 2 has shown that annual volume changes in the dunes along the Holland coast are in the order of  $0-50 \text{ m}^3/\text{m}/\text{yr}$  due to combined marine and aeolian forcing. Examples along the Dutch coast have shown that submarine volume changes due to bar migration at the foreshore can be in the order of  $20 \text{ m}^3/\text{m}$  in one week (see for instance the example given in van Rijn et al., 2003)

The difference in morphological timescale between the 'upper foreshore' and the 'backshore' has been formulated conceptually by Cowell et al. (2003). Figure 3.2 shows the conceptual illustration of the spatial distribution of the morphological timescale by Cowell et al. (2003). The measured different order of aeolian and marine processes described above supports the concept of Figure 3.2. For understanding measured coastal morphology at any time and location it is important to account for the difference in timescale and the nature of processes (marine/aeolian) occurring. Analyzing measured morphological profiles collected at short timescales could possibly specify this conceptual difference in timescale.

### 3.1.1 Cross shore interaction between foreshore, beach and dune

The data which is analyzed in Chapter 2 provide an aggregated image of the annual development of the dune volume and cross shore profile. This development is the result of morphological changes due to both marine and aeolian processes on the annual timescale. On the shorter (seasonal) timescale, periods and locations exist where marine processes dominate and periods and locations where aeolian

processes dominate. In winter months, water levels typically reach higher levels due to the occurrence of storm events and large parts of the beach and sometimes the dunes are influenced by marine processes. In summer months, water levels typically reach lower levels due to the lack of storm events leaving large parts of the beach and dunes influenced by aeolian processes only. Available morphological data collected on the monthly timescale can be used to identify the specific contribution of marine and aeolian processes on the coastal morphology.

Few morphological datasets are available that cover both the morphology of beach and dunes on short timescales. Therefore morphological interactions between beaches and dunes are poorly documented. Datasets that include coastal profile measurements on the monthly timescale are however available. Some datasets include the beach only such as the data collected at Noordwijk in the Netherlands (Quartel et al., 2008) and the data collected at Narrabeen in Australia (Short and Trembanis, 2004). The morphological dataset collected at Duck NC includes beach, dune and foreshore (Howd and Birkemeier, 1987; Lee and Birkemeier, 1993) but the upper beach and dune part within this dataset is hard to interpret due to irregular measurement intervals. The morphological dataset collected at Vlugtenburg, the Netherlands, presented in de Vries et al. (2011b) covers foreshore and beach on a monthly timescale on a nourished site.

### 3.1.2 Chapters Aim

In this Chapter it is aimed to describe measured cross shore interaction between beach and dunes at three behaviorally different field sites. The key interest is the (relative) effects of marine and aeolian processes and their difference in morphological timescale. Of the three sites, two are located on the storm dominated Holland coast (one natural beach and one nourished beach) and one is located on the swell dominated SE Australian coast. This spread of sites is expected to render the findings and conclusions of this chapter generally applicable.

## 3.2 Field sites

In this Chapter, the three field sites are discussed. At these three sites morphological data is collected in a similar and comparable way at monthly time intervals. The most important characteristics of the field sites and the survey programs are summarized in table 3.1. In short, the tidal ranges are similar but the wave climates and the beach' mean grain sizes differ between the Australian and Dutch beaches.

### 3.2.1 Vlugtenburg Beach

Morphological data has been collected at Vlugtenburg beach in the Netherlands at monthly intervals between 2008 and 2012. Vlugtenburg beach is located at the south west of the Holland coast (see Figure 3.3). In 2008 this beach has been

Location	Noordwijk (NLD)	Vlugtenburg (NLD)	Narrabeen (AUS)
Field Characteristics			
Wave climate	sea (1.2m 5s)	sea (1.2m 5s)	swell (1.6m 10s)
Dominant wind direction	side/onshore	side/onshore	onshore
Grain size ( $D_{50}$ )	0.3	0.3	0.3-0.4
Classification (Short and Hesp, 1982)	Dissipative	Dissipative	Intermediate
Tide range	1.8	2	2
Survey parameters			
Survey period	10-2001 till 10-2004	7-2009 till 12-2012	7-2005 till 4-2010
frequency	monthly	monthly	monthly
Cross shore extend	+3 to -1 m NAP	+6 to -10 m NAP	+6 till 0 m
alongshore distance	1.5 km	1.8 km	3.6 km
Nr of transect locations	31	22	5

Table 3.1: Overview of survey parameters for the different measurement locations

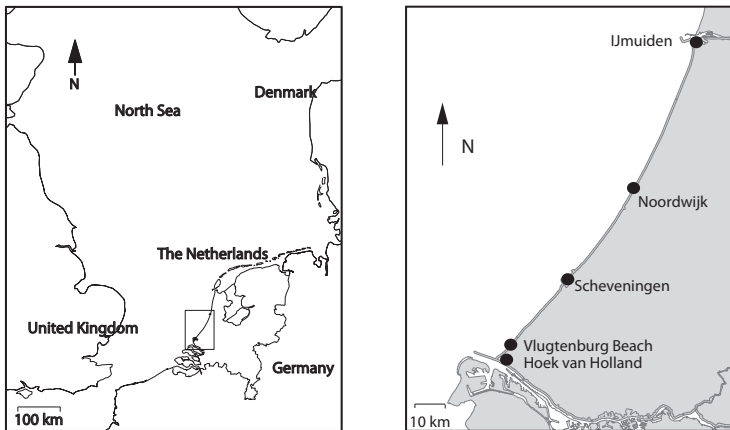


Figure 3.3: Vlugtenburg and Noordwijk measurement locations.

nourished and since then, several aspects of this beach including foreshore and dune behavior have been studied (de Vries et al., 2011b; de Schipper et al., 2012).

Figure 3.4 shows the cross shore profile before and after the 2008 nourishment. The 2009 post nourishment profile includes a new artificial dune and a dune valley behind it before reconnecting to the old (2008) dune profile. For the current study we focus on the upper beach of the profile until the +3 m NAP level. The +3 m level is chosen as an upper limit while normally the dune foot is located at this level. No dunefoot is however present in this artificially made profile but for consistency considerations this upper limit is maintained.

Generally, mean wave heights and periods along the Dutch coast are 1.2 m and 5 s respectively where alongshore differences in wave climate are small (Wijnberg and Terwindt, 1995). The tide is semi diurnal with a neap spring cycle of 1.2 and 2.2 m, respectively. Beach slopes in the inter tidal zone are roughly between 1:40 and 1:50. The beach at this site can generally be categorized as a dissipative beach according to the geographical framework presented by Short and Hesp (1982).

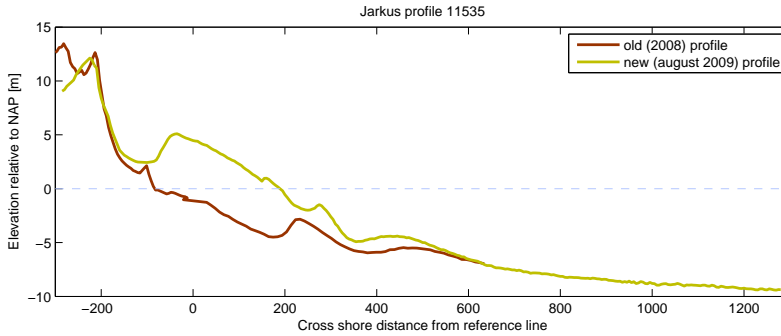


Figure 3.4: Cross shore profile at the Vlugtenburg location before and after the 2008 nourishment.

Dissipative beaches are characterized by a large potential wave induced onshore sediment transport which could provide an abundant source of sand for aeolian processes.

The wind climate is dominated by mainly west to southwest winds. These directions are oblique to normal incident with a large onshore component. This large onshore component governs cross shore sediment transport towards the dunes and dune formation.

The morphological measurements consist of monthly topographical measurements of 22 cross shore profiles encompassing both the marine and aeolian zone. Profile spacing is 70-80 m resulting in a domain that covers 1.8 km alongshore. The marine part of the profile is measured using the TUDelft jetski (van Son et al., 2009) and the aeolian part is measured using conventional RTK GPS techniques.

The sand surface at the upper beach is characterized by a shell layer where micro scale bed forms are present. The shell layer is formed due to erosion of lighter material on the surface by aeolian processes where the heavier material stays behind. The micro scale bed forms are significant and mainly anthropogenic created as a result of footsteps and car tracks. The topography changes at the upper beach are relatively small with respect to the intertidal area (de Vries et al., 2011b).

The closest tide station is located at Hoek van Holland which is located 2 km south of Vlugtenburg inside the area shadowed by large harbor moles, see Figure 3.3.

### Decadal behavior

Decadal behavior at the Vlugtenburg site is analyzed using the JARKUS dataset presented in Chapter 2. Analyzing the decadal behavior of the beach and dunes during the relevant time at the Vlugtenburg site is however hampered by the large nourishment. Behavior before and after the nourishment are therefore separated. Table 3.2 shows the results of the fitted linear trends at the relevant locations



Alongshore [km]	Avg DV change [m <sup>3</sup> /m/yr]	linear corr [-]
114.88	19.40	0.99
115.10	24.65	0.99
115.35	29.47	0.95
115.60	28.26	0.89
115.86	40.12	0.98
116.11	17.46	0.96
116.36	23.08	0.99
116.62	26.62	0.97

Table 3.2: Derived dune volume changes for the Vlugtenburg area [1996-2008]

(114.88-116.62) for the pre-nourishment period 1996-2008.

Figure 3.5 shows the development of the dune volume for the period between 1996 and 2012. It is shown that after a period of apparent linear development until 2008, the volume increases instantly due to the nourishment. After the nourishment the dune volume remains to increase at most transect locations. A more detailed comparison of the behavior before and after the nourishment is not made at this stage. This is due to the limited post nourishment data available at the time of writing.

### 3.2.2 Noordwijk

Noordwijk is located along the Dutch coast some 35 km north of Vlugtenburg, see Figure 3.3. Quartel et al. (2008) collected morphological data at Noordwijk beach in the Netherlands between November 2001 and November 2004 with monthly intervals. Data is collected using conventional RTK GPS techniques and covers the beach between the low water line and the dunefoot at roughly -1 m and +3 m NAP respectively.

Quartel et al. (2008) collected and analyzed this dataset to investigate seasonal patterns of beach accretion and erosion in monthly observed morphologies at a storm-dominated coast and to relate these patterns to variations in the wave forcing conditions. Through defining cross shore zones and quantifying their horizontal extent and volumes, Quartel et al. (2008) found that while variability in beach width was typically governed by hydrodynamic forcing, variability in beach volume was not. Although it can be assumed that beach volume is some product between beach width and an average vertical level, the variability in vertical morphology could play a governing role. This variability in vertical morphology remains not addressed.

Like Vlugtenburg, Noordwijk can be characterized as a dissipative beach in the framework presented by Short and Hesp (1982) with a mild beach slope and a potential abundance of sediment supply to the aeolian system. The beach slope is however steeper (1:20-1:25) than at Vlugtenburg. The closest tide stations are

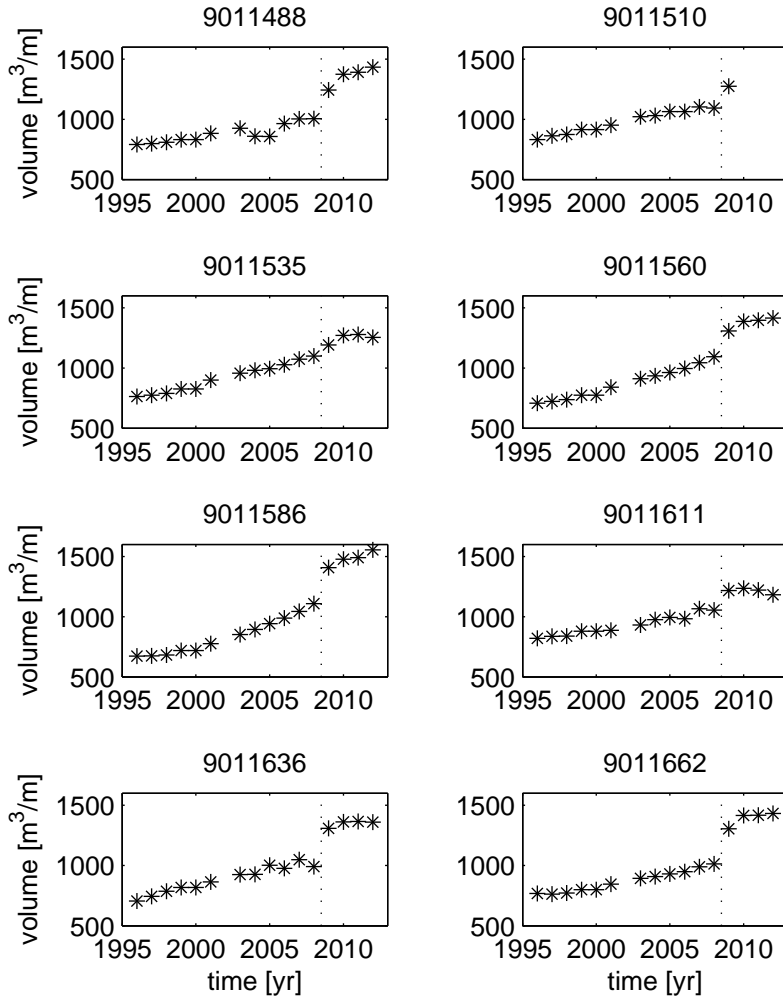


Figure 3.5: Volume development of individual profiles measured at Vlugtenburg beach.

Alongshore [km]	Avg DV change [m <sup>3</sup> /m/yr]	linear corr [-]
81.25	7.70	0.97
81.50	7.51	0.98
81.75	5.49	0.98
82.00	5.94	0.96
82.25	2.31	0.30
82.50	9.63	0.97
82.75	11.14	0.97

Table 3.3: Derived dune volume changes for the noordwijk area [1996-2008]

located offshore at Meetpost Noordwijk and onshore at the Harbor of IJmuiden

### Decadal behavior

Using the analysis presented in Chapter 2 at the considered time and location the dune behavior can be quantified. The Noordwijk area extends from 81.25 up to 82.75 km including 7 JARKUS transect locations, (see Chapter 2 for background on JARKUS transect locations). Figure 3.6 shows the development of dune volume for the period 1996-2008 (the years including and 4 years around the seasonal measurements). The measured volumes are further quantified in Table 3.3 where it is indicated that a positive linear trend (corrcoef > 0.95) is found for 6 out of the 7 transect locations. Moreover, average dune volume changes are roughly in the order of 5-10 m<sup>3</sup>/m/yr.

The volume changes are significantly lower than the volume changes related to the Vlugtenburg site. This could possibly be explained by the difference in beach slope argued in Chapter 2 where it is found that steeper beaches correlate with smaller dune volume changes relative to milder beach slopes which correspond to larger dune volume changes.

### 3.2.3 Narrabeen

Narrabeen beach has been surveyed since 1976 (Short and Trembanis, 2004). Between July 2005 and April 2010 monthly high resolution profiles measurements are available for 5 profiles located along the entire 3-4 km beach (Harley et al., 2011). The surveyed profiles are indicated in Figure 3.7 and cover the beach and intertidal zone. The dune area is relatively small (close to non-existent) where roads and buildings are located very close to the beach. As a result, decadal behavior of the dune is not documented in a comparable way with respect to the Dutch sites. The closest tide station is located around 10 km south of Narrabeen beach inside the Sydney harbor region.

The Narrabeen beach is discussed by Short and Hesp (1982) to be an intermediate beach which is characterized by an almost continuous exchange of sediment between aeolian beach and surf zone.

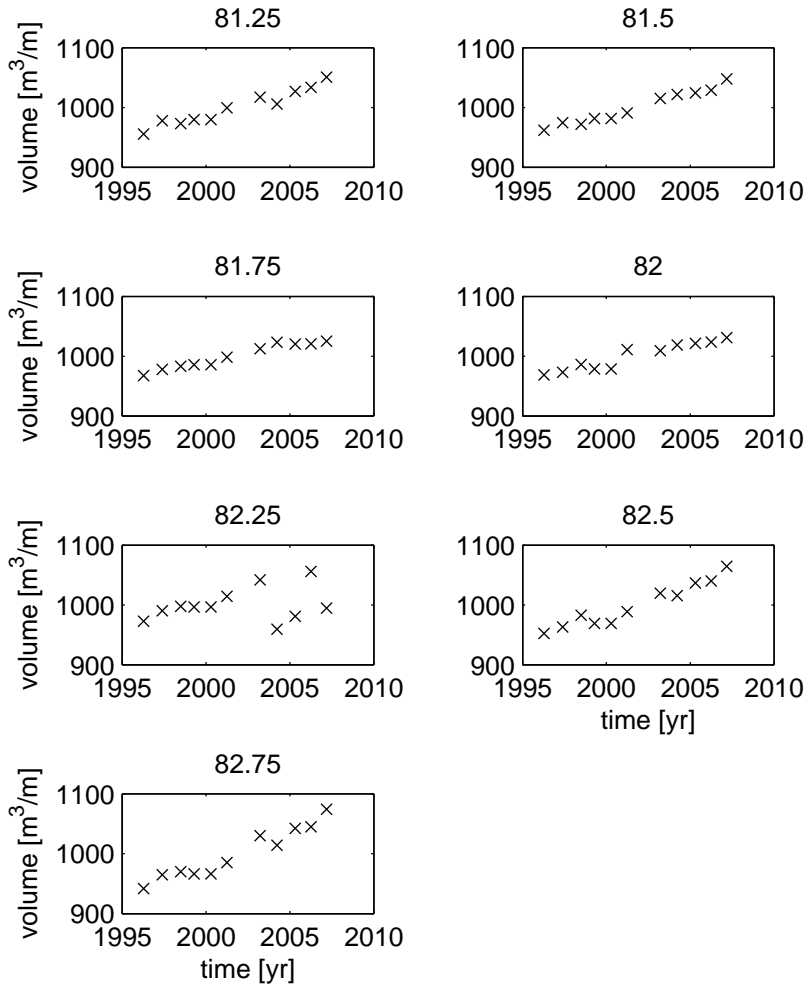


Figure 3.6: Volume development of the dune area at the Noordwijk transect locations.

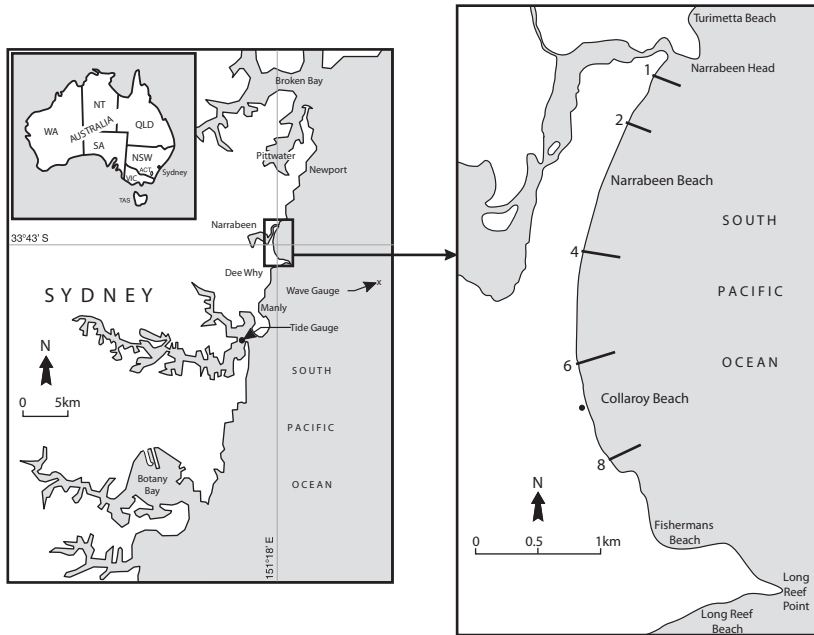


Figure 3.7: Overview of the Sydney field site. Adapted from Harley et al. (2011).

### 3.3 Analysis & Results

In order to analyze morphological variability in cross shore direction, 3 consecutive surveys (2 months blocks) are analyzed separately for every profile of the morphological datasets. The left panels of Figure 3.8 show three arbitrary consecutive surveys at a single transect location for each site. Differences between sites are highlighted as the axis scaling of the left panels in Figure 3.8 is identical. The Vlugtenburg cross shore beach profile is rather mild with respect to the Narrabeen and Noordwijk cross shore profile. The Narrabeen profile is significantly steeper than both Dutch beach profiles. Following the theory presented by Wright and Short (1984), this could possibly be explained by the differences in wave climate where Narrabeen is mainly swell dominated and the Dutch sites are mainly dominated by sea waves.

In the example depicted in the left panels of Figure 3.8 it is clear that the most landward part of the beach (above Mean Sea Level, MSL) is relatively static when compared to the seawards part of the beach (especially below MSL). The seaward end of the beach shows relatively large vertical variability of the local bed level. This difference in variability of the local bed level can be assessed using the vertical variance with respect to the mean profile of the three consecutive surveys. The corresponding vertical variance is shown in the right panels of Figure 3.8 where it is clearly shown that the variance of the bed level varies along the cross shore

profile.

### 3.3.1 Defining a discrete separation point between the marine and aeolian zone

The relatively large vertical variance measured at the seaward end of the beach (below MSL) indicates a relative dynamic zone most likely due to the influence of marine processes. The derived small vertical variance at the landward end of the beach (above MSL) indicates a relative static zone most likely due to the lack of marine processes and the limited effects of aeolian processes on the morphology. Using the right panels of Figure 3.8, a distinct separation point ( $S_p$ ) between the static upper beach and dynamic lower beach can be derived using an assumed threshold value for vertical variance ( $= 0.01 \text{ m}^2$ ).

The time series of measured transects allows to extract a time series of  $S_p$  for each location. Extracting  $S_p$ , overlapping windows of three consecutive surveys are used. At this stage, the vertical level of  $S_p$  is considered while the vertical level is comparable between transect locations and field sites. Figures 3.9-3.11 show an overview of the development of the vertical level of  $S_p$  for the three field sites. The left panels show the vertical level of the extracted  $S_p$  for all measured locations and for all time intervals considered. Some temporal and spatial variability is present. The right panels of Figures 3.9-3.11 show the spatial average over all alongshore transect locations. The spatial average can be used to focus upon the temporal variability.

The average level of  $S_p$  found is few meters above mean sea level at all three sites. It appears to be trivial that the found  $S_p$  levels correspond with the maximum level of which marine processes have influenced the profile morphology.

The  $S_p$  level derived at Narrabeen is generally higher than for the other two sites. While the tide range is similar between sites this is most probably due to the (swell) wave climate in combination with the relatively steep profile. Steep beach slopes and long period waves at Narrabeen lead to reflective conditions where runup levels are expected to be relatively high. This in contrast to the Dutch sites where profile slopes are milder and the wave climate is characterized by sea waves.

Focusing on the possible temporal variability due to marine processes, the level of the spatially averaged separation point at each site (Right panels of Figures 3.9-3.11) is used for autocorrelation and cross correlation with measured maximum water levels.

Autocorrelations of the timeseries of  $S_p$  levels indicate no significant seasonal (cyclic) behavior of  $S_p$  levels at any of the three sites. Timeseries of measured maximum water levels indicate no seasonal signal in measured maximum water levels at Narrabeen. For the Noordwijk and Hoek van Holland tide stations, significant seasonal signals with a period of 12-14 months are found in the measured maximum water levels.

Cross correlating the corresponding  $S_p$  levels with measured maximum water levels does not lead to significant (zero lag) correlations for the Noordwijk ( $r = -0.31$ ,  $p = 0.054$ ) and Narrabeen ( $r = 0.25$ ,  $p = 0.076$ ) site. For the Vlugtenburg

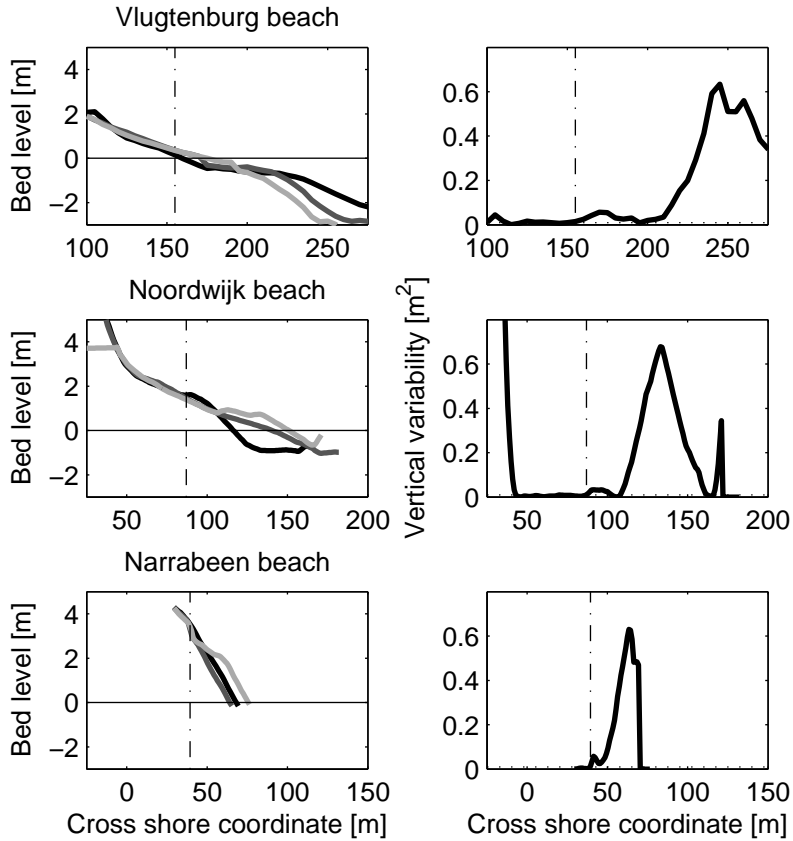


Figure 3.8: The left panels show two arbitrary cross shore morphological profiles measured consecutively at the three field sites. The right panels show the spatial distribution of the vertical variance with respect to the morphological profiles shown in the left panels. The vertical dash-dotted lines show the horizontal location of the generically derived separation point ( $S_p$ ).

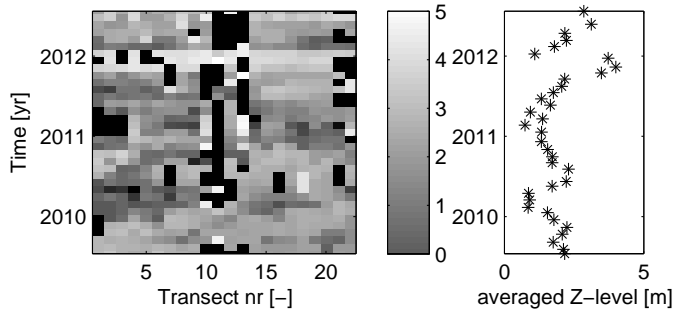


Figure 3.9: Derived separation points from Vlugtenburg data. Left panels colorbar indicates vertical level of  $S_p$  where missing values are filled in with black. Right panel shows a spatially averaged temporal variability.

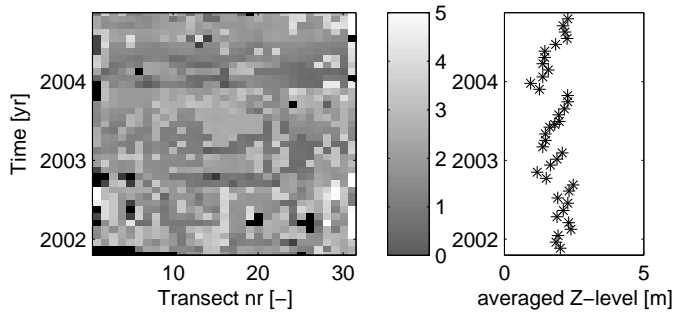


Figure 3.10: Derived separation points from Noordwijk data. Left panels colorbar indicates vertical level of  $S_p$  where missing values are filled in with black. Right panel shows a spatially averaged temporal variability.

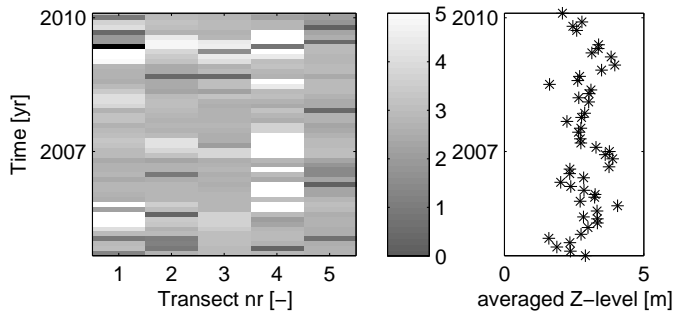


Figure 3.11: Derived separation points from Narrabeen data. Left panels colorbar indicates vertical level of  $S_p$  where missing values are filled in with black. Right panel shows a spatially averaged temporal variability.



site a small but significant correlation ( $r = 0.53$ ,  $p = 0.001$ ) is however found. The limited correlation with measured maximum water levels could mean that some other process governs the vertical extend of the marine influences. Wind and wave conditions as well as morphological feedback could be of important relevance.

Some spatial variability of the derived  $S_p$  level is present at all sites. Earlier analysis by de Vries et al. (2011b) have shown that  $S_p$  levels could possibly be governed partially by spatially varying foreshore parameters such as foreshore slope at this site. Spatial variability in  $S_p$  levels could also be associated with alongshore varying signatures in sedimentology such as the distribution of sediment after an event or a nourishment.

### 3.3.2 Separation point and profile development

To further illustrate the difference in cross shore morphological variability for each of the sites, additional examples are given. Figures 3.12, 3.13 and 3.14 show all measured profiles at arbitrary transect locations for the Vlugtenburg, Narrabeen and Noordwijk field sites respectively. For each of the examples the development of the vertical level as a function of time is shown at three cross shore locations. The three cross shore locations are such that the most landward point is located at the upper beach above maximum high tide levels and the most seaward point is around mean sea level.

It is shown that vertical variability is small at the most landward point considered at all three field sites. Large periods of limited vertical evolution are measured. Moving to the measured point into the more seaward direction it is shown that the vertical level is static during large periods of time at all three field sites. At some moment in time possibly during a marine event there is some large vertical change after which the bed level remains to be static again. Temporarily, the static upper beach has likely been dynamic due to high water levels. Considering a point at the seaward end of the beach, near the mean sea level line, the elevation time series show much more variability in time. This increased variability is likely governed by the regular occurrence of marine processes at this location.

Focusing on the example given in Figure 3.12, the local morphological situation at the cross shore location of 10 m has been governed by aeolian processes only. These aeolian processes did not account for large morphological variability. At a cross shore location of 40 m the local morphology has been determined by aeolian but also marine processes (after 2012). After 2012 the profile has been influenced by marine processes where the footprint of the marine processes remains unaltered by the proceeding period of aeolian conditions only. Therefore it could be concluded that, at this locations, while the induced morphological dynamics due to aeolian processes is much smaller than due to marine processes, the cross shore coastal profile at any time is much determined by preceding marine processes. At a cross shore location of 150 m, marine induced morphological dynamics overshadow any aeolian influences.

A similar conclusion can be drawn looking at the bottom panel (black stars) of Figure 3.13. After a large period of limited vertical changes at the considered

location an event in 2007 causes erosion in the upper profile and hence large morphological changes at the considered location. The large morphological change due to marine processes leaves a relatively large footprint on the morphology which is unlikely to be changed significantly on the short term by aeolian processes.

At the Noordwijk location shown in Figure 3.14, similar behavior is measured. At the most landward considered cross shore location (at the upper beach) measured vertical evolution is small relative to the more seaward locations.

## 3.4 Discussion

### 3.4.1 Marine-, aeolian processes and beach morphology

During the timescales considered, the aeolian zone shows morphological variability which is of smaller order than the morphological variability of the marine zone. This is illustrated by the distribution of variance in cross shore direction shown in Figure 3.8 and the examples of vertical bed level development at specific cross shore locations shown in Figures 3.12, 3.13 and 3.14.

In line with the concept presented in Figure 3.2, the morphological changes induced by marine processes are measured to be larger than morphological changes due to aeolian processes. The separation point between aeolian and marine processes can be identified while the change in vertical variance is explicit at the monthly timescale. The  $S_p$  levels are found to vary in time because during relatively short events (such as storms) the marine zone extends to cover the (under regular conditions) aeolian beach until the dunes inducing relatively large morphological changes at the dunefront but also at the (under regular conditions) aeolian beach.

At the Dutch sites considered, the dunes were growing implying that some aeolian activity was present. With the exception of events however, there have been no measured signs of significant accretion or erosion at the upper beach. On all three considered sites, the measured vertical variability due to aeolian processes only (at the upper beach) is very limited. As a result it seems plausible to assume that the measured temporal variability of the profile shape is mainly determined by (previous) marine processes. The assumption that beach morphology is mainly governed by marine processes could be valid for many coastal situations where marine processes regularly influence the beach. While properties of the beach (such as the beach slope discussed in Chapter 2) are likely to influence aeolian processes, aeolian processes could also be indirectly governed by marine conditions at many locations. This (in)direct coupling between the marine and aeolian system supports the earlier described concept by Short and Hesp (1982).

### 3.4.2 The intertidal zone as source area for aeolian transport

The aeolian zone in cross shore direction consists of the beach until the waterline and adjacent dunes. At the dutch sites, Noordwijk and Vlugtenburg, data of annual dune volume changes are available. Typical values of sedimentation at

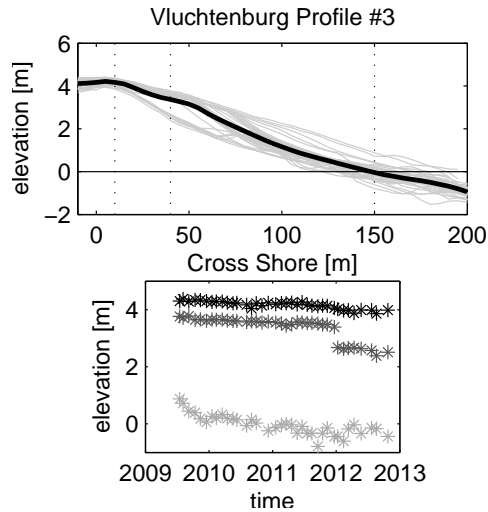


Figure 3.12: Top panel shows in gray all measured profiles at an arbitrary transect location at Vlugtenburg (profile #3). The black line represents the temporal mean of all gray profiles. At three cross shore locations the evolution of the bed level is plotted in time in the bottom panels. The three cross shore locations are indicated at the top panel with the vertical dotted lines.

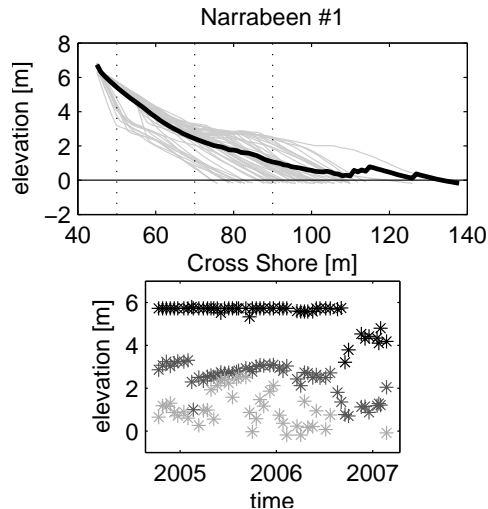


Figure 3.13: Top panel shows in gray all measured profiles at an arbitrary transect location at Narrabeen (profile #1). The black line represents the temporal mean of all gray profiles. At three cross shore locations the evolution of the bed level is plotted in time in the bottom panels. The three cross shore locations are indicated at the top panel with the vertical dotted lines.

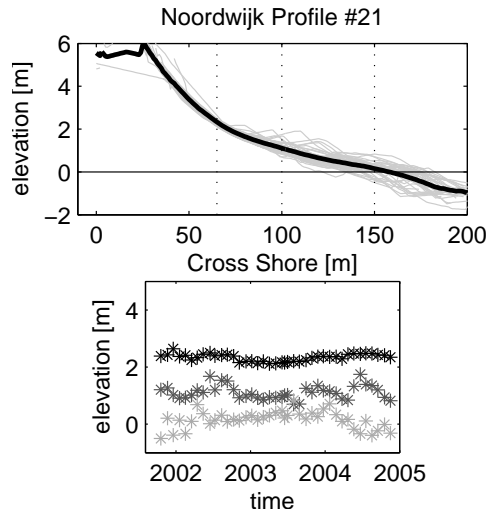


Figure 3.14: Top panel shows in gray all measured profiles at an arbitrary transect location at Noordwijk (profile #21). The black line represents the temporal mean of all gray profiles. At three cross shore locations the evolution of the bed level is plotted in time in the bottom panels. The three cross shore locations are indicated at the top panel with the vertical dotted lines.

the dunes are in the order of 5-10  $\text{m}^3/\text{m}/\text{yr}$  at Noordwijk and 20-40  $\text{m}^3/\text{m}/\text{yr}$  at Vlughtenburg (see Chapter 2 and Tables 3.2 and 3.3). Assuming the source for this sediment to be at the dry beach one might expect a significant decrease in bed level at the dry beach due to aeolian erosion of the dry beach. With a typical beach width of around 70-90 meters a general decrease in bed level in the order of 10-60 cm each year could be expected. Such a general decrease is not found in any of the analyzed measurements. As a result, the source for aeolian sediment transport towards the dunes should lie in the intertidal zone.

The intertidal zone separates the marine from the aeolian zone. At all three locations a clear separation point can be defined based on the spatial distribution of the vertical variability of the bed level. This point delineates the marine and aeolian zones. The vertical level of this separation point is located just above mean sea level. Where seaward of this point, morphological changes are much governed by marine processes. Landward of this point, morphological changes are governed by aeolian processes.

Previous authors have stressed the importance of the intertidal zone as an important zone for aeolian sediment transport processes (e.g. Carter (1976); van der Wal (1998)). The main physical argument for the intertidal zone to be important is that during high tide, marine processes rework the sediment bed and during low tide well mixed sediment at the bed is available for aeolian transport. On the dry beach where no marine processes occur, aeolian processes cause the grains at

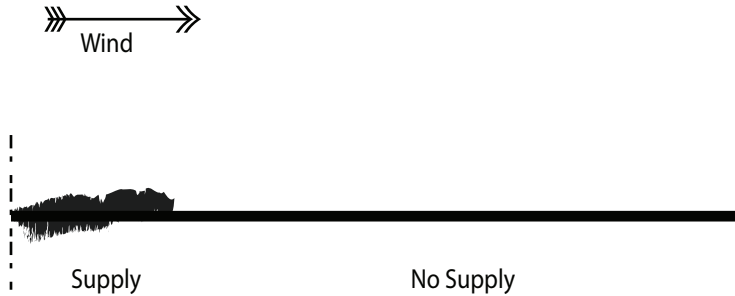


Figure 3.15: Spatial representation of the concept of supply and no supply zones.

the bed to be sorted over time where the light grains erode and the heavier grains stay behind. After a period of aeolian surface sorting, a desert pavement can prevent sediment grains to be picked up resulting in the sediment surface to stabilize. The occurrence of a relatively stable bed in the aeolian zone is supported by the presented data.

### 3.4.3 A model for spatial zonation

From the previous reasoning it could be assumed that the sand which is found in the dunes originates (partly at least) from the marine zone. This apparent supply from the marine zone to the aeolian zone could be due to the mobilization of sediment by wind in the intertidal zone during low water only. This mobilized sediment could then be transported in the direction of the dunes where the beach only allows for a transport zone where erosion and sedimentation is limited. Figure 3.15 shows a spatial representation of such a proposed system. In the proposed system of Figure 3.15 the beach remains static while sediment transport occurs from the intertidal zone towards the dunes. Since the proposed spatial representation is supported by the analyzed data, it provides a starting point when addressing aeolian transport processes on beaches. In the next Chapters (4 and 5) this spatial models is adopted to explain specific characteristics of aeolian sediment transport processes.

## 3.5 Conclusions

Based on the data analysis it is concluded that:

- Measured morphological changes, at the beach of the analyzed cross shore profiles, due to marine processes are significantly larger than morphological changes due to aeolian processes. A separation point between marine and aeolian zones can be extracted from consecutive morphological measurements. This separation point is found to be dynamic in time and space. This dynamic border can only partly be explained by fluctuations in water levels and

are most likely partly governed by wave conditions and local morphological conditions.

- The upper beach remains stable under aeolian forcing while limited morphological changes occur. Therefore no significant erosion or sedimentation due to aeolian transport is measured. These limited morphological changes at the upper beach indicate small transport gradients related to aeolian transports. The limited morphological activity at the upper beach could be attributed to armoring due to sediment sorting processes at the bed surface. Armoring of the surface layer occurs when the smaller and lighter sediment erodes leaving the heavier sediment which is more difficult to erode at the bed.

Due to the limited morphological activity at the upper beach, the upper beach is unlikely to function as a large source area for aeolian transport processes. A large sediment supply to the aeolian system is expected to originate from the intertidal zone. At the lower beach, tides cause aeolian processes to be interchanged with marine processes. Therefore armoring of the surface layer does not occur while marine processes mix the surface layer. As a result the sand at the surface layer of the intertidal zone is easier to erode than on the upper beach.

- Marine induced morphological changes appear to be of larger order than aeolian induced morphological changes. The shape of the profile at any time is therefore likely to be governed by (previous) marine processes rather than aeolian processes.

## Chapter 4

# Aeolian sediment transport rates in supply limited situations

### *A numerical implementation*

---

This chapter is submitted as an article to Aeolian Research (submitted April 2013). No changes have been made with respect to the AR submission other than this text.

The aim of this chapter is to present a new model to estimate aeolian sediment transport rates in supply limited situations. A 1D linear advection model is presented where sediment transport rates are calculated as a function of wind using traditional sediment transport formulations where a limited sediment supply magnitude is explicitly taken into account.

Lessons learned:

- The presented model successfully explains several physical observations such as the occurrence of a fetch effect, intermittency in sediment transport and the dominant role of supply.
  - Limited supply can cause fetch effects where sediment transport rates increase in the direction of the wind. The length of these fetch effects (critical fetch) is dependent on supply magnitude.
  - When supply is limited, variability in sediment transport rates show limited correlation with traditional sediment transport formulations. Alternatively, a linear relationship between wind and sediment transport could be adopted.
  - Fitting linear relationships between velocity and sediment transport rates to the simulated data, the magnitude of the fitted linear relationship provides information on source magnitude.
  - Field data collected at supply limited locations (beaches) provide evidence that linear relationships between wind and transport rates can also be found in the field and are governed by supply magnitude.
  - For the model to be applicable in future applications predicting aeolian sediment transport, threshold velocities should be accounted for and supply magnitudes should be a given. Gaining knowledge on the supply magnitude is of major concern while current quantitative knowledge on sediment supply is limited.
- 
-

## 4.1 Introduction

The aim of this paper is to present a new way of describing aeolian sediment transport on a beach. A general problem in modeling aeolian sediment transport on a beach is the over-prediction of the actual transport rate (Kroon and Hoekstra, 1990; Sarre, 1989; Sherman et al., 1998; Sherman and Li, 2012). Without notable exceptions, existing models to calculate aeolian sediment transport rates are based on higher power functions with respect to the wind induced shear velocity ( $u_*$ ) derived from the pioneering work by Bagnold (1954). Bagnold identified the main factors governing the aeolian transport rates ( $q$ ), in a wind tunnel and in a desert, as the grain diameter ( $d$ ) relative to a reference grain diameter ( $D$ ), the air density ( $\rho$ ), the gravitational acceleration ( $g$ ), the drag velocity ( $u_*$ ) and an empirical coefficient ( $C_b$ ).

$$q = C_b \frac{\rho}{g} \sqrt{\frac{d}{D}} (u_*)^3 \quad (4.1)$$

This work was followed by Kawamura (1951) who slightly reformulated the equation and added a threshold drag velocity ( $u_{*t}$ ).

$$q = C_k \frac{\rho}{g} (u_* - u_{*t})(u_* + u_{*t})^2 \quad (4.2)$$

The threshold drag velocity is dependent on the grain diameter ( $D$ ), the gravitational acceleration ( $g$ ), the density of the sand grains ( $\rho_s$ ), the density of the air ( $\rho$ ) and an empirical coefficient ( $A$ ) (Bagnold, 1954).

$$u_{*t} = A \sqrt{Dg(\rho_s - \rho)/\rho} \quad (4.3)$$

In some studies (e.g. Bagnold, 1954; Arens, 1996) Equations (4.1), (4.2) and (4.3) are pragmatically adapted towards:

$$q = \alpha C_b \frac{\rho}{g} \sqrt{\frac{d}{D}} (u - u_t)^3 \quad (4.4)$$

where wind speed is written instead of drag velocity. Parameter  $\alpha$  accounts for the conversion between the drag velocity and wind velocity where a logarithmic velocity profile is assumed.

For beach situations, several authors have formulated similar relations and compared measured sediment transport rates with modeled sediment transport rates with variable success and only after modifying calibration parameters to match sediment transport rates, see Sherman and Li (2012) and references therein for an overview. Calibration parameters are commonly stated to be functions of supply limiting environmental parameters (Nickling and Davidson-Arnott, 1990). Generic methods to derive calibration parameters are unavailable which limits the predictive skill of any of the present sand transport models (Sherman and Li, 2012). On beaches, sediment supply is governed by various variables (Houser,



2009). Relevant variables on beaches are surface moisture content (Davidson-Arnott et al., 2005), beach slope (Hardisty and Whitehouse, 1988; de Vries et al., 2012), fetch length (Bauer and Davidson-Arnott, 2002), the presence of vegetation (Arens, 1996) and the presence of lag deposits armoring the sand surface layer (van der Wal, 1998)

Some of these supply variables vary on timescales in the (order minutes to hours). Process measurements have confirmed that sediment transport rates at a beach are very variable due to supply limiting effects (Davidson-Arnott et al., 2005; Bauer et al., 2009; Davidson-Arnott and Bauer, 2009).

While the range of discussed governing parameters is large, variability in transport rates are often ascribed to a combination of wind direction and beach geometry resulting in a 'fetch effect' (see Delgado-Fernandez (2010) for an overview). The fetch effect is an increase of the aeolian sediment transport rate with distance downwind over an erodible surface. The fetch distance required to reach the wind driven transport capacity is called critical fetch distance (see Figure 4.1 for a conceptual representation after Bauer and Davidson-Arnott (2002)). Various reports are available on the effect of fetch, where the measured critical fetch distances measured in the field vary from 20-200 m (Davidson-Arnott and Law, 1990; Davidson-Arnott et al., 2008) to no measured fetch effects at all (Lynch et al., 2008; Jackson and Cooper, 1999).

Mechanisms responsible for fetch effects and the existence of a critical fetch on beaches are described by Delgado-Fernandez (2010) to be:

1. The onset of a saltation cascade increasing sediment transport until wind driven transport capacity is met.
2. The reduced rate of particle ejection.

Where (1) is typically relevant when sediment supply is abundant and critical fetch distances are short, (2) represents a fetch effect related to supply limitation. Especially the longer measured fetch distances (up to several hundreds of meters) are suggested to occur due to this reduced particle ejection rate (Delgado-Fernandez, 2010).

On beaches, sediment is transported across the beach during onshore or oblique onshore winds. During (oblique) onshore winds, there is no sediment supply at the seaward side of the waterline. As a result, the region of increasing sediment transport rates in the direction of the wind due to the fetch effect starts with zero sediment transport at the waterline. The spatial area of increase in sediment transport rates adjacent to the waterline often includes the intertidal zone. In the intertidal zone, both fetch distance and ejection rate are dynamic variables. Aeolian transport in the intertidal zone could be governed by variable moisture content of the sand surface, intertidal morphology (ridge and runnel systems) in combination with fetch distance (Anthony et al., 2009) and salt crust formation. Within the tidal cycle the fetch distance varies but also lag deposits are reworked by wave action resulting in a renewal of sediment that is available for transport (Carter, 1976). Therefore, within a tidal cycle the sediment supply can increase.

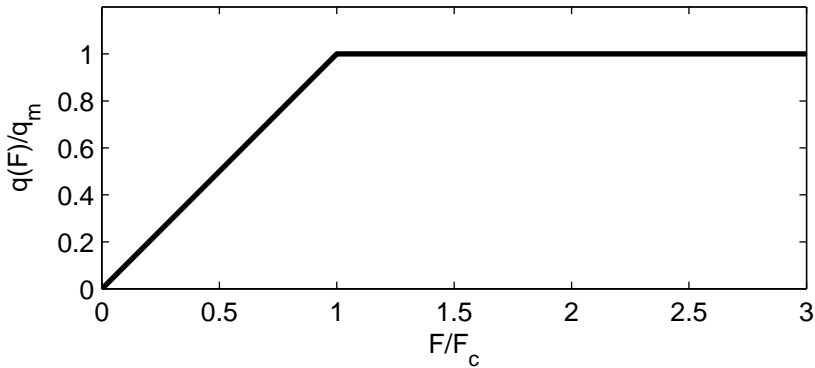


Figure 4.1: Conceptual representation of the fetch effect, where transport increases with increasing fetch towards a certain limit. Reference is made to Bauer and Davidson-Arnott (2002) who suggests similar curves including a smoother transition between the increasing and stable transport.

Following this reasoning, van der Wal (1998) suggests that at low tide and during onshore winds, transport initiated at the intertidal zone could be an important source for sediment transport towards the dunes. This is also supported by the review of Houser (2009).

Current state-of-the-art saltation models predicting aeolian sediment transport rates, often include a parameter which could represent fetch effects. For instance Sauermann et al. (2001) include a parameter (their  $\gamma$ ) to account for a time or length scale of saturation transients. However, the possibility of implementing supply limitations by limiting ejection rates is currently not explored.

This paper aims to gain insight in the spatial and temporal development of aeolian sediment transport rates and gradients. An idealized model is proposed to capture the many facets of supply limitations. In the next section the model concept is formulated together with its equations and spatial domain. Then the results of three particular cases are used to illustrate the model's potential of representing physical processes. In the following section a comparison with field data is made followed by a discussion and conclusion.

## 4.2 Model concept

The proposed model aims to calculate wind driven aeolian sediment transport rates and the sediment exchange with the bed while sediment availability could vary in space and time. Therefore, two sediment concentration ( $C$  [ $\text{kg}/\text{m}^3$ ]) parameters are defined: 1. the sediment concentration corresponding to the equilibrium concentration related to wind forcing ( $C_u$ ); 2. the actual sediment concentration ( $C_c$ ). Additionally, a layer of erodible sediment at the bed ( $S_e$ ) is defined which accommodates potential deposition and indicates the supply potential. These three

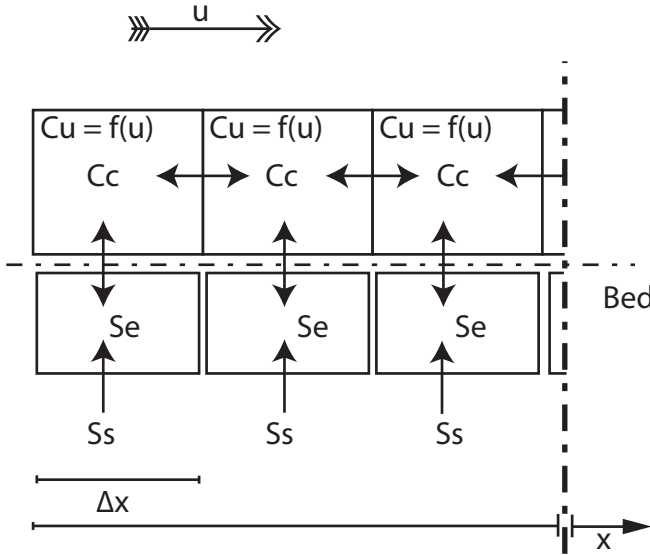


Figure 4.2: Arrangement of the spatial domain indicating concentration parameters where:  $S_e$  is the available sediment on the bed;  $C_c$  is the sediment concentration of the air;  $C_u$  is the wind driven sediment concentration via a sediment transport formulation.

sediment parameters are calculated following the arrangement presented in Figure 4.2.

It is assumed that the sediment speed is proportional to the wind speed. As a result, sediment concentrations ( $C$ ) and sediment transport rates ( $Q$  [ $\text{kg}/\text{m}^2\text{s}$ ]) are related via:

$$Q = u_w C \quad (4.5)$$

where  $u_w$  is the wind velocity at some height (often 10 m) above the bed.

To calculate the equilibrium concentration corresponding to the wind driven sediment transport capacity, a Bagnold type (3<sup>rd</sup> power) function is applied. For the purpose of focusing on wind ( $u_w$  [ $\text{m}/\text{s}$ ]) only as a varying parameter keeping all other parameters constant, the 3<sup>rd</sup> power function (Equation (4.1) assuming a logarithmic velocity profile) is simplified towards:

$$Q_u \propto u_w^3 \quad (4.6)$$

where  $Q_u$  [ $\text{Kg}/\text{m}^2\text{s}$ ] represents the wind driven sediment transport capacity. The 3<sup>rd</sup> power function implies the sediment concentration ( $C$  presented in Equation (4.5)) to be proportional to  $u_w^2$ . As a result:

$$C_u = \propto u_w^2 \quad (4.7)$$

For practical reasons the 3<sup>rd</sup> power sediment transport formulation is normalized to generate 1 at  $u_w = 10$  m/s

Referring to the spatial arrangement presented in Figure 4.2, a one dimensional linear advection model is adopted:

$$\frac{\partial hC_c}{\partial t} + \frac{\partial uhC_c}{\partial x} = E - D \quad (4.8)$$

where  $h$  is the height of the saltation layer and  $u$  is the sediment speed assumed to be proportional to  $u_w$ . At this stage  $h$  is assumed to be constant in space and time and  $u$  can vary in time but is assumed to be constant in space.

$D$  is the potential deposition per spatial entity consisting of the existing concentration times the height divided by a timescale for deposition.

$$D = \frac{hC_c}{T_1} \quad (4.9)$$

$E$  is the erosion per spatial entity which can be supply limited. The magnitude of  $E$  can be controlled by the equilibrium concentration as an upper limit or by the potential deposition  $D$  increased by the available erodible sediment at the bed ( $S_e$ ). Both possibilities could have different timescales.

$$E = \min \left( \frac{hC_u}{T_2}, \frac{hC_c + S_e}{T_3} \right) \quad (4.10)$$

Substituting (4.9) and (4.10) in (4.8) gives :

$$\frac{\partial C_c}{\partial t} + u \frac{\partial C_c}{\partial x} = \min \left( \frac{C_u}{T_2}, \frac{C_c + S_e/h}{T_3} \right) - \frac{C_c}{T_1} \quad (4.11)$$

There are three distinct timescales formulated and used in Equation 4.11. These timescales represent different timescales of sediment pick up and sediment deposition. While all three timescales are a measure of interaction between saltating sediment and the bed surface, it could be argued that the timescale of saltation for an individual grain can be used as a proxy for all three timescales. Therefore it seems reasonable to assume that to first order  $T = T_1 = T_2 = T_3$ . This assumption reduces Equation (4.11) to:

$$\frac{\partial C_c}{\partial t} + u \frac{\partial C_c}{\partial x} = \frac{\min(C_u - C_c, S_e/h)}{T} \quad (4.12)$$

Davidson-Arnott et al. (2008) report that the saltation system responds very quickly to fluctuations in windspeed (O 1-2 s.). Therefore we initially choose  $T = 1$  s.

The magnitude of erodible sediment at the bed is defined by the difference in erosion and deposition increased by the external supply at the bed; the ejection rate ( $S_s$ ).

$$\frac{\partial S_e}{\partial t} = S_s - \frac{\min(C_u - C_c, S_e/h)}{T} \quad (4.13)$$

$C_c$	Sediment transport concentration	Kg/m <sup>3</sup>
$h$	Height of the transport layer	m
$u$	Sediment velocity	m/s
$E$	Erosion	Kg/m <sup>2</sup> s
$D$	Deposition	Kg/m <sup>2</sup> s
$C_u$	Equilibrium concentration	Kg/m <sup>3</sup>
$Q$	Sediment transport rate	Kg/m <sup>2</sup> s
$Q_u$	Wind driven transport capacity	Kg/m <sup>2</sup> s
$S_e$	Amount of erodible sediment at the bed	Kg/m <sup>2</sup>
$S_s$	Ejection Rate at the bed	Kg/m <sup>2</sup> s
$T_1$	Timescale of deposition	s
$T_2$	Timescale of erosion (pick up)	s
$T_3$	Timescale of erosion (pick up)	s
$T$	Timescale for adapting sediment concentrations	s
$\lambda$	Spatial fraction of the supply zone (between 0-1)	-

Table 4.1: List of Symbols

Equations (4.12) and (4.13) are used as governing model equations in the remainder of this paper. In all cases it is assumed that at the initial stage  $t = 0$  there is no erodible sediment present at the bed ( $S_e(x, 0) = 0$ ) and there is no sediment in transport ( $C_c(x, 0) = 0$ ). Moreover, it is assumed that there is no sediment supply from the upwind boundary at any time ( $C_c(1, t) = 0$ )

Supply limitation on beaches implies the existence of zones where sediment is relatively difficult to pick up and zones where sediment is relatively easy to pick up. To illustrate the presented model it is chosen to adopt a situation where at low tide the intertidal zone at the upwind side of the domain governs the sediment supply. At the upper beach adjacent to this supply zone, supply is assumed to be negligible due to the limiting effects of armoring of the bed surface layer. Comparable physical situations are to some extent described by Carter (1976) and van der Wal (1998).

Total supply at the supply zone is a function of the dimension of the supply zone and the sediment ejection rate at the bed. At this stage it is assumed that the ejection rate is constant in time and that in cases where the ejection rate is larger than can be eroded by wind, 'ejected' sediment directly accumulates at the bed. Physically this could represent a drying beach where sediment is 'ejected' in a passive system and could later be mobilized when wind speeds increase.

Figure 4.3 shows this idealized system where a discrete zone of supply and no-supply is indicated. Winds are assumed to blow from left to right leading to transport from the supply zone over the no-supply zone towards the downwind boundary. The spatial domain consists of a 100 m long line element where this distance represents the typical order of beach width. The supply zone is represented by some fraction ( $\lambda$ ) of the total length of the domain originating from the most upwind point. Unless otherwise stated  $\lambda$  is initially assumed 0.2 which leads

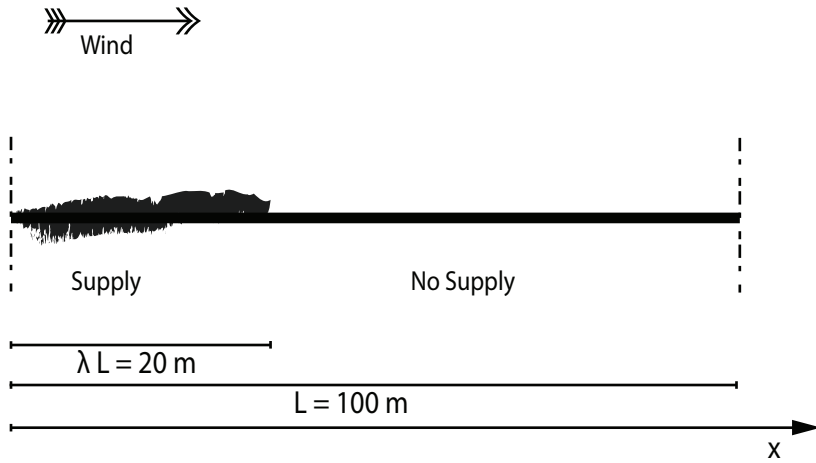


Figure 4.3: Simple schematic of a supply limited system. Winds are assumed from left to right.

to a 20 m supply zone.

## 4.3 Results

Three test cases are discussed where in each case either wind speed ( $u_w$ ) or ejection rates ( $S_s$ ) are varied. The total supply magnitude can also be varied while varying  $\lambda$  rather than ejection rates, results are found to be similar downwind of the supply zone. Therefore only ejection rates are varied to illustrate the concept of supply limitations.

### 4.3.1 Test Case I; Continuous wind

In the first test case a continuous constant wind of 7.5 m/s is applied. The constant wind leads to a steady state solution in time. Figure 4.4 shows the steady state solutions of the spatial distribution of the sediment transport rates while ejection rates in the supply zone are varied. Ejection rates outside the supply zone are assumed zero indicating a non erodible layer.

It is shown that sediment transport rates increase in the direction of the wind over the supply zone. Where no supply is present the transport rates are constant. When supply is relatively small ( $\beta < 1$  in Figure 4.4), maximum transports are reached at the downwind border of the supply zone. When supply is sufficiently large to achieve the wind driven transport capacity in the supply zone ( $\beta > 1$  in Figure 4.4), maximum sediment transport rates occur somewhere in the supply zone. The exact location of this maximum is a function of both wind speed and supply magnitude.

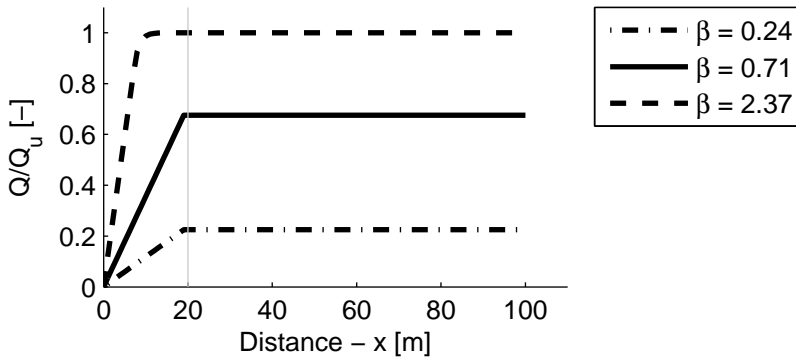


Figure 4.4: Spatial distribution of modeled sediment transport rates ( $Q$ ) normalised with wind driven transport capacity ( $Q_u$ ) with constant wind ( $u = 7.5$  m/s). Source magnitude is varied using parameter  $\beta$  which represents the spatially integrated source magnitude normalized with the wind driven transport capacity (if  $\beta < 1$  supply is smaller than wind driven transport capacity). The vertical gray line indicates the border of the supply/no supply zones.

Where supply is limited, transport at any location is governed by ejection rates. When upwind supply is larger than the transport capacity of the wind, the transport capacity of the wind determines the transport rates.

In case the wind driven transport capacity is reached in the supply zone. The abundant supply in the supply zone (downwind of the maximum in sediment transport rates) accumulates over time resulting in an increasing sediment availability at the bed ( $S_e$ , not shown).

### 4.3.2 Test Case II; Increasing and decreasing winds

In practice, beach situations winds fluctuate and therefore wind fluctuations are introduced in this case. The temporal development of the applied wind time series start with a period of constant moderate wind (6 m/s) followed by a very mild wind (4 m/s). The relatively mild wind is followed by a constant strong wind (9 m/s), see right top panel of Figure 4.5. Figure 4.5 also shows the spatial and temporal distributions of sediment transport calculated for these wind series. The left panels indicate the sediment transport rates ( $Q$ ) normalized with the equilibrium sediment transport rates when  $u = 10$  m/s ( $\max(Q_u)$ ).

At  $t = 150$  s. and  $t = 300$  s. the left panels show a steady state solution where the wind driven transport capacity ( $Q_u$ ) is reached similar to the situation described in the previous test case. The middle panels show that the surplus of source material leads to an increase in erodible sediment at the bed in the supply zone.

At  $t = 450$  s. the left panel indicates a steady state solution where the wind

driven sediment transport capacity is lower than at the previous interval. The middle panel shows the continuation of sediment build up in the supply zone. Moreover, while wind decreases the transport capacity of the wind decreases. As a result, an overload situation occurs causing sedimentation over the entire domain.

At  $t = 600$  s. the wind has increased again, as has the transport capacity of the wind. As a result the sediment available at the bed is picked up. Moreover, the sediment that has been accumulated in the supply zone is gradually picked up by the wind. The left panel shows that the sediment transport concentration is relatively large (equal to the transport capacity) in the supply zone since the previously deposited sand in this area is eroding. The middle panel indicates that the erodible sediment stored at the bed during previous conditions is partly re-mobilized resulting in erosion over the entire domain.

At  $t = 750$  s. and  $t = 900$  s. the erosion of the previously accumulated source material continues. Left panels show the re-mobilization of the previously accumulated sediment. The sediment transport concentration at the downwind boundary reaches temporally high values (equal to the transport capacity) since abundant sediment is available for transport. When all the previously accumulated sand is re-mobilized and transported to the downwind boundary a new steady state solution is found at  $t = 900$  s. The steady state at  $t = 900$  s represents a supply limited solution. The middle panels show that since sand is re-mobilized no sediment concentration at the bed is present.

The right panels show the temporal variability of the wind, the sediment transport concentration at the downwind boundary ( $x = 101$  m) and the sediment transport rates at the downwind boundary. The bottom right panel indicates that the actual sediment transport rates deviate from the wind driven sediment transport capacity at some occasions. The temporal variability of the calculated sediment transport rates at the downwind boundary are the results of temporal variability in the wind speed but also due to the temporal variability in sediment availability in the supply zone. This temporal variability of supply in the supply zone is in this case governed by the accumulation of sediment during relatively mild winds and the re-mobilization of supply during relatively high winds.

### 4.3.3 Test Case III; Random wind (short term variability)

In reality winds fluctuate on the timescale in the order of seconds. To model short term variability in wind conditions a time series of wind conditions is generated using a random generator. Winds fluctuate randomly between 0 and 10 m/s leading to a mean wind speed of 5 m/s where variability around the mean is normally distributed. These chosen values are not necessary representative for real life conditions but allows for including the concept of wind fluctuations.

Results are shown in Figure 4.6 where the right panels show the fluctuating winds and the corresponding fluctuating sediment transport concentrations and sediment transport rates at the downwind boundary of the assumed domain.

The left and middle panels show again snapshots of the spatial distribution of the sediment transport concentration (normalized with  $\max(Q_u)$ ) and the erodible



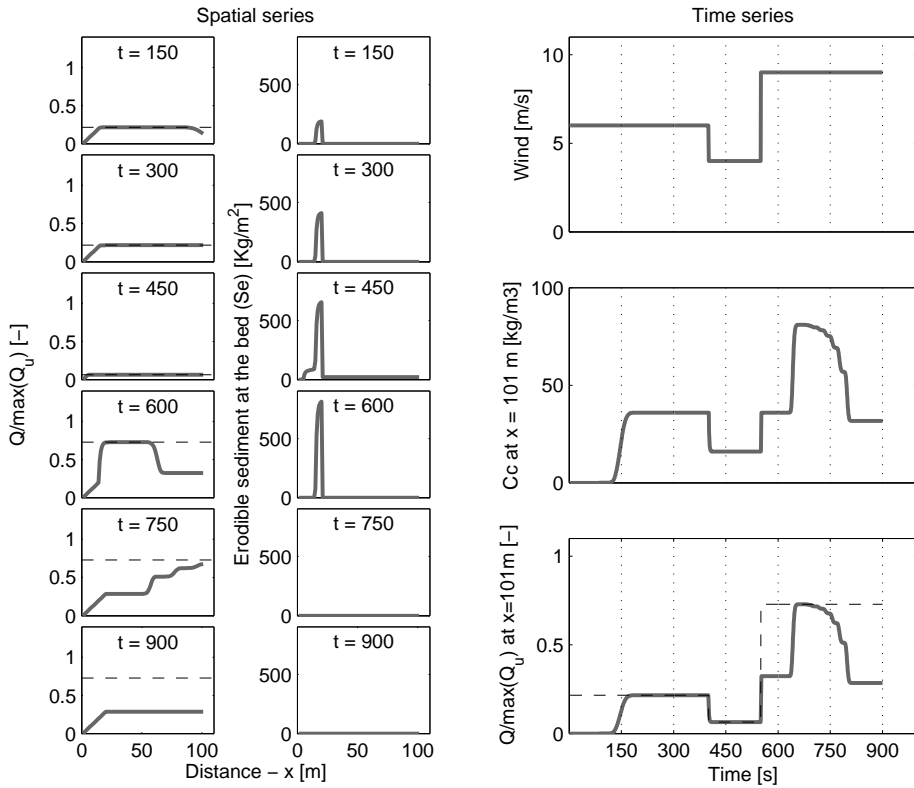


Figure 4.5: Left panels show snapshots in time of the spatial distribution of the sediment transport concentration. Middle panels show snapshots in time of the spatial distribution of the sediment concentration at the bed. Right panels show the time series of the wind (top), the time series of the sediment transport concentration at  $x = 101$  m (middle), the time series of the sediment transport rates (normalized with  $\max(Q_u)$  when  $u = 10$  m/s) at  $x = 101$  m (bottom). Dashed lines in left panels and right bottom panel indicate the momentary value of the wind driven sediment transport capacity. Vertical dotted lines indicate the relevant snapshot times for the left and middle panels.

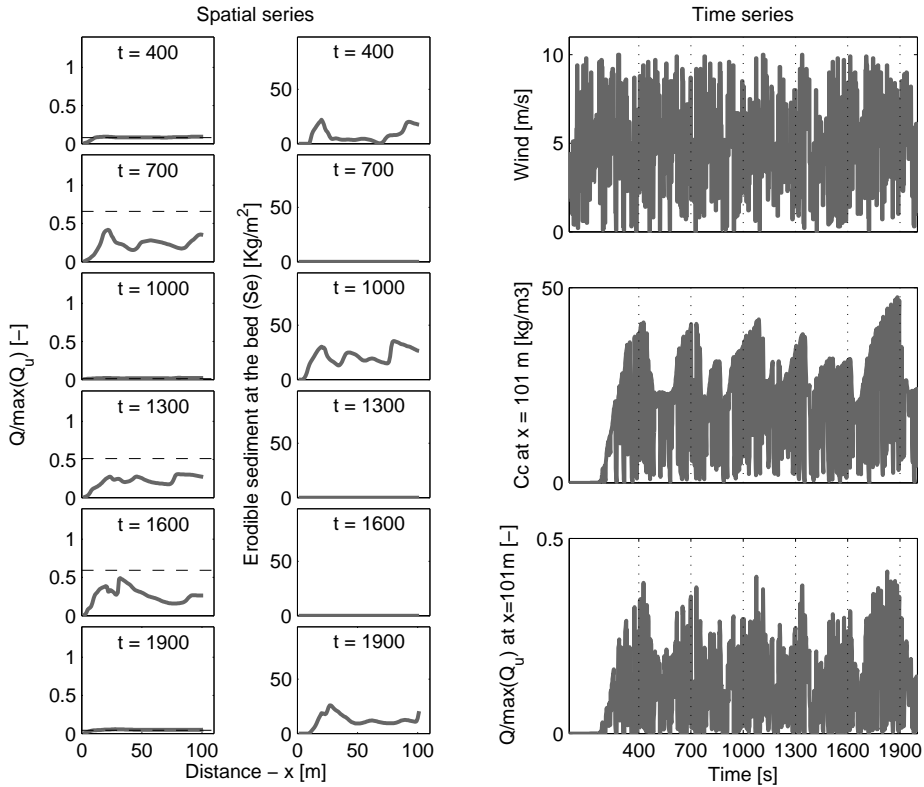


Figure 4.6: Left panels show snapshots in time of the spatial distribution of the sediment transport concentration. Middle panels show snapshots in time of the spatial distribution of the sediment concentration at the bed. Right panels show the time series of the wind (top), the time series of the sediment transport concentration at  $x = 101$  m (middle), the time series of the sediment transport rates at  $x = 101$  m (bottom). Dashed lines in left panels indicate the momentary value of the wind driven sediment transport capacity. Vertical dotted lines indicate the relevant snapshot times for the left and middle panels.

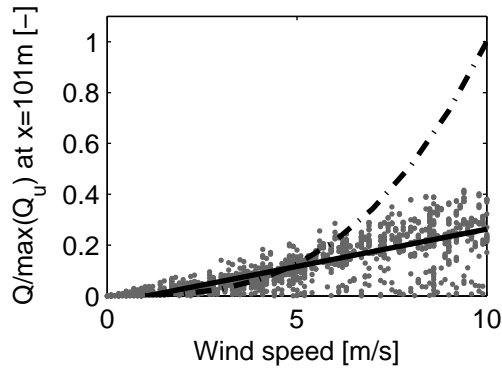


Figure 4.7: Relation between wind speed and sediment transport rates at the downwind boundary. The gray dots represent the data presented in the right panels of figure 4.6. The solid line represents the linear fit ( $R^2 = 0.83$ ). The dash-dotted line indicates the used sediment transport formulation for sediment pick up.

sediment at the bed. It shows that while winds are fluctuating on a short timescale, very often no wind driven transport capacity is reached. When winds are relatively mild ( $t=400$  &  $t=1000$  &  $t=1900$ ) and wind driven transport capacity is reached, sedimentation occurs indicated by the positive sediment concentration available for transport ( $S_e$ ). This sedimentation is temporary and the proceeding stronger winds re-mobilize the sediment.

Figure 4.7 shows the relation between wind and calculated sediment transport rates ( $Q$  [kg/s]) at the downwind boundary. The calculated sediment transport rates deviate from the initial 3<sup>rd</sup> power sediment transport function, especially when wind speeds are relatively large.

A linear model is fitted providing a significant fit ( $R^2 = 0.83$ ). The linear fit represents:

$$Q(t) = \bar{C}_c \times (u_w(t) - u_t) \quad (4.14)$$

where  $\bar{C}_c$  represents the mean sediment transport concentration and  $u_t$  a threshold wind velocity. While this threshold could be expected to be zero based on Equation (4.7), it is found that due to a combination of supply limitations and erosion/sedimentation timescales ( $T$ ) the fitted threshold velocity is slightly positive for the considered case ( $u_t = 1.03$  m/s).

Assuming a supply limited system where the total supply is mobilized towards the downwind boundary, it could be assumed that the total transport, during a given period ( $P$ ), at the downwind boundary equals the supply during that same period. Therefore, the total sediment supply can be estimated using:

$$\int_{t=0}^P \int_{x=0}^L \frac{S_s(x)}{h} dx dt \approx \int_{t=0}^P Q_{(x=101m)}(t) dt \quad (4.15)$$

Equations (4.14) and (4.15) provide an explicit link between a fitted (linear) relation for sediment transport rates as a function of wind speed and supply magnitude. This link could be used determining variability in supply magnitude when analysing field data.

## 4.4 Comparison with field data

There are several datasets available where wind speed and sediment transport rates are collected at the beach (see amongst others Arens (1996); Davidson-Arnott et al. (2005); Jackson and Cooper (1999)). Based on the theoretical approach presented in this paper it could be argued that when interpreting these data, fitting linear trends could provide parameters related to the supply limited system. The variable of interest is variability in supply magnitude over space and time.

As a first step however, it should be validated if the linear fit is providing similar or possibly better results than the conventional 3<sup>rd</sup> power fit. Therefore, linear and 3<sup>rd</sup> power functions are fitted to data previously collected and presented by Arens (1996).

Arens (1996) has collected data on aeolian transport on the Dutch site of Schiermonnikoog during a period of about three months. Sediment transports were measured using saltiphones which counts the number of impacts of sand grains on a microphone. A wind station was used to measure wind speed and direction at 5 m above the sand surface on the beach. Subsets of the data are selected based on the activity of the aeolian system and further specified in Arens (1996) (their Table 1). In this paper the same data subsets are used for analysis and the results table presented in Arens (1996) is updated.

In an effort to describe aeolian sediment transport as a function to wind speed, Arens (1996) has fitted 3<sup>rd</sup> power relationships between wind speed and sediment transport (saltiphone counts). In this paper linear relationships are added to the analysis and the fit quality is added represented by ( $r$ ). The results are shown in Figure 4.8 and Table 4.2. A nonzero intersect with the velocity axis can be derived indicating that a threshold velocity is present. As a result the fitted linear relation can be written after Equation (4.14) as:

$$Q_s(t) = \begin{cases} \bar{C}_{cs} \times (u_w - u_t) & \text{if } u_w > u_t \\ 0 & \text{if } u_w < u_t \end{cases} \quad (4.16)$$

where  $Q_s$  [counts m<sup>-2</sup>] represents the measured sediment transport rate with the saltiphone and  $C_{cs}$  [counts m<sup>-3</sup>] is the derived proxy for sediment concentrations based on the saltiphone measurements. Currently there are no methods available to convert the sediment transport rates based on counting grains towards sediment volumes (or total sediment mass) however, a relationship close to linear could be expected.

The fitted 3<sup>rd</sup> power function is similar to the function previously fitted by Arens (1996) rewritten as:

$$Q_s(t) = A_s \times (u_w - u_t)^3 \quad (4.17)$$

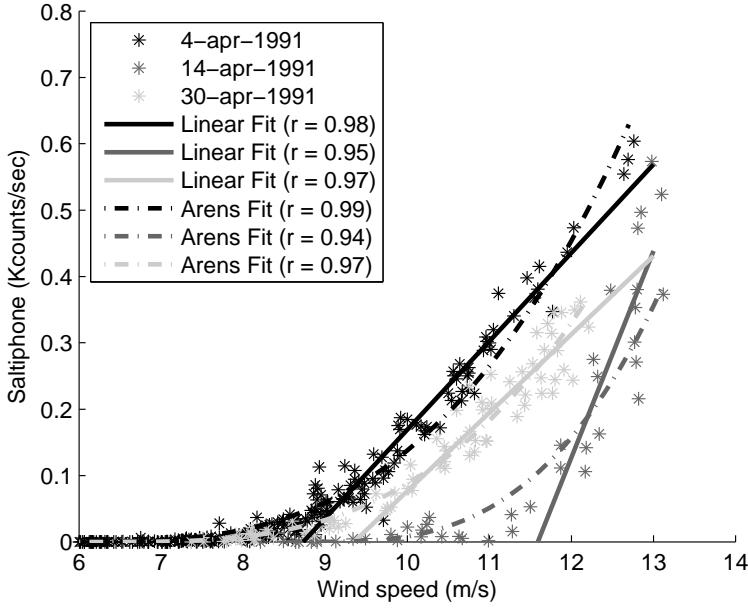


Figure 4.8: Data presented in Arens (1996) where the initial higher order fit (see Arens (1996) for details) is given as well as the linear fit.

where in line with Equation (4.4):

$$A_s = \alpha C_b \frac{\rho}{g} \sqrt{\frac{d}{D}} \kappa \quad (4.18)$$

where  $\kappa$  [counts/Kg] accounts for the (assumed linear) conversion between counted sediment and sediment mass. As a result,  $A_s$  [counts  $s^2$   $m^{-4}$ ] is a non dimensionless parameter which is composed of several unknown variables consisting of a combination of physical and empirical parameters. Due to the large range of empirical and physical parameters it is very difficult to relate values for  $A_s$  after fitting data back to these governing parameters.

For the cases shown in Figure 4.8 and Table 4.2 it is shown that the linear fit provides a similar quality fit ( $r$ ) than the conventional 3<sup>rd</sup> power fit. Some variability is present in both parameters indicating that both the threshold wind velocity and the sediment concentration ( $C_{cs}$ ) vary in time.

The advantage is that the linear fit provides not only an aggregated value for threshold velocity but also a direct estimation of the average sediment concentration ( $\bar{C}_{cs}$ ) which can be used to derive a measure for supply using Equations (4.14) and (4.15). Based on this reasoning, supply could possibly indexed as a function of additional parameters not excluding the parameters presented in Equation (4.18).

Survey period: 3 March - 27 May 1991							
Day nr.	Duration (hours)	Linear fit			3rd power fit		
		$\bar{C}_{cs}$	$u_t$	$r$	$A_s$	$u_t$	$r$
78	1	0.167	9.9	0.80	0.033	8.1	0.80
78	22	0.177	12.6	0.65	0.067	11.3	0.61
80	1	0.037	14.7	0.57	0.181	14.4	0.45
83	6	0.085	9.0	0.96	0.036	7.8	0.96
84	40	0.121	8.8	0.96	0.010	5.9	0.95
89	4	0.019	8.4	0.86	0.014	7.4	0.87
91	3	0.017	0.1	0.27	0.026	7.8	0.12
94	42	0.133	8.7	0.98	0.010	5.9	0.99
97	19	0.258	10.6	0.97	0.026	8.0	0.97
98	5	0.045	10.4	0.53	0.096	10.0	0.37
101	5	0.012	6.9	0.63	0.007	5.9	0.60
103	7	0.311	11.6	0.95	0.024	8.8	0.94
105	32	0.016	1.7	0.19	0.039	9.4	0.03
114	2	0.025	7.3	0.97	0.149	7.0	0.95
115	10	0.060	8.1	0.90	0.016	6.7	0.91
116	11	0.074	8.3	0.97	0.019	6.7	0.97
117	3	0.036	7.8	0.96	0.020	6.7	0.95
120	14	0.118	9.4	0.97	0.009	6.4	0.97
121	13	0.047	8.7	0.79	0.013	7.2	0.76
121	7	0.141	11.1	0.71	0.040	9.5	0.69
122	5	0.047	11.6	0.59	0.013	9.6	0.58
124	8	0.319	10.6	0.89	0.161	9.4	0.90
134	25	0.035	11.2	0.29	0.042	9.3	0.26

Table 4.2: Fitting parameters fitting linear and 3rd power functions to the Arens (1996) data. The 3rd power results are identical to the Arens (1996) results. The gray rows represent the data plotted in Figure 4.8

## 4.5 Discussion

### 4.5.1 Supply limited vs Abundant supply

In situations where supply is abundant (wind tunnels, deserts), Bagnold type formulations have been confirmed by many authors to represent the relevant physical parameters for aeolian sediment transport. Results from the presented supply limited model suggest that when supply is limited (and constant), a linear relationship between wind speed and sediment transport rates is to be expected. Therefore a distinction between regimes and representative models could be appropriate. To explore these different regimes and the inevitable transitions between them, the supply limited model is used for different magnitudes of supply from a situation where there is hardly any supply to a situation where supply is abundant. Figure 4.9 shows the results of fitting linear and 3<sup>rd</sup> power models at the downwind boundary ( $x = 101$  m) where a wide range of supply magnitudes have been applied. Three cases are shown in the top panels: A. where supply is of smaller order than the demand (integrated wind driven transport capacity); B. where supply is of similar order than the demand; C. where supply is of larger order than the demand. The middle panel shows the 'goodness of fit' for the fitted cubic and linear relations as a function of source magnitude. It is shown that while supply is limited the linear model fits best where if supply is abundant the 3<sup>rd</sup> power model fits best. There is a transition where supply is of the same order than the demand.

The bottom panel of Figure 4.9 shows the relation between the calculated total (integrated) sediment transport rates ( $Q_{(x=101m)}$ ) via Equations (4.14) and (4.15). The average sediment transport concentration ( $\bar{C}_t$ ) is derived fitting the linear relations and is multiplied with the velocity timeseries before integrating over time. The dashed line represents the line where supply and sediment transport rates are in balance (via Equation (4.15)). It is shown that especially when supply is small, the derived sediment transport rates are well defined by the supply. When supply is larger, magnitudes deviate due to the 'limited' capacity of the wind.

### 4.5.2 Variability in Supply

Currently it is assumed that the supply magnitude is constant in time. In reality the supply is likely to vary with a timescale in the order of seconds to hours where variations in supply can be caused by tide (inundation of the supply zone) or precipitation. It is shown that linear fits between wind speed and sediment transport rates are to be expected while supply is limited and constant. If it is assumed that winds vary independent from and on a shorter timescale than supply magnitudes however, it could theoretically be expected that the average supply governs the average sediment concentration ( $\bar{C}_c$ ) keeping the linear dependence on wind speed. Therefore Equations (4.14) and (4.15) can be used to derive varying sediment supply using field measurements.

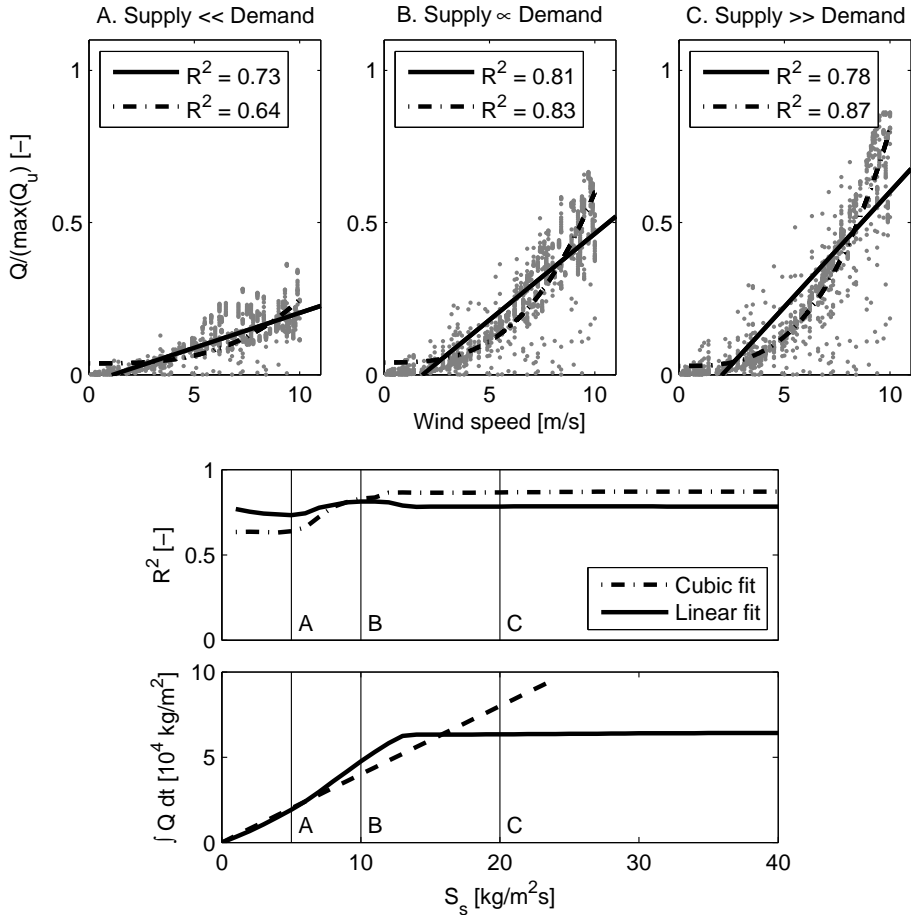


Figure 4.9: Top panels show the relation between wind speed and sediment transport rates for three different supply magnitudes. Both linear and 3<sup>rd</sup> power curves are fitted. Middle panel shows the development of the 'goodness of fit' where supply magnitude is varied. Bottom panel shows the derived total transports (via the integration of Equation (4.14)) as a function of supply magnitude. The dashed line in the bottom panel represents Equation (4.15) where the total transports are assumed equal to the total supply. The vertical lines in bottom and middle panels correspond to the cases shown in the top panels.



### 4.5.3 Threshold velocity for transport

The model presented in the previous sections considers sediment velocity which is assumed to be proportional to wind velocity and no threshold velocity is implemented in the erosion term in the model equations (Equation (4.7)). In future development of the model for supply limited conditions a threshold velocity could easily be accounted for. However, including a threshold velocity in the erosion terms requires additional assumptions. First an (empirical) assumption on threshold velocity is needed and second an assumption on how wind speed and sediment speed are related. In the current model the sediment speed and wind speed are assumed to be equal. Introducing both of these assumption and possibly additional assumption is beyond the scope of this paper but possibly subject for further research.

### 4.5.4 Fetch effects

Test Case I shows steady state solutions of the spatial distributions of sediment transport rates. Fetch effects are previously described as an increase of the aeolian sediment transport rate with distance downwind over an erodible surface towards a certain maximum. Where the maximum is the wind driven transport capacity. It is often suggested that a generic value of a critical fetch distance could be derived for different situations. The results and underlying described physics behind Test Case I could explain the varying reports on measured fetch distance in field situations. In the modeled cases the fetch distance needed to achieve a maximum sediment transport rate is governed by ejection rates and wind speed both of which can vary on short timescales in field situations. While other possible governing processes of fetch effects are ignored in this study (such as the onset of the saltation cascade), the described processes make the analysis on the nature of measured fetch effects in the field tedious, if not impossible in supply limited situations. The main complicating issue is that in the proposed model, the transport maximum (horizontal part of the curves in Figure 4.4) does not necessarily equal the wind driven sediment transport capacity due to supply limitations. Only when supply is abundant, a wind driven transport capacity could theoretically be reached. Therefore, the critical fetch concept is found to be unsuitable to describe spatial variability in measured sediment transport rates for supply limited situations and it is proposed to focus on quantifying the variability in supply instead.

### 4.5.5 Implications for future modeling

Several authors have recognized the over prediction of sediment transport rates using Bagnold type formulations. These over predictions are commonly linked to supply limiting factors keeping the 3<sup>rd</sup> power Bagnold type relation intact. As a result, these predictions remain very sensitive for variability in wind conditions.

In the proposed approach, sediment transport is dependent on the wind speed (1<sup>st</sup> order) and source magnitude. Compared to current sediment transport models, the dependence on wind speed is reduced and the dependence on source mag-

nitude is highlighted. The relative reduction of the dependence on wind could possibly shift the focus of current aeolian sediment transport models from solving complex wind field towards modeling source parameters.

## 4.6 Conclusions

A model for aeolian transport in supply limited situations is presented based on a 1D linear advection model where a Bagnold type 3<sup>rd</sup> power sediment transport formulation is implemented. Applying the model to three test cases it is concluded that:

- Aeolian sediment transport rates are dependent on wind speed and supply where both variables can govern total sediment transports. When supply is limited, wind driven equilibrium transports do not occur and supply governs the transport. When supply is abundant, wind driven equilibrium transports occur and wind governs transport.
- In supply limited systems, the length of increase in sediment transport rates in the direction of the wind, often ascribed to the fetch effect, can be governed by supply magnitude.
- In supply limited systems, aeolian sediment transport can be estimated using linear models. While conventional 3<sup>rd</sup> power sediment transport functions can be used to calculate a wind driven transport capacity, this capacity is not reached in supply limited systems. Sediment transport rates are governed by the magnitude of the source instead.
- Field data indicate that when measuring sediment transport rates and wind velocity simultaneously in a supply limited system, a linear relationship can be observed. While this observation qualitatively validates the linear model, the fitted linear relationship can be used to quantify the source present. This linear relationship can be relevant to apply to several available field data sets.
- According to the presented model, observed fetch effects in the field could be a by-product of supply limitations. The conventional fetch effect concept suggests a generic principle where the fetch distance versus critical fetch distance is an important parameter governing total transport. However, the critical fetch distance can be governed by the temporal and spatial variability of the supply instead. Therefore, determining critical fetch distances generically is very difficult if not impossible without quantifying supply magnitudes.

## Chapter 5

# Aeolian sediment transport rates in supply limited situations

### *An analysis of field data*

---

This chapter is in preparation to be submitted as an article. No changes have been made with respect to the text of the article manuscript. As a result, this Chapter is legible individually but parts of the introduction overlap somewhat with the introduction of Chapter 4.

The aim of this chapter is to test generic relations between wind and aeolian sediment transport, using field data. These transport relations can possibly be used to predict aggregated transports on the beach. Data of wind velocity and sediment transport rates are collected during a 5 day field campaign at Vlugtenburg beach located in The Netherlands.

Lessons learned:

- The variability in measured transports is to a large extent governed by the tide elevation. This indicates an explicit link between aeolian sediment transport rates and the intertidal area. During the measurements, the sediment supply in the intertidal area is considered of larger order than at the upper beach.
  - According to fetch theories, sediment transports increase in the direction of the wind until wind driven transport capacity is reached at critical fetch distance. While fetch alike effects are measured, conventional fetch theories are not confirmed because it is unclear if a wind driven transport capacity is reached. If wind driven transport capacity is not reached, the relationship between wind speed and sediment transport rates does not follow traditional formulations.
  - The linear model proposed in Chapter 4, slightly adapted to be applicable to this field data, is used to successfully fit the measured data. The fitting parameters of the linear model represent the threshold velocity for transport and average sediment concentration.
  - For this particular dataset the derived threshold velocities show limited spatial and temporal variability but the derived averaged sediment concentrations show significant spatial and temporal variability. This carefully suggests that during the experiment the variability in measured sediment transports are not governed by the variability in threshold velocity for transport.
- 
-

## 5.1 Introduction

In this paper generic relations are tested between wind and aeolian sediment transport which can be used to predict aggregated transports on the beach. Traditionally, relations between wind and aeolian transport are based on higher power functions with respect to the wind induced shear velocity ( $u_*$ ) derived from the pioneering work by Bagnold (1954). Bagnold identified the main factors influencing aeolian transport rates ( $q$ ) as the grain diameter ( $d$ ) relative to a reference grain diameter ( $D$ ), the air density ( $\rho$ ), the gravitational acceleration ( $g$ ), the drag velocity ( $u_*$ ) and an empirical coefficient ( $C_b$ ).

$$q = C_b \frac{\rho}{g} \sqrt{\frac{d}{D}} (u_*)^3 \quad (5.1)$$

In practical situations however, a threshold wind velocity is present. The threshold drag velocity is dependent on the grain diameter ( $D$ ), the gravitational acceleration ( $g$ ), the density of the sand grains ( $\rho_s$ ), the density of the air ( $\rho$ ) and an empirical coefficient ( $A$ ) (Bagnold, 1954).

$$u_{t*} = A \sqrt{Dg(\rho_s - \rho)/\rho} \quad (5.2)$$

Implementing the concept of threshold velocity, Bagnold (1954) derives that the aeolian sediment transport rates vary as the cube of excess wind velocity over and above the constant threshold velocity at which the sediment begins to move.

$$q = \alpha C_b \frac{\rho}{g} \sqrt{\frac{d}{D}} (u - u_t)^3 \quad (5.3)$$

Note that in Equation (5.3) wind speed is written instead of drag velocity. Parameter  $\alpha$  accounts for the conversion between the drag velocity and wind velocity where a logarithmic velocity profile is assumed.

Adopting the cubic 'Bagnold type' formulations for predicting aeolian sediment transport on beaches leads to a general over-prediction of the actual sediment transport rates on the longer timescale (Kroon and Hoekstra, 1990; Sarre, 1989; Sherman et al., 1998; Sherman and Li, 2012). These over-predictions are often suggested to be governed by supply limitations (Nickling and Davidson-Arnott, 1990). On beaches, sediment supply is governed by various variables such as surface moisture content (Davidson-Arnott et al., 2005), beach slope (Hardisty and Whitehouse, 1988; de Vries et al., 2012), fetch length (Bauer and Davidson-Arnott, 2002), the presence of vegetation Arens (1996) and the presence of lag deposits armoring the sand surface layer (van der Wal, 1998). Some of these supply variables vary on short timescales (order minutes to hours) and process measurements have often confirmed that sediment transport rates at a beach are very variable due to supply limiting effects (e.g. Davidson-Arnott et al., 2005; Bauer et al., 2009; Davidson-Arnott and Bauer, 2009).

The fetch effect is often described as a supply limiting parameter due to a combination of wind direction and beach geometry (many references possible, see

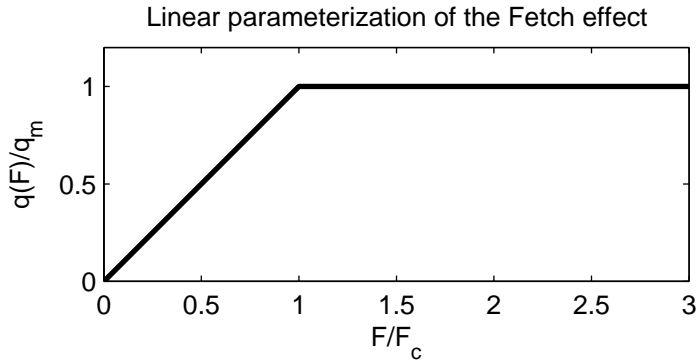


Figure 5.1: Conceptual representation of the fetch effect, where transport increases with increasing fetch towards a certain limit. Reference is made to Bauer and Davidson-Arnott (2002) who suggests similar curves including a smoother transition between the increasing and stable transport.

for an overview Delgado-Fernandez (2010)). The fetch effect is an increase of the aeolian sediment transport rate with distance downwind over an erodible surface. The fetch distance needed to reach the transport capacity is called critical fetch distance (see Figure 5.1 for a conceptual representation after Bauer and Davidson-Arnott (2002)). While various reports are available on the effect of fetch, the measured critical fetch distances vary from 20-200 m to no measured fetch effects at all (Delgado-Fernandez, 2010; Lynch et al., 2008; Jackson and Cooper, 1999). In Chapter 4 it is argued that these varying reports could possibly be explained by spatial and temporal variability in supply magnitude.

In the intertidal zone, both fetch and supply magnitude are dynamic variables in space and time. Spatial variability in aeolian transport in the intertidal zone could be governed by a variable moisture content of the sand surface, intertidal morphology (ridge and runnel systems) in combination with fetch distance (Anthony et al., 2009) and salt crust formation. Temporal variability of sediment transport within the tidal cycle could be due the varying tide level causing varying fetch distances but also varying surface characteristics. Surface characteristics vary while surface moisture varies but also stabilizing lag deposits could be reworked by wave action. This reworking of stabilizing lag deposits can result in a renewal of sediment available for transport (Carter, 1976) within a tidal cycle contributing to an increase of sediment supply. Following this reasoning, van der Wal (1998) suggests that at low tide and during onshore winds, transport initiates at the intertidal zone which could function as an important sediment source for sediment transport towards the dunes.

Modeling aeolian sediment transport rates, supply limitations are often accounted for in a pragmatic way by adding empirical parameters to Bagnold type formulations when fitting field data (e.g. Arens, 1996; Kroon and Hoekstra, 1990).

While generic models for these empirical parameters are unavailable, the use of process formulations is undermined. Therefore quantitative prediction capabilities of aeolian sediment transport rates in the field using these models are very limited (Sherman and Li (2012); Bauer et al. (1996)).

In Chapter 4, a model is suggested where aeolian sediment transport on beaches is linearly related to wind speed. This linear relation is proposed based on a numerical model including supply limitations. It is argued that sediment transport rates could be determined to a great extent by the available supply rather than the higher order function of the wind speed. At this stage the formulated linear model does not have predictive skills, however it provides a tool to assess the variability in supply magnitude during field experiments where sediment transport rates and wind velocities are measured.

This paper aims to establish a sediment transport relation which can be used to predict average values of aeolian sediment transport in both the short ( $O$  seconds) and the longer ( $O$  hours) timescale. A field experiment is designed to quantify transports and transport gradients on the beach. The measurement data are used to fit both Bagnold type sediment transport formulations and linear sediment transport relations with respect to wind speed. It is tested if the fitted models can account for the measured variability in transports in space and time.

## 5.2 Measurement location and experimental design

Field measurements have been conducted from 6-10 December 2010 at Vlugtenburg beach located at the south west of the Holland coast (see Figure 5.2). In 2008 this beach has been nourished and since then, several aspects of this beach including foreshore and dune behavior have been studied (de Vries et al., 2011b; de Schipper et al., 2012).

Generally, mean wave heights and periods along the Dutch coast are 1.2 m and 5 s respectively where alongshore differences in wave climate are small (Wijnberg and Terwindt, 1995). The tide is semi diurnal with a neap spring cycle of 1.2 and 2.2 m, respectively. Beach slopes in the inter tidal zone are roughly between 1:40 and 1:50. The beach at this site can generally be categorized as a dissipative beach according to the geographical framework presented by Short and Hesp (1982))

While the tidal range is in the order of 2 m, the horizontal excursion of the tide on the beach is on the order of 80-100 m. As a result, the tide creates a significant temporal variability of beach width and therefore wind fetch during (oblique) onshore winds. Measurements of water levels are available from a nearby tide station at Hoek van Holland.

The wind climate is dominated by mainly west to southwest winds. These directions are oblique to normal incident with a large onshore component This large onshore component governs cross shore sediment transport towards the dunes and dune formation.

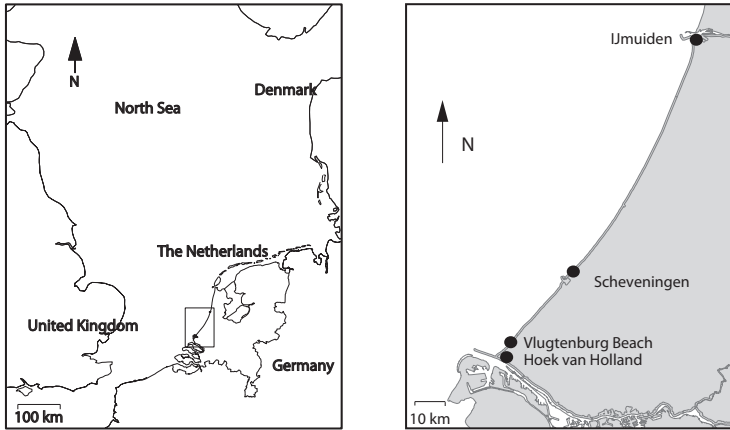


Figure 5.2: Measurement location

The intertidal zone generally has a concave morphology where the seaward side has a relatively mild slope and the slope increases when moving toward the upper beach (landward side), see Figure 5.3. Intertidal morphology is characterized by dynamic intertidal bar systems and local topography changes are relatively large due to wave and tide forces. Swash processes are of large importance in this zone. The surface in the intertidal zone is relatively smooth containing no micro scale bed forms with the exception of runnels (intertidal troughs) in which sometimes bed ripples occur as a result of currents during high waters.

The upper beach is characterized by a constant sloping surface from the waterline towards the dunes. At the measurement site both the beach and the dunes are artificially constructed. Generally, at Dutch beaches the dune foot is located around the +3 m NAP level. At this artificial beach no dune foot is present and we have chosen to introduce an artificial landward boundary of the beach at the +5 m contour. The sand surface at the upper beach is characterized by a shell layer where micro scale bed forms are present. The shell layer is formed due to erosion of lighter material on the surface by aeolian processes where the heavier material stays behind. The micro scale bed forms are significant and mainly anthropogenic created as a result of footsteps and car tracks. The topography changes at the upper beach are relatively small with respect to the intertidal area (de Vries et al., 2011b).

While it is aimed to measure gradients in sediment transport across the beach, 5 saltiphones (Spaan and van den Abeele, 1991) are used. The saltiphones are placed perpendicular to the wind during onshore conditions. The hart of the saltiphones' sensors is located 10cm above the sand surface at any time. The 5 Saltiphones are moved throughout the experiment over 4 positions (A-D). Figures 5.3 and 5.4 (right panel) show the locations of the Saltiphones and wind station. During part of the experiment Saltiphones are located in and near the intertidal

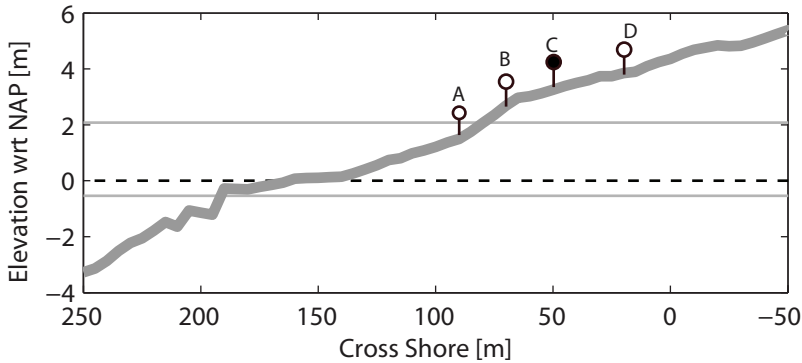


Figure 5.3: Cross shore profile where locations of saltiphones are depicted (top view shown in Figure 5.4). At location C, a fixed saltiphone and the wind station is situated. The horizontal gray lines indicate the high water level and low water level. The dashed black line indicate vertical reference level (NAP)

Meas.	Begin time	End time	Remarks
Sub I	00.00 9-12	9.30 9-12	Saltiphones placed close to each other.
Sub II	10.00 9-12	15.20 9-12	Saltiphones placed in an array within the intertidal zone. Tide is mid-tide and falling

Table 5.1: Details of subsets

zone. The right panel of Figure 5.4 shows the measured wind conditions at location C indicating the dominant cross shore direction.

Saltiphones record cumulative counts per second. To reduce the size of the data stream, the data of every 5th second is stored. Wind conditions are momentary values which are logged at the same 5 second intervals at a fixed location (C) at 2 meters above the sand bed.

### 5.3 Results

Figure 5.5 gives an overview of the measured data at location C. The measurements are cut in two separate subsets where the saltiphone setup has changed. Table 5.1 shows an overview of the details of the subsets. One saltiphone is fixed at position C at the upper beach during the full measurement campaign. Measurement Sub I is for calibration purposes where it is checked if all saltiphones give similar values when placed close to each other (results are discussed in Appendix A). Sub II is used to focus on spatial gradients in sediment transport.

Saltiphones have a discrete maximum measurement capacity of around 1000-1200 counts. If transport is occurring this measurement capacity is often reached



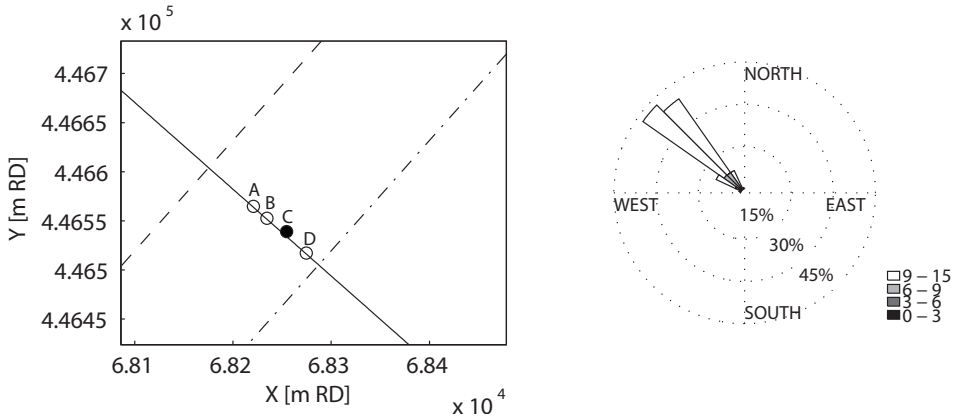


Figure 5.4: Left panel shows a schematized top view of the measurement locations. Black circles indicate saltiphone locations. Filled circle indicates the position of the wind station. The dashed line indicates the waterline and the dashed dotted line indicates the landward reference. Black solid line indicates profile shown in Figure 5.3. Right panel shows the measured wind conditions (in m/s).

(see Figure 5.5) biasing any quantitative measure based on measured counts. Since we are interested in gradients over the beach and all sensors are assumed to be equally biased we use total counts as a proxy for saltation intensity.

### 5.3.1 Temporal variability of aggregated parameters

Figure 5.6 shows 30 minutes averaged of measured and derived parameters. Wind velocities and directions are measured to be fairly stable (around 10 m/s and 300 degrees), especially after 4.00h. Simultaneously, large variable transport rates are measured at location C. This variability in time of the total counts shows a periodic signal where autocorrelations indicate a periodicity of 12,5 hours which coincides with the tidal period. Correlating the variable signal of the total counts with the measured tide at Hoek van Holland, a significant (95% confidence) negative correlation is found ( $R = -0.68$ ). This indicates that the variability in tidal elevation explains a large part (46%) of the measured variability in total counts. High tides correspond with a narrow beach and low transport an low tides correspond with a wide beach and large transport where the transports rates are measured at the upper beach.

### 5.3.2 Relation between Wind speed and sediment transport rates

In line with the work of Bagnold, a higher order function between wind speed and sediment transport rates corrected with the threshold velocities is fitted. Following

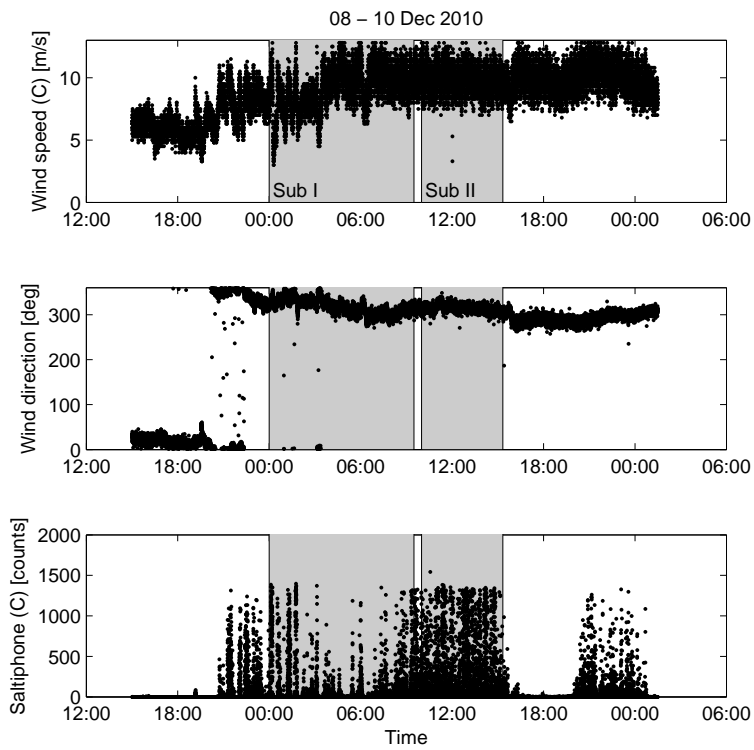


Figure 5.5: Data from the full length of the experiment. One saltiphone is continuously located at a fixed location C. Gray areas identify measurement sub-series.

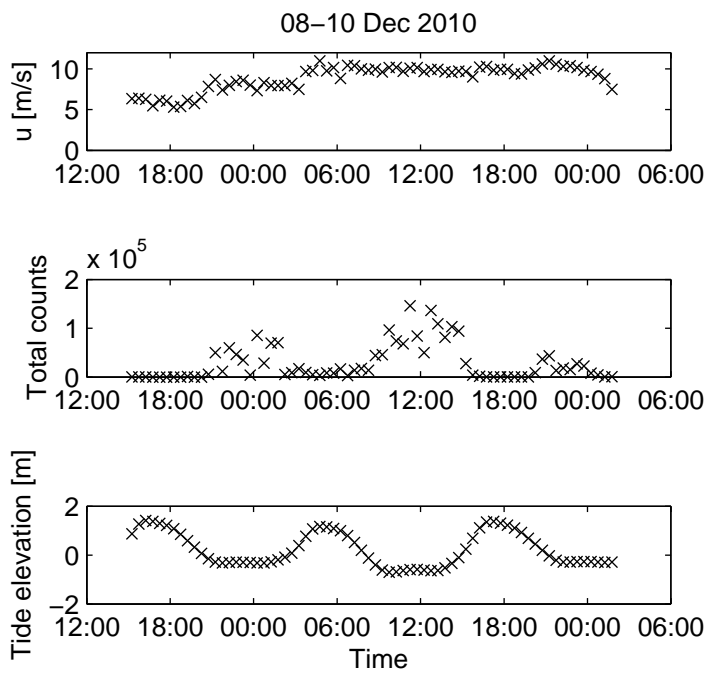


Figure 5.6: Measured data aggregated over 30 minute intervals. Top panel shows average wind conditions. Middle panel shows total counts. Bottom panel shows vertical tide.

Equation (5.3), a generic form of such a higher order function is given by:

$$Q_s(t) = A_{\text{cub}} \frac{(u(t) - ut_{\text{cub}})^3}{g} \quad (5.4)$$

where  $Q_s$  [counts/(s m<sup>2</sup>)] is the measured sediment transport rate by the saltiphone and  $g$  [m/s<sup>2</sup>] is the gravitational constant.  $A_{\text{cub}}$  [counts/m<sup>3</sup>] is an empirical constant representing environmental properties including grains size, density and supply. The  $ut_{\text{cub}}$  [m/s] is the threshold velocity which is also governed by bed properties. Since time series of wind speed ( $u(t)$  [m/s]) and sediment transport rates ( $Q_s(t)$ ) are measured, the unknown constants  $A_{\text{cub}}$  and  $ut_{\text{cub}}$  are derived for specific time intervals.

Additionally the linear model proposed in Chapter 4 is fitted. The linear model presents a description of aeolian sediment transport rates assuming a relatively constant sediment transport concentration which is governed by supply. While wind speed is assumed proportional to sediment speed ( $u_s(t)$  [m/s]) and fluctuating on a timescale shorter than the average sediment concentration ( $\bar{C}_c$  [kg/m<sup>3</sup>]), sediment transport rates can be represented using:

$$Q_s(t) = \bar{C}_c \times u_s(t) \quad (5.5)$$

For this field case however, it is necessary to assume the relationship between sediment speed and wind speed including a threshold wind speed. While no plausible alternatives are present, it is at this stage (pragmatically) assumed that the sediment velocity is proportional to the excess wind velocity over the threshold wind velocity. Therefore:

$$Q_s(t) = A_{\text{lin}} \times (u(t) - ut_{\text{lin}}(t)) \quad (5.6)$$

where  $A_{\text{lin}}$  [counts/m<sup>3</sup>] is an empirical constant representing environmental properties including average sediment concentration. The  $ut_{\text{lin}}$  [m/s] is the threshold velocity which is also governed by bed properties. Note that the parameters presented in Equation 5.6 are similar (same physical meaning and dimension) to the parameters in Equation (5.4) and are therefore inter comparable.

### Fitting results

Figure 5.7 illustrates the procedure for fitting the relations discussed above. For the purpose of fitting, the dataset is subdivided in 30 minute intervals identical to the intervals of the derived aggregated parameters in Figure 5.6. For every time interval of 30 minutes, the measured sediment transports are binned with respect to wind speed. For each wind speed bin, a binned average is calculated. Both the cubic (Equation (5.4)) and the linear curves (Equation (5.6)) are fitted to the binned averaged transports. The measured wind speeds which deviate twice the standard deviation from the mean measured wind speed are discarded to minimize the possible influence of outliers in bins (which are only a marginal part of the dataset) on the fitting procedure. Results contain the value of the threshold velocities ( $ut_{\text{lin}}$  and  $ut_{\text{cub}}$  which are restricted to be larger than 0) and

the empirical constants ( $A_{lin}$  and  $A_{cub}$ ) for both fits. Moreover, the coefficients of correlation ( $r$ ) are derived for both fits. Figure 5.7 shows the linear and cubic fit indicating similar coefficients of correlation for a particular time window.

Applying the above for the full dataset, fitting parameters for every 30 minute window are obtained. Figure 5.8 shows the correlation coefficient, threshold velocity and (empirical) fitting constant for the linear and cubic fit applied to all measured 30 minutes intervals. It is shown that the correlation coefficient is similar for both fitting methods where the average correlation coefficient is 0.88 for both methods.

The derived threshold velocities using the linear fit show a relatively constant distribution with a mean threshold velocity of 8.8 m/s (standard deviation 1.8 m/s). For the cubic fit the average of the derived threshold velocities is 5.7 m/s (standard deviation 3.5 m/s). Overall, the derived threshold velocities using the cubic fit are smaller and fluctuate more with respect to the linear fit.

### Relevance of fitted models

By fitting models to measured data it is tried to derive a generic relationship which can eventually be used for predicting sediment transport. In this case the interest is predicting sediment transport rates as a function of wind speed, threshold wind speed and an empirical constant representing environmental parameters. The models are fitted using process data (O seconds) within a discrete time window of 30 minutes. The predictions of interest are of aggregated nature where for the moment a single and aggregated model per 30 minute time window is derived. After fitting the linear and cubic models, it is tested if the aggregated sediment transports are related to aggregated parameters such as the mean wind velocity, derived threshold velocity and the derived empirical constant. A time series is available for all of the derived parameters and correlations between parameters are to be expected. Table 5.2 shows the linear correlations between the derived parameters. Gray cells indicate that the linear correlation is found to be significant (at 95% confidence).

In Table 5.2 it is shown that aggregated parameters are significantly correlated. A significant negative correlation is found between total transport and tide level. This dependence is illustrated before in Figure 5.6. A significant correlation is also found between total transport and average wind velocities indicating the dependence of wind. Wind and tide seem to correlate as well.

The dependence between tide and wind speed could be governed by the height of the wind speed sensor relative to the water level. During low tide the difference between the height of the sensor and the water level is larger than during high tide. Assuming an increasing wind velocity with height, a higher wind speed measurement is expected during low tide. The dependence between tide and wind speed could also be coincidental.

The time series of the fitting parameters of the cubic fit show limited correlation with the time series of the total counts. Where especially a correlation is expected between the time series of the empirical parameter ( $A_{cub}$ ) and the time

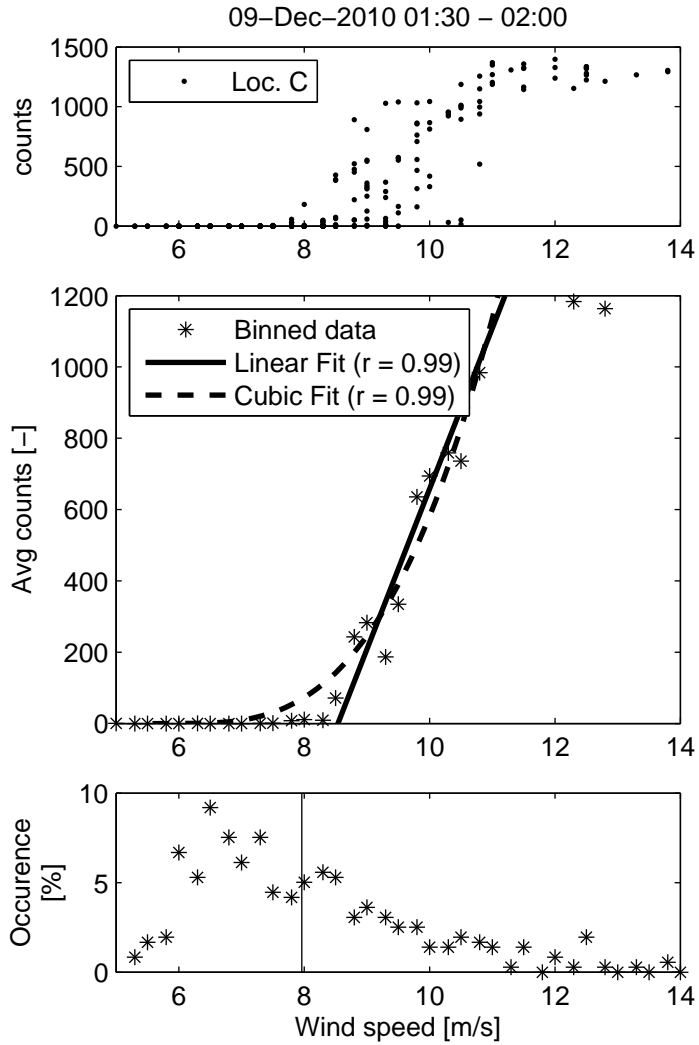


Figure 5.7: Top panel shows measured counts for saltiphone at location C. Middle panel shows mean counts for binned wind speeds together with their best linear and cubic fit. Bottom panel shows wind speed mass distribution.

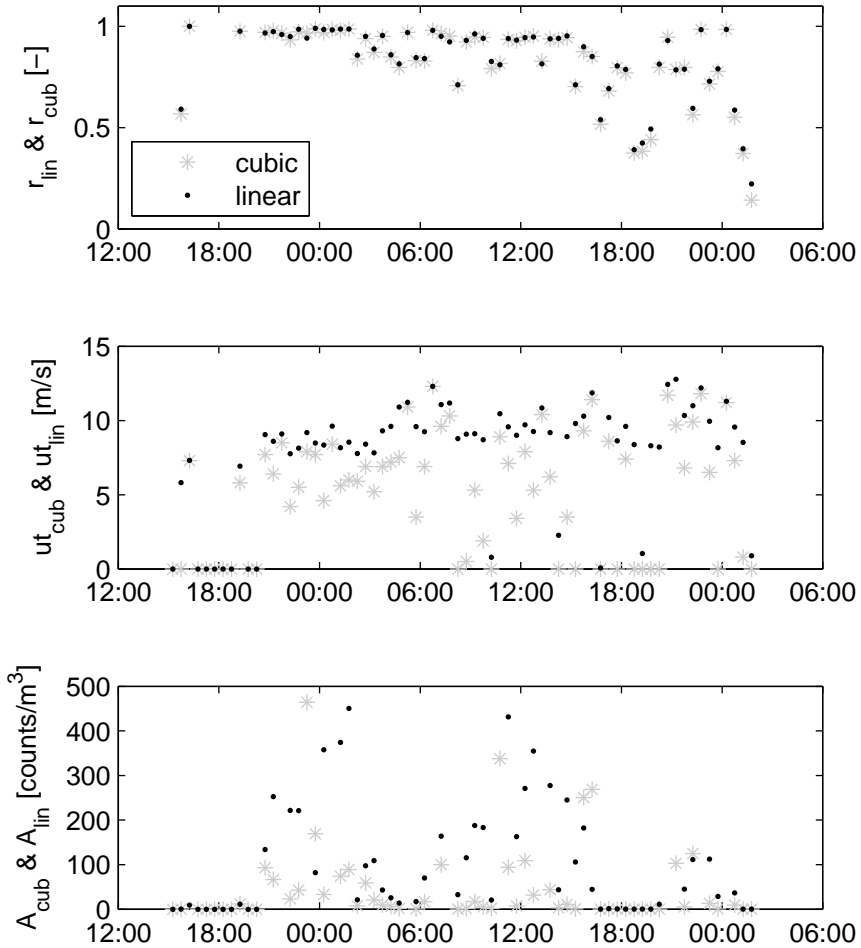


Figure 5.8: Overview of fitting data for every 30 minute interval. Top panel shows linear correlation coefficients for both linear and cubic fits. Middle panel shows the derived threshold velocities. Bottom panel shows the fitting constants. Gray stars represent the cubic fit where black dots represent the linear fit.

	Total counts	Average wind	Tide
Aggregated parameters			
Total counts	1.00	0.29	-0.66
Average wind	0.29	1.00	-0.25
Tide	-0.66	-0.25	1.00
Cubic fit			
$A_{\text{cub}}$	-0.10	0.15	0.05
$ut_{\text{cub}}$	0.09	0.39	-0.17
$(\text{Average wind} - ut_{\text{cub}})^3$	-0.04	0.19	0.08
Linear fit			
$A_{\text{lin}}$	0.24	0.30	-0.31
$ut_{\text{lin}}$	0.19	0.67	-0.26
$(\text{Average wind} - ut_{\text{lin}})$	-0.10	-0.34	0.21

Table 5.2: Linear correlations between parameters. Significant correlation at  $(2/\sqrt{n} = 0.24)$ .

series of the total counts, no correlation is found. Therefore, variability in measured average transports cannot be explained by variability of the fitted empirical parameter. This could be caused by the large relative importance of the wind speed and threshold wind speed which is induced by to the 3<sup>rd</sup> power exponent. Therefore, variability due to wind overshadows possible variability due to other parameters which makes the fitted model coefficients to a large extent dependent on the occurring winds on the short timescale.

The time series of the fitted parameters of the linear fit show that the empirical constant ( $A_{\text{lin}}$ ) correlates significantly with the measured total counts. This indicates that the empirical parameter derived using the linear model represents to some extent the variability in sediment transport rates. Moreover the empirical parameter correlates significantly with the tide suggesting some relation between the empirical parameter and source conditions.

Remarkably, fitting both relations (linear and cubic), the time series of the derived threshold velocities ( $u_{\text{lin}}$  and  $u_{\text{cub}}$ ) do not correlate with the time series of total counts. This indicates that in both cases variability in threshold velocity does not explain any variability in total counts during this particular experiment. During previous experiments presented by Arens (1996), significant variability in fitted threshold velocities (using a cubic fit) are found. These varying threshold velocities found by Arens (1996) could be attributed to varying environmental conditions which vary on a longer timescale than the measurements presented in this paper (such as precipitation).

### 5.3.3 Spatial gradients in transport.

While transports are measured at different locations during the experiment a comparison between measured transport at different locations can be made.



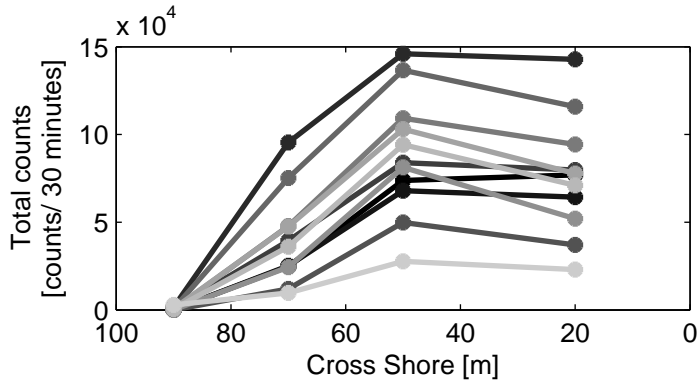


Figure 5.9: Measurements of total counts for 11, 30 minute intervals at 4 saltiphone locations. Colors and lines indicate corresponding intervals. Winds are from left to right in the figure. Total transports increase in downwind direction up to a certain limit in all depicted cases.

### Spatial gradients in total transports

Spatial gradients in total transports are analyzed using a subset of the dataset. Data Subset II (see Sub II area in Figure 5.5) contains data where saltiphones are placed in a cross shore array. The cross shore array is partially located in the intertidal zone and consists of 4 saltiphones. In line with the previous section, 30 minute data intervals are used to derive aggregated parameters at each location. Figure 5.9 shows measured total counts for 11 intervals of 30 minutes. There is a clear positive gradient present in the direction of the wind for all 30 minute intervals. The increase stops after a certain distance in the direction of the wind where a more or less stable value for total saltiphone counts is found.

This observation supports the general assumption that some transport capacity is reached after a certain fetch distance is exceeded. In line with fetch theories, the critical fetch distance can be estimated to be around 40 m. However, while wind speeds are fairly constant, the measured transports at the most landwards saltiphones show (temporal) variability which cannot be attributed to variability in wind speed. Earlier it is shown that this variability might be attributed to environmental variables such as the tide (see Section 5.3.1).

This increase of transport in the direction of the wind could be explained by supply limitations as shown in Chapter 4. Following this reasoning and spatial representation presented in Chapters 3 & 4, the inter tidal zone could function as a discrete supply zone with a length of about 40 m. At the upper beach (in downwind direction of the supply zone) supply could be of smaller order (because of armoring of the surface etc.) which leads to no significant increase of transport rates in downwind direction.

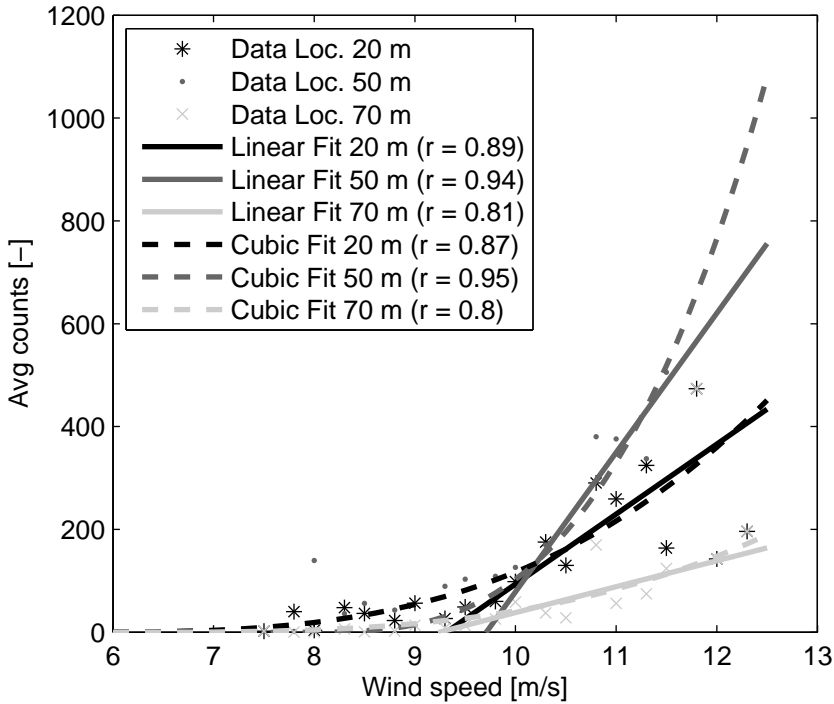


Figure 5.10: Velocity binned data of average counts including linear fits for three locations measured simultaneously.

### Spatial differences while fitting the linear model

Figure 5.10 shows the binned distribution of measured wind speeds and averaged measured transports [counts/s] at three different locations. Although the presented measurements are obtained simultaneously, the steepness of the linear fit ( $A_{lin}$ ) differs. In the downwind direction the average sediment transport concentration represented by  $A_{lin}$  increases indicating a pick-up of available sediment in downwind direction. At the same time, the intersection with the x-axis (threshold velocity) are comparable for all three locations. This indicates that these threshold velocities (using this model for data analysis) show no variations over measurement locations.

Analyzing a larger part of the time series, the linear model is fitted to the 30 minute intervals of two subsets (Sub I and Sub II in Figure 5.5). Fitting the linear model, three aggregated parameters are extracted: 1. The linear correlation coefficient indicating the quality of the fit; 2. The linear fitting coefficient ( $A_{lin}$ ) indicating the average sediment transport concentration [count/m<sup>3</sup>]; 3. The derived threshold velocity [m/s]. In Figure 5.11 the results are shown.

During series Sub I, all sensors are placed at location C. Therefore, no signif-

icant differences in parameters are to be expected. The measurements in Figure 5.11 confirm that during this data series different sensors show similar derived parameters. N.B. some temporal variability in derived averaged sediment transport concentration is found which could be attributed to the tide discussed in section 5.3.1. The derived threshold velocity seems to be fairly constant.

During series Sub II sensors are placed at different locations. Significant differences in average sediment concentration ( $A_{\text{lin}}$ ) are found. This can be related to the relative positions of the sensors. Generally, the average sediment concentration increases ( $A_{\text{lin}}$ ) in downwind direction indicating pick up of sediment between the sensors. While average sediment concentrations vary, the derived threshold velocities seem to converge and show no consistent spatial dependence. This is somewhat surprising as it could be expected that threshold velocities are higher closer to the intertidal area. Instead, it is found that threshold velocities spatially converge while average sediment transport concentrations vary in space.

## 5.4 Discussion

### 5.4.1 Measured cross shore gradients and the role of supply

The measured cross shore gradients in transport rates, depicted in Figure 5.9, are mostly located in and around the intertidal zone during low tide. While a transport gradient indicates an area of erosion, this indicates that this (lower beach) area is an important sediment source during the experiment. At the upper beach, the gradients are less pronounced if not nonexistent. This indicates that there is limited sediment pick up at the upper beach. If no sediment is picked up at any part of the spatial domain, this suggests either no supply in the corresponding spatial domain or the wind driven transport capacity is reached. Keeping in mind that the wind conditions show limited variability the conclusion is that the upper beach does not significantly contribute to supply and the variability in measured transports at the upper beach is governed by variability in upwind supply. At the same time, it could be concluded that the wind driven sediment transport capacity might not be reached at any moment during the experiment.

Based on these measurements we conclude that during these measurements, a large part of the sediment transport over the beach originates in the intertidal area. This could be explained by the reduction of sediment ejection rates due to the presence of lag deposits on the upper beach. The presence of these lag deposits could result from sediment sorting at the bed surface by aeolian processes. In the intertidal area no lag deposits due to aeolian sorting processes are formed due to the additional dynamics induced by marine processes reworking the upper layer of the bed.

As a result, the amount of sediment available at the bed for aeolian transport (sediment supply) is likely to vary spatially where a zone of supply is present near the intertidal zone and a zone of reduced supply at the upper beach. This concept of spatially varying supply is depicted in Figure 5.12 and is supported by the

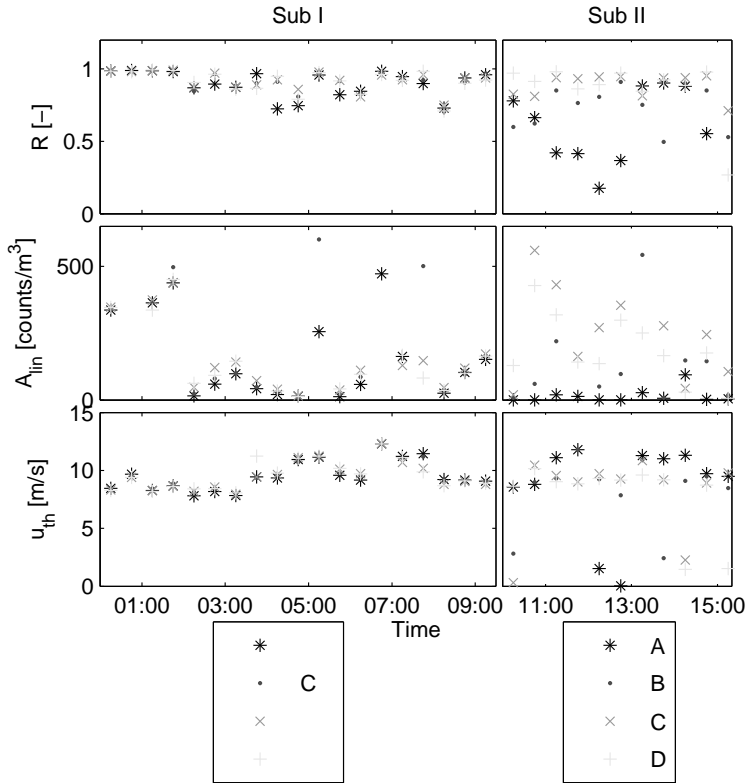


Figure 5.11: Time series of fitting parameters applying the linear model on Sub I and Sub II subsets of the data series. Top panels show goodness of fit  $R$ , middle panels show the derived average sediment concentration, bottom panel shows the derived threshold velocities. Legend at the bottom indicates measurement locations corresponding to Figure 5.3

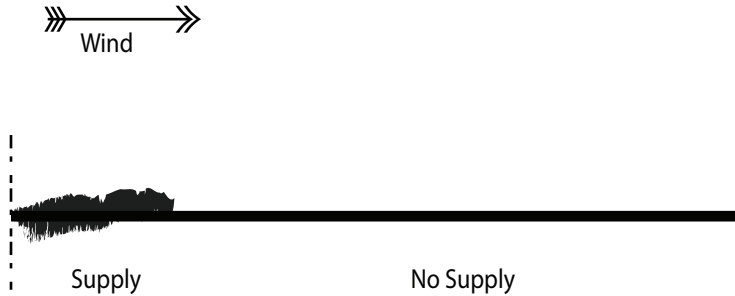


Figure 5.12: Spatial representation of the concept of supply and no supply zones.

results given in Chapter 3 and used in the model presented in Chapter 4.

### 5.4.2 The Fetch effect

A general definition of the fetch effect is given by Delgado-Fernandez (2010) as "an increase of the aeolian sediment transport rate with distance downwind over an erodible surface". After a sufficient distance downwind (critical fetch) a wind driven transport capacity is reached.

While we measure such an increase in transport in downwind direction our findings are not consistent with critical fetch theories. The observations show a constant transport rate in downwind direction comparable to the critical fetch theory, but this constant transport rate seems to be governed by the lack of additional supply (limited sediment ejection rates) in downwind direction rather than the realization of a wind driven transport capacity. The fetch effect measured in this case seems to be driven by supply only.

The explicit influence of supply on fetch effects complicates the prediction of sediment transport rates using fetch theories. While the critical fetch distance can be (and in this case *is*) a direct function of supply, the current critical fetch models should be expanded to account for a fetch effect due to supply limitations next to the fetch effect due to the realization of a wind driven transport capacity. The relative importance of both effects is unknown at this stage but the varying reports on measured critical fetch distances in literature (20-200 m see Delgado-Fernandez (2010)) point to the large relative importance of supply effects where wind driven transport capacity may not have been reached at many times.

### 5.4.3 Transport capacity vs Supply limitations

Many transport formulations take wind velocity as a measure of the amount of sediment transport. Given a certain wind velocity some transport capacity can be calculated. The transport capacity cannot be met if there is insufficient supply.

This has major implications for current sediment transport formulations. Traditionally, supply is being corrected for using an empirical constant with the cubic 'Bagnold type' formulation as a basis (see for instance Sherman and Li, 2012). As a result variability in transport due to variability in wind conditions is dominant over variability in supply. Since the variability of supply can have a dominant influence over the variability due to wind, Bagnold type formulations prove to be invalid in supply limited situations. Alternatively, transport formulations for supply limited situations are needed. The fitted linear model shows some potential to represent supply limited situations and can be used to estimate variability in sediment supply. Currently there is very limited knowledge on the quantification of sediment supply in beach situations. Additional knowledge on the quantification of the supply is of major interest when assessing the relevant importance between wind driven transport capacity and supply limiting effects. Field data available from previous studies could be used to fit the linear model in an effort to gain insight in variability of sediment supply on beaches.

## 5.5 Conclusions

Results of a 3 days field campaign where sediment transport rates and wind speeds are measured on a Dutch beach are presented. The measured sediment transport rates are analyzed by fitting cubic and linear models with respect to wind speed. Based on the measurements and analysis it is concluded that:

1. A significant gradient in sediment transport over the beach is found during onshore winds. Sediment transport increases in the direction of the wind until a certain limit. The distance over which transport increases is around 40 m while after 20 m in downwind direction increasing transport is found in all cases and after 50 m in downwind direction a stable value is found in all cases. The strongest increase is found in the intertidal area at low tides. The increase in transport in downwind direction is accredited to supply limited transport conditions where the maximum sediment transport is governed by supply rather than wind driven transport capacity.
2. At the measurement site, the intertidal area plays a governing role with respect to sediment supply and aeolian transport on the beach. There is less transport activity at the upper beach when the intertidal area is inundated. Therefore, the water level partly governs the sediment transport on the beach. At the upper beach during high water levels less sediment transport is measured than during low water levels. This can be expressed in the amount of total counts but also in an increase of average transport concentration (derived fitting a linear model).
3. Fitting linear relationships between wind and sediment transport magnitudes provide reasonable fits which are of equal quality compared to conventional cubic relationships:

- Fitting the linear relationships, aggregated values of threshold velocities and (relative) sediment transport concentrations are directly quantified. Derived and aggregated threshold velocities show relatively constant values with only limited temporal and spatial variability. The corresponding empirical constants (aggregated sediment transport concentrations) show variability which correlate with the tidal phase indicating dependence on source.
  - Fitting the cubic relationships, aggregated values of threshold velocities and empirical constants are directly quantified. Derived and aggregated threshold velocities show a highly variable signal in time with no consistent mean. The corresponding empirical constants show no variability that correlate to the corresponding measured transports.
4. Supply limitations can have a dominant effect on aeolian sediment transport rates over wind speed. This causes existing sediment transport formulations where sediment transport rates are proportional to a higher power of the wind speed to be invalid in supply limited situations. Alternatively, a linear (supply limited) model could be adopted where existing data can be used to quantify sediment supply and calibrate the supply model.

## Appendix A Saltiphone calibration

In this appendix it is shown that all 5 saltiphones measure similar sediment transport amounts when placed at the same position. Data series Sub I (see table 5.1) is discussed.

### Sub I

Saltiphones are placed close to each other and should produce similar output. Figure 5.13 shows that measured wind is between 8-12 m/s from NW directions. Figure 5.14 shows that total measured counts compare well to one another as well as the maximum and mean measured counts.

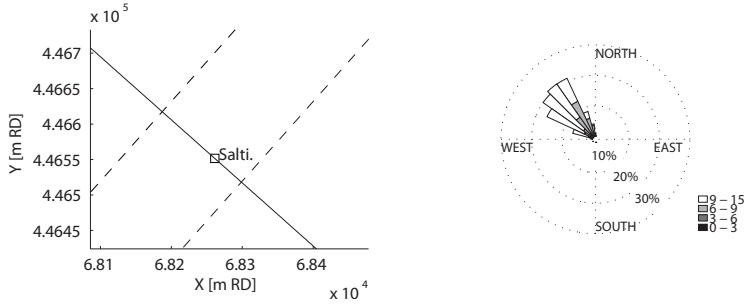


Figure 5.13: Left panel shows saltiphone setup where the dashed lines represent the waterline and the fence line. Right panel shows wind rose representing conditions during measurement.

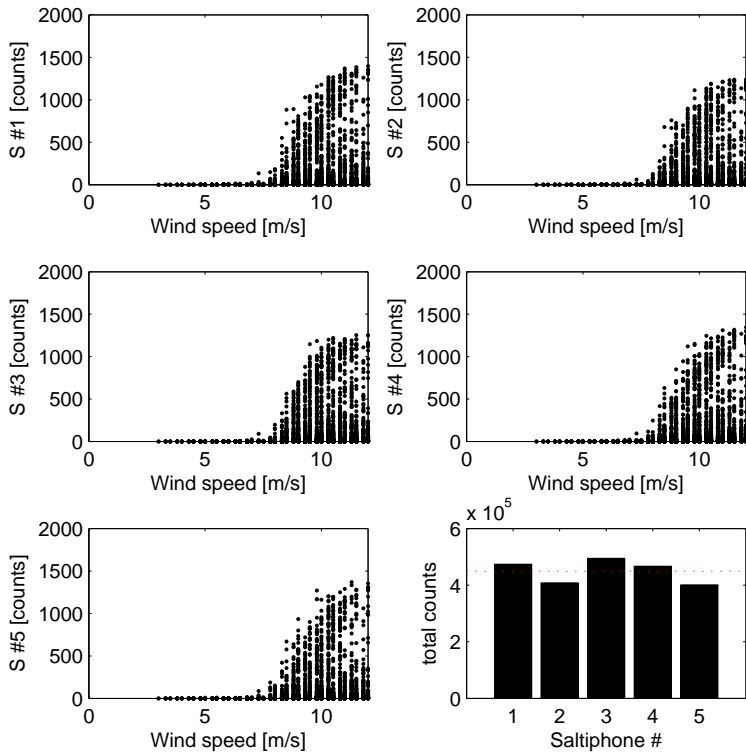


Figure 5.14: Comparison between saltiphones during Sub I. Panels 1-5; dots show all measured saltiphone counts in relation to measured wind speeds. Panel 6 shows the total counts over the measurement.



## Chapter 6

# Conclusions and Perspective

## 6.1 Conclusions

In the previous chapters, dune development and aeolian transport is discussed using different angles of approach. The most important general conclusions are that:

1. In beach situations, the system of aeolian sediment transport can be supply limited. This is reflected through the lack of correlation between dune volume changes and wind conditions on the annual timescale in Chapter 2, the difference in morphological activity in the cross shore profile presented in Chapter 3, the derived linear relation between sediment transport and wind speed in Chapter 4 and the limited correlation between aeolian sediment transport rates and wind speed on the process timescale presented in Chapter 5.
2. An important governing parameter of aeolian sediment transport rates in a supply limited system is the supply magnitude which can vary in space and time. This is reflected in the dependence between beach slope and dune volume changes derived in Chapter 2, the modeled sediment transport rates using varying source magnitude in Chapter 4 and the large correlation between the measured sediment transport rates and tide elevation presented in Chapter 5.
3. Based on this thesis and several available studies on supply limited systems it is concluded that current knowledge on the quantification of sediment supply is very limited.

The conclusions of the previous chapters are summarized in more detail below.

### 6.1.1 Measured morphologic behavior along the Holland coast

Dune behavior along the Holland coast is analyzed using the Dutch JARKUS dataset in Chapter 2. Based on this analysis it is concluded that:

1. Dune volume changes along the Holland coast are often found to be linear in time. A constant dune growth rate can be defined at many transect locations and is used to quantify dune growth rates. The linear dune growth rates at the Holland coast are found to be in the order 0-40m<sup>3</sup>/m/yr. These fitted relations could simplify future predictions of dune volume changes.

The spatial scale of fluctuation of the auto correlation of dune volume changes in alongshore direction is in the order of 2 km when averaging over 5-10 years. On shorter timescales, smaller alongshore correlation distances are found.

2. No significant correlation is found between the variability of yearly wind conditions (RDP) and yearly dune volume changes. This suggests that traditional aeolian transport models developed for desert dunes overestimate the importance of variability in wind conditions for aeolian transport rates across the beach towards the foredunes.
3. Significant temporal correlation is found between variability of yearly beach gradients and dune volume change for part of the analyzed spatial domain (11% of the transect locations). This correlation is likely to be governed by transport limiting processes with respect to aeolian transport.
4. Significant spatial correlations are found between 5 year averaged beach slopes and dune volume changes. Moreover, it is found that alongshore variability of the 5 year averaged beach slope explains 27% of the alongshore variability of the 5 year averaged dune volume changes.
5. In future modeling of yearly to decadal dune volume changes, variability of transport limiting parameters is of interest rather than time varying forcing conditions such as varying wind speeds and drift potentials.
6. The capacity of aeolian processes to build dunes is of similar order to the capacity of (extreme) marine events to erode dunes. Alongshore variability in dune volume changes at decadal scales is therefore likely to be governed by aeolian processes as well as marine erosion.

### 6.1.2 Seasonal development of the cross shore profile

In Chapter 3 morphological cross shore profiles measured at monthly intervals are analyzed. The analyzed data covers three different field sites. Based on the the data analysis it is concluded that:

- Measured morphological changes, at the beach of the analyzed cross shore profiles, due to marine processes are significantly larger than morphological changes due to aeolian processes. A separation point between marine and aeolian zones can be extracted from consecutive morphological measurements. This separation point is found to be dynamic in time and space. This dynamic border can only partly be explained by fluctuations in water levels and are most likely partly governed by wave conditions and local morphological conditions.
- The upper beach remains stable under aeolian forcing while limited morphological changes occur. Therefore no significant erosion or sedimentation due to aeolian transport is measured. These limited morphological changes at the upper beach indicate small transport gradients related to aeolian transports. The limited morphological activity at the upper beach could be attributed to armoring due to sediment sorting processes at the bed surface. Armoring of the surface layer occurs when the smaller and lighter sediment erodes leaving the heavier sediment which is more difficult to erode at the bed.

Due to the limited morphological activity at the upper beach, the upper beach is unlikely to function as a large source area for aeolian transport processes. A large sediment supply to the aeolian system is expected to originate from the intertidal zone. At the lower beach, tides cause aeolian processes to be interchanged with marine processes. Therefore armoring of the surface layer does not occur while marine processes mix the surface layer. As a result the sand at the surface layer of the intertidal zone is easier to erode than on the upper beach.

- Marine induced morphological changes appear to be of larger order than aeolian induced morphological changes. The shape of the profile at any time is therefore likely to be governed by (previous) marine processes rather than aeolian processes.

### 6.1.3 A numerical implementation of processes

In Chapter 4, a model for aeolian transport in supply limited situations is presented. It is concluded that:

1. In supply limited systems, aeolian sediment transport can be predicted using linear models. While conventional 3<sup>rd</sup> power sediment transport functions can be used to calculate a wind driven transport capacity, this capacity is not reached in supply limited systems. Sediment transport rates are governed by the magnitude of the source instead.
2. Measuring sediment transport rates and wind velocity simultaneously in a supply limited system, a linear relationship is expected if supply is constant. The fitted linear relationship can be used to quantify the source present. This linear relationship could be relevant to apply to several available field data sets.
3. Fetch effects are a by-product of supply limitations. A fetch effect suggests a generic principle where the fetch distance versus critical fetch distance is an important parameter governing total transport. However, the critical fetch distance is likely to be governed by the temporal and spatial variability of the supply and determining critical fetch distances generically is very difficult if not impossible without quantifying supply magnitudes.

### 6.1.4 Measured aeolian sediment transport processes

Results of a 3 days field campaign where sediment transport rates and wind speeds are measured on a Dutch beach are presented. The measured sediment transport rates are analyzed by fitting cubic and linear models with respect to wind speed. Based on the measurements and analysis it is concluded that:

1. A significant gradient in sediment transport over the beach is found during onshore winds. Sediment transport increases in the direction of the wind

until a certain limit. The distance over which transport increases is around 40 m while after 20 m in downwind direction increasing transport is found in all cases and after 50 m in downwind direction a stable value is found in all cases. The strongest increase is found in the intertidal area at low tides. The increase in transport in downwind direction is accredited to supply limited transport conditions where the maximum sediment transport is governed by supply rather than wind driven transport capacity.

2. At the measurement site, the intertidal area plays a governing role with respect to sediment supply and aeolian transport on the beach. There is less transport activity at the upper beach when the intertidal area is inundated. Therefore, the water level partly governs the sediment transport on the beach. At the upper beach during high water levels less sediment transport is measured than during low water levels. This can be expressed in the amount of total counts but also in an increase of average transport concentration (derived fitting a linear model).
3. Fitting linear relationships between wind and sediment transport magnitudes provide reasonable fits which are of equal quality compared to conventional cubic relationships:
  - Fitting the linear relationships, aggregated values of threshold velocities and (relative) sediment transport concentrations are directly quantified. Derived and aggregated threshold velocities show relatively constant values with only limited temporal and spatial variability. The corresponding empirical constants (aggregated sediment transport concentrations) show variability which correlate with the tidal phase indicating dependence on source.
  - Fitting the cubic relationships, aggregated values of threshold velocities and empirical constants are directly quantified. Derived and aggregated threshold velocities show a highly variable signal in time with no consistent mean. The corresponding empirical constants show no variability that correlate to the corresponding measured transports.
4. Supply limitations can have a dominant effect on aeolian sediment transport rates over wind speed. This causes existing sediment transport formulations where sediment transport rates are proportional to a higher power of the wind speed to be invalid in supply limited situations. Alternatively, a linear (supply limited) model could be adopted where existing data can be used to quantify sediment supply and calibrate the supply model.

## 6.2 Perspective

Below a perspective is given with respect to research on aeolian sediment transport in coastal environments and with respect to building with nature management strategies.

### 6.2.1 Research on aeolian sediment transport in coastal environments

Throughout this thesis it is shown that supply limitations can govern aeolian sediment transport rates on beaches. In the cases described in this thesis, sediment supply is the main governing parameter for aeolian sediment transport rates. A general lack of knowledge exists on the magnitude of the supply to the aeolian system. Several parameters influencing aeolian sediment transport rates have however been identified. Especially surface conditions such as sediment sorting, moisture content and shell pavements are known to have a significant influence on sediment supply. While these parameters have been studied, quantification of their relative importance with respect to aeolian sediment transport remains a major challenge. Especially while surface conditions can vary across the beach due to the distinct influence of marine and aeolian processes. In this thesis a methodology of quantifying supply magnitude is carefully suggested which can be of help to re-analyze existing data with the aim of determining the relative importance of supply limiting parameters.

Next to supply limiting parameters on the beach the sediment exchange between the marine and aeolian zone is shown to be important for aeolian sediment transport rates. It is shown that the effects of tide dependent marine processes can govern aeolian sediment transport rates. This effect could be attributed due to the sediment mixing at the surface due to marine processes where the mixed sediment at the surface layer in the intertidal zone could possibly be easier to erode than the sorted sediment at the upper beach. This makes the intertidal area an area of interest when trying to quantify sediment supply, aeolian transport and dune development. Sediment mixing is suggested above to be influencing aeolian sediment transport and sediment exchange between the intertidal zone and aeolian zone. Considering the wide range of scales relevant to sediment transport (marine and aeolian) the mechanisms of sediment exchange and the quantification of this sediment exchange are likely to be beyond sediment mixing alone. To increase the knowledge on quantifying sediment transport on beaches, processes of sediment exchange between marine and aeolian zones should be of interest of future research.

In this thesis, the morphology of coastal dunes has not been addressed in detail. Development of dunes has been described in literature and (despite some major contributions) are not fully understood yet. This work focuses on quantifying sediment transport towards the dunes. The work presented in this thesis could possibly be used as a boundary condition for studies on dune morphology.

### 6.2.2 Building with nature

Building with Nature aims to use natural processes to do part of the engineering work. In the case of dune development due to natural aeolian processes, it is found that the system of sediment transport is limited by sediment supply. While the exact magnitude of sediment supply and the exact capacity of the wind is

unknown, it is evident that wind driven transport capacity is not utilized at all times. Therefore, dune development in terms of dune volume changes might be stimulated by artificially changing source conditions. Source conditions might be changed applying beach and foreshore nourishments.

In the case of beach nourishments the dry beach is generally widened. This leads initially to a measurable increase in sediment transport and dune volume changes (van der Wal, 1998) which can be attributed to an increased sediment supply. This increase is however temporarily where sediment sorting and armoring at the sediment surface limits sediment supply from the bed towards the aeolian system.

In the case of shoreface nourishments the foreshore slope is generally flattened. This causes presently unknown effects on the conditions in the intertidal zone. The intertidal zone is an explicit area of interest because of its possible governing role with respect to sediment supply to the aeolian system. An increased knowledge on intertidal dynamics might therefore contribute to the design of future nourishments.

## References

- Aarninkhof, S., van Dalen J.A., Mulder, J., Rijks, D., May 2010. Sustainable development of nourished shorelines: Innovations in project design and realization. In: Proceedings of PIANC MMX Congress. Liverpool UK.
- Allen, J., 1982. Simple models for the shape and symmetry of tidal sand waves: (1) statically stable equilibrium forms. *Marine Geology* 48 (1-2), 31 – 49.
- Anthony, E. J., Ruz, M.-H., Vanhe, S., 2009. Aeolian sand transport over complex intertidal bar-trough beach topography. *Geomorphology* 105 (1-2), 95–105.
- Arens, S. M., 1996. Rates of aeolian transport on a beach in a temperate humid climate. *Geomorphology* 17 (1-3), 3 – 18.
- Arens, S. M., Mulder, J. P., Slings, Q. L., Geelen, L. H., Damsma, P., 2012. Dynamic dune management, integrating objectives of nature development and coastal safety: Examples from the Netherlands. *Geomorphology* (0), –.
- Bagnold, R. A., 1954. *The physics of blown sand and desert dunes*, 2nd Edition. Methuen, London.
- Bagnold, R. A., 1973. The nature of saltation and of 'bed-load' transport in water. *Proceedings of the Royal Society of London. Series A, Mathematical and Physical Sciences* 332 (1591), pp. 473–504.
- Bauer, B. O., Davidson-Arnott, R., Nordstrom, K. F., Ollerhead, J., Jackson, N. L., 1996. Indeterminacy in aeolian sediment transport across beaches. *Journal of Coastal Research* 12, 641–653.
- Bauer, B. O., Davidson-Arnott, R. G. D., 2002. A general framework for modeling sediment supply to coastal dunes including wind angle, beach geometry, and fetch effects. *Geomorphology* 49 (1-2), 89–108.
- Bauer, B. O., Davidson-Arnott, R. G. D., Hesp, P. A., Namikas, S. L., Ollerhead, J., Walker, I. J., 2009. Aeolian sediment transport on a beach: Surface moisture, wind fetch, and mean transport. *Geomorphology* 105 (1-2), 106–116.
- Bochev-van der Burgh, L., Wijnberg, K., Hulscher, S., 2011. Decadal-scale morphologic variability of managed coastal dunes. *Coastal Engineering* 58 (9), 927 – 936.
- Callaghan, D. P., Nielsen, P., Short, A., Ranasinghe, R., 2008. Statistical simulation of wave climate and extreme beach erosion. *Coastal Engineering* 55 (5), 375–390.
- Carter, R. W. G., 1976. Formation, maintenance and geomorphological significance of an aeolian shell pavement. *Journal of Sedimentary Research* 46 (2), 418–429.

- Chatfield, C., 1996. The analysis of time series; an introduction. Chapman and Hall.
- Cowell, P. J., Stive, M. J. F., Niedoroda, A. W., de Vriend, H. J., Swift, D. J. P., Kaminsky, G. M., Capobianco, M., 2003. The coastal-tract (part 1): A conceptual approach to aggregated modeling of low-order coastal change. *Journal of Coastal Research* 19 (4), 812–827.
- Damsma, T., April 2009. Dune growth on natural and nourished beaches: 'a new perspective'. Master's thesis, Delft University of Technology.
- Davidson-Arnott, R. G. D., Bauer, B. O., 2009. Aeolian sediment transport on a beach: Thresholds, intermittency, and high frequency variability. *Geomorphology* 105 (1-2), 117–126.
- Davidson-Arnott, R. G. D., Law, M. N., 1990. Seasonal patterns and controls on sediment supply to coastal foredunes, long point, lake erie. In: Nordstrom, K. F., Psuty, N. P., Carter, R. W. G. (Eds.), *Coastal Dunes: Form and Process*. John Wiley & Sons Ltd., pp. 177–200.
- Davidson-Arnott, R. G. D., MacQuarrie, K., Aagaard, T., 2005. The effect of wind gusts, moisture content and fetch length on sand transport on a beach. *Geomorphology* 68 (1-2), 115–129.
- Davidson-Arnott, R. G. D., Yang, Y., Ollerhead, J., Hesp, P. A., Walker, I. J., 2008. The effects of surface moisture on aeolian sediment transport threshold and mass flux on a beach. *Earth Surface Processes and Landforms* 33 (1), 55–74.
- de Schipper, M., de Vries, S., Ranasinghe, R., Reniers, A., Stive, M., 2012. Morphological developments after a beach and shoreface nourishment at vlugtenburg beach. In: *NCK-days 2012 : Crossing borders in coastal research : jubilee conference proceedings*. pp. 115–118.
- de Vries, S., Arens, B., Stive, M., Ranasinghe, R., 2011a. Dune growth trends and the effect of beach width on annual timescales. In: *Coastal Sediments 2011*. pp. 712–724.
- de Vries, S., de Schipper, M., Stive, M., Ranasinghe, R., 2011b. Sediment exchange between the sub-aqueous and sub-aerial coastal zones. *Proceedings of the International Conference on Coastal Engineering* 1 (32).
- de Vries, S., Southgate, H., Kanning, W., Ranasinghe, R., 2012. Dune behavior and aeolian transport on decadal timescales. *Coastal Engineering* 67 (0), 41 – 53.
- Delgado-Fernandez, I., 2010. A review of the application of the fetch effect to modelling sand supply to coastal foredunes. *Aeolian Research* 2 (2-3), 61 – 70.



- den Heijer, C., Baart, F., van Koningsveld, M., 2012. Assessment of dune failure along the dutch coast using a fully probabilistic approach. *Geomorphology* 143144 (0), 95 – 103.
- Edelman, T., 1972. Dune erosion during storm conditions. In: *Proceedings of the 13th Conference on Coastal Engineering*. Vancouver, Canada, pp. 1305–1311.
- Fryberger, S., 1979. Dune forms and wind regime. *A Study of Global Sand Seas*, USGS Professional Paper 1052, 137–169.
- Guillen, J., Stive, M. J. F., Capobianco, M., 1999. Shoreline evolution of the holland coast on a decadal scale. *Earth Surface Processes and Landforms* 24 (6), 517–536.
- Hardisty, J., Whitehouse, R. J. S., Apr. 1988. Evidence for a new sand transport process from experiments on saharan dunes. *Nature* 332 (6164), 532–534.
- Harley, M. D., Turner, I. L., Short, A. D., Ranasinghe, R., 2011. Assessment and integration of conventional, rtk-gps and image-derived beach survey methods for daily to decadal coastal monitoring. *Coastal Engineering* 58 (2), 194 – 205.
- Houser, C., 2009. Synchronization of transport and supply in beach-dune interaction. *Progress in Physical Geography* 33 (6), 733–746.
- Howd, P., Birkemeier, W., 1987. Beach and nearshore survey data: 1981-1984 cerc field research facility, technical report cerc-87-9. Tech. rep., U.S. Army Engineer Waterways Experiment Station, Vicksburg, MS.
- Iversen, J. D., Rasmussen, K. R., 1994. The effect of surface slope on saltation threshold. *Sedimentology* 41 (4), 721–728.
- Iversen, J. D., Rasmussen, K. R., 1999. The effect of wind speed and bed slope on sand transport. *Sedimentology* 46 (4), 723–731.
- Jackson, D. W. T., Cooper, J. A. G., 1999. Beach fetch distance and aeolian sediment transport. *Sedimentology* 46 (3), 517–522.
- Jungerius, P. D., Witter, J. V., Boxel, J. H. V., 1991. The effects of changing wind regimes on the development of blowouts in the coastal dunes of the netherlands. *Landscape Ecology* 6, 41–48.
- Kawamura, 1951. Study on sand movement by wind. *Reports of Physical Sciences Research Institute of Tokyo University* 5 (3-4), 95–112.
- Kriebel, D. L., Dean, R. G., 1985. Numerical simulation of time-dependent beach and dune erosion. *Coastal Engineering* 9 (3), 221 – 245.
- Kroon, A., Hoekstra, P., 1990. Eolian sediment transport on a natural beach. *Journal of Coastal Research* 6, 367–380.

- Larson, M., Erikson, L., Hanson, H., 2004. An analytical model to predict dune erosion due to wave impact. *Coastal Engineering* 51 (8-9), 675 – 696.
- Lee, G., Birkemeier, W., 1993. Beach and nearshore survey data: 1985-1991 cerc field research facility, technical report cerc-93-3. Tech. rep., U.S. Army Engineer Waterways Experiment Station, Vicksburg, MS.
- Lynch, K., Jackson, D. W. T., Cooper, J. A. G., 2008. Aeolian fetch distance and secondary airflow effects: the influence of micro-scale variables on meso-scale foredune development. *Earth Surface Processes and Landforms* 33 (7), 991–1005.
- Ministry of transport and Public Works, December 1990. A new coastal defence policy for the netherlands. The Hague, The Netherlands.
- Nickling, W., Davidson-Arnott, R., 1990. Aeolian sediment transport on beaches and coastal sand dunes. In: Davidson-Arnott, R. (Ed.), *Proceedings of the Symposium on Coastal Sand Dunes*. National Research Council of Canada, pp. 1–35.
- Pye, K., Blott, S. J., 2008. Decadal-scale variation in dune erosion and accretion rates: An investigation of the significance of changing storm tide frequency and magnitude on the sefton coast, uk. *Geomorphology* 102 (3-4), 652–666.
- Quartel, S., Kroon, A., Ruessink, B. G., 2008. Seasonal accretion and erosion patterns of a microtidal sandy beach. *Marine Geology* 250 (1-2), 19–33.
- Ranasinghe, R., Callaghan, D., Stive, M., 2011. Estimating coastal recession due to sea level rise: beyond the bruun rule. *Climatic Change*, 1–14.
- Ruessink, B. G., Jeuken, M. C. J. L., 2002. Dunefoot dynamics along the dutch coast. *Earth Surface Processes and Landforms* 27 (10), 1043–1056.
- Sarre, R. D., 1989. Aeolian sand drift from the intertidal zone on a temperate beach: Potential and actual rates. *Earth Surface Processes and Landforms* 14 (3), 247–258.
- Sauermann, G., Kroy, K., Herrmann, H. J., Aug 2001. Continuum saltation model for sand dunes. *Phys. Rev. E* 64 (3), 031305.
- Sherman, D. J., Jackson, D. W. T., Namikas, S. L., Wang, J., 1998. Wind-blown sand on beaches: an evaluation of models. *Geomorphology* 22 (2), 113 – 133.
- Sherman, D. J., Li, B., 2012. Predicting aeolian sand transport rates: A reevaluation of models. *Aeolian Research* 3 (4), 371 – 378.
- Short, A. D., Hesp, P. A., 1982. Wave, beach and dune interactions in southeastern australia. *Marine Geology* 48 (3-4), 259–284.
- Short, A. D., Trembanis, A. C., 2004. Decadal scale patterns in beach oscillation and rotation narrabeen beach, australia-time series, pca and wavelet analysis. *Journal of Coastal Research*, 523–532.

- Sørensen, M., 2004. On the rate of aeolian sand transport. *Geomorphology* 59 (1-4), 53 – 62.
- Southgate, H. N., 2011. Data-based yearly forecasting of beach volumes along the dutch north sea coast. *Coastal Engineering* 58 (8), 749 – 760.
- Spaan, W., van den Abeele, G., 1991. Wind borne particle measurements with acoustic sensors. *Soil Technology* 4 (1), 51 – 63.
- van de Graaff, J., 1977. Dune erosion during a storm surge. *Coastal Engineering* 1, 99–134.
- van de Graaff, J., 1986. Probabilistic design of dunes; an example from the netherlands. *Coastal Engineering* 9 (5), 479–500.
- van der Wal, D., 1998. Effects of fetch and surface texture on aeolian sand transport on two nourished beaches. *Journal of Arid Environments* 39 (3), 533–547.
- van Rijn, L., Walstra, D., Grasmeyer, B., Sutherland, J., Pan, S., Sierra, J., 2003. The predictability of cross-shore bed evolution of sandy beaches at the time scale of storms and seasons using process-based profile models. *Coastal Engineering* 47 (3), 295 – 327.
- van Son, S., Lindenbergh, R., de Schipper, M., de Vries, S., Duijnmayor, K., 2009. Using a personal watercraft for monitoring bathymetric changes at storm scale. In: *International Hydrographic Conference*. Cape Town, South Africa.
- Van Straaten, L., 1961. Directional effects of winds, waves and currents along the dutch north sea coast. *Geologie en Mijnbouw* 40, 333–346 (Part 1) and 363–391 (Part 2).
- Vellinga, P., 1986. Beach and dune erosion during storm surges. Ph.D. thesis, Delft University of Technology.
- Waterman, R., 2010. Integrated coastal policy via Building with Nature. Ph.D. thesis, Delft University of Technology.
- Wijnberg, K., Bochev-van der Burgh, L., Hulscher, S., 2011. Coastal management and long-term foredune behavior: characterizing semi-natural foredune evolution. *Journal of Coastal Research Special Issue* 64, 329–333.
- Wijnberg, K. M., Terwindt, J. H. J., 1995. Extracting decadal morphological behaviour from high-resolution, long-term bathymetric surveys along the holland coast using eigenfunction analysis. *Marine Geology* 126 (1-4), 301 – 330.
- WL/Delft Hydraulics, 1978. (in Dutch) Duinafslag ten gevolge van de stormvloed op 3 januari 1976. Tech. rep., Waterloopkundig Laboratorium.
- WL/Delft Hydraulics, 1984. (in Dutch) Duinafslag ten gevolge van de stormvloed op 1 en 2 februari 1983. Tech. rep., Waterloopkundig Laboratorium.

- Wolf, J., Flather, R., 2005. Modelling waves and surges during the 1953 storm. *Philosophical Transactions of the Royal Society A: Mathematical, Physical and Engineering Sciences* 363 (1831), 1359–1375.
- Wolman, M. G., Miller, J. P., 1960. Magnitude and frequency of forces in geomorphic processes. *The Journal of Geology* 68 (1), pp. 54–74.
- Wright, L., Short, A., 1984. Morphodynamic variability of surf zones and beaches: A synthesis. *Marine Geology* 56 (1-4), 93 – 118.

## Curriculum Vitae

Sierd de Vries was born in Gouda on October 15<sup>th</sup> 1981. He grew up in Gouda where he graduated from Goudsche Scholen Gemeenschap (VWO), 1999. In 2000 he started his academic education at Delft University of Technology. He graduated at the section of Hydraulic engineering in 2007 under the supervision of Professor M.J.F. Stive.

In 2007 he started at Delft University of Technology on a temporary contract together with Matthieu de Schipper. Together they developed field capacity for the section of Hydraulic engineering with the intention of starting a PhD in a later stage. In 2007 and 2008 (one and a half year) a Jetski capable of measuring coastal topography was build and tested. Moreover, a technique to measure parameters of coastal waves was developed. Early 2009, a PhD project was started within the Building with Nature project. This project resulted in this dissertation.

In 2009 he co-founded a private company (Shore Monitoring & Research) which aimed to exploit the developed field capacity at the University commercially. Especially the TUDelft jetski is still not only used for research purposes but it is also used for commercial projects.

Currently he is working 3 days a week as a post-doc researcher at Delft University within a research project related to the Zandmotor in Holland (NeMo). Two days a week he works for the company (Shore Monitoring & Research) he currently owns together with 2 associates. His associates are his colleague Matthieu de Schipper and a former MSc. student Roeland de Zeeuw.

## Publications

### Journal Articles

- de Vries, S., Hill, D., de Schipper, M., Stive, M., 2011. Remote sensing of surf zone waves using stereo imaging. *Coastal Engineering* 58 (3), 239 – 250.
- de Vries, S., Southgate, H., Kanning, W., Ranasinghe, R., 2012. Dune behavior and aeolian transport on decadal timescales. *Coastal Engineering* 67 (0), 41 – 53.
- de Vries, S., van Thiel de Vries, J., van Rijn, L., Ranasinghe, R., Submitted to *Aeolian Research*. Aeolian sediment transport in supply limited situations; a numerical implementation. *Aeolian Research*.
- de Vries, S., Arens, S., de Schipper, M., in preparation. Aeolian sediment transport in supply limited situations; an analysis on field data.

### Conference proceedings

- de Vries, S., Arens, B., Stive, M., Ranasinghe, R., 2011a. Dune growth trends and the effect of beach width on annual timescales. In: *Coastal Sediments 2011*. pp. 712–724.
- de Vries, S., Arens, S., Stive, M., Ranasinghe, R., 2012. A new modelling concept for aeolian sediment transport on beaches. In: *EGU General Assembly Conference Abstracts*. Vol. 14. p. 214.
- de Vries, S., de Schipper, M., Stive, M., Ranasinghe, R., 2011b. Sediment exchange between the sub-aqueous and sub-aerial coastal zones. *Proceedings of the International Conference on Coastal Engineering* 1 (32).
- de Vries, S., de Schipper, M., van Thiel de Vries, J., Uijtewaal, W., Stive, M., 2008. Using stereo photo measurements to analyse the surfability of ship induced waves. In: Dasmiani, L., Mossa, M. (Eds.), *Second International Conference on the Application of Physical Modelling to Port and Coastal Protection*. pp. 37–46.
- de Vries, S., Hill, D., de Schipper, M., Stive, M., 2009. Using stereo photogrammetry to measure coastal waves. *Journal of Coastal Research* SI 56, 1484–1488.
- de Vries, S., Southgate, H., Kanning, W., Ranasinghe, R., 2012. Dune development and aeolian transport along the holland coast. In: *NCK-days 2012 : Crossing borders in coastal research : jubilee conference proceedings*. pp. 125–129.
- de Vries, S., Stive, M., van Rijn, L., Ranasinghe, R., 2012. A new conceptual model for aeolian transport rates on beaches. In: *Proceedings of the International Conference on Coastal Engineering*.

## Co-authored publications

- Baart, F., Den Bieman, J., van Koningsveld, M., Luijendijk, A., Parteli, E., Plant, N., Roelvink, J., Storms, J., de Vries, S., van Thiel de Vries, J., et al., 2012. An integrated coastal model for aeolian and hydrodynamic sediment transport. In: EGU General Assembly Conference Abstracts. Vol. 14. p. 12842.
- de Groot, A., de Vries, S., Keijsers, J., Riksen, M., Ye, Q., Poortinga, A., Arens, S., Bochev-Van der Burgh, L., Wijnberg, K., Schretlen, J., van Thiel de Vries, J., 2012. Measuring and modeling coastal dune development in the netherlands. In: NCK-days 2012 : Crossing borders in coastal research : jubilee conference proceedings. pp. 105–110.
- de Schipper, M., de Vries, S., Henriquez, M., Reiniers, A., de Koning Gans, H., Labeur, R., Stive, M., 2008. Surfing waves generated by a hull. In: Proceedings of the 31st International Conference Coastal Engineering. pp. 761–773.
- de Schipper, M., de Vries, S., Ranasinghe, R., Reniers, A., Stive, M., 2012. Morphological developments after a beach and shoreface nourishment at vlugtenburg beach. In: NCK-days 2012 : Crossing borders in coastal research : jubilee conference proceedings. pp. 115–118.
- de Schipper, M., de Zeeuw, R., de Vries, S., Stive, M., Terwindt, J., 2011. Horizontal adcp measurements of waves and currents in the very nearshore. In: Current, Waves and Turbulence Measurements (CWTM), 2011 IEEE/OES 10th. IEEE, pp. 159–166.
- Lindenbergh, R., Soudarissanane, S., De Vries, S., Coquet, M., De Schipper, M., Hejbudzka, K., Duijnmayr, K., Van Goor, B., Cohen, A., 2010. Eolian sand transport monitored by terrestrial laser scanning. In: International Archives of Photogrammetry, Remote Sensing and Spatial Information Sciences. Vol. XXXVIII, Part 5. International Society of Photogrammetry and Remote Sensing (ISPRS), pp. 393–398.
- Sénechal, N., Ardhuin, F., Abadie, S., Almar, R., Arnaud, G., Austin, M., Barnoud, J., Barthélémy, E., Berni, C., et al., 2008. Ecors truc vert: qualification des modèles de houle et de morphodynamique. Xmes Journes Nationales Gnie Ctier Gnie Civil, 635–654.
- van Son, S., Lindenbergh, R., de Schipper, M., de Vries, S., Duijnmayr, K., 2009. Using a personal watercraft for monitoring bathymetric changes at storm scale. In: International Hydrographic Conference. Cape Town, South Africa.

## Acknowledgments

This thesis was funded by the innovation program Building with Nature. The Building with Nature program is funded from several sources, including the Subsidiereregeling Innovatieketen Water (SIW, Staatscourant nrs 953 and 17009) sponsored by the Dutch Ministry of Transport, Public Works and Water Management and partner contributions of the participants to the Foundation EcoShape. The program receives co-funding from the European Fund for Regional Development EFRO and the Municipality of Dordrecht. From the Building with Nature team I would specifically like to thank Stefan Aarninkhof for being a great case manager.

Several people have made a notable contribution in various stages during the completion of this thesis. This thesis could not have been completed without the formal and personal contribution of these people.

First of all I would like to thank Professor Marcel Stive for the confidence in me in the beginning and during the full period of my employment at the TUDelft. This employment is not over yet and continues today for an extended period and I am looking forward to give it my best. Thank you for introducing me to the world of coastal engineering and especially for the introduction to field work sending me to the Truc Vert experiment in France in 2009. Moreover, thank you for your support with starting our company in 2009.

Thanks to Rosh Ranasinghe who has been an inspiring supervisor and co-promotor. The members of the committee, Dr. Arens, Prof. Hoekstra, Prof. Hanson, Prof. Roelvink, Dr.ir. van Thiel de Vries, Prof. Hanson and Prof. Uijtewaal are thanked for their interest and useful comments.

Howard Southgate, Jaap van Thiel de Vries and Bas Arens have made specific contributions to this thesis' content in both writing and collecting/analyzing data, thanks a lot.

The people at Deltares and Utrecht University who were always happy to provide me with generous advice and hospitality are thanked. Gerben Ruessink, Bert van der Valk, Jan Mulder, Leo van Rijn, Ad van der Spek, Pieter Koen Tonnon, Leo Senbering, Dano Roelvink and Ap van Dongeren, thank you !

Then I would like to thank my TUDelft PhD colleagues starting with my friend, office mate, professional associate, co-author and of course drinking partner, Matthieu de Schipper. Despite the fundamental differences on how we think about important details of our lives, not the least cars, I feel we will keep seeing each other for a while.

Martijn Henriques and Chu Ao, thanks for sharing good and less good times at the office. Thanks to PhD colleagues, Nicolette Volp, Wim Kanning, Ruben Jongejan, Meagan Wengrove, Marije Smit, Ronald Brouwer, Menno Eelkema, Joao Mill Homens, Judith Bosboom, Max Radermacher, Fedor Baart, Cees den Heijer, Bas Huisman, Bas Hoonhout, Saulo Meirelles Nunes Da Rocha and Timothy Price for discussing interesting topics on and off office hours, I hope we will continue meeting each other in the future.

Roeland de Zeeuw has made a significant contribution making the field activ-



ities of myself but also the TUDelft possible. I am happy to share the interest in field measurements in the way we currently do.

I would like to thank my parents, sister and family, their contribution to this work and my personal/professional life in general can not be overestimated.

Finally I would like to thank Marion ! Words cannot describe how much you have been contributing to any detail of the past period. Hopefully we continue discovering the world together starting tomorrow again.

Sierd de Vries, August 2013.